Gravitational waves from compact binary coalescences

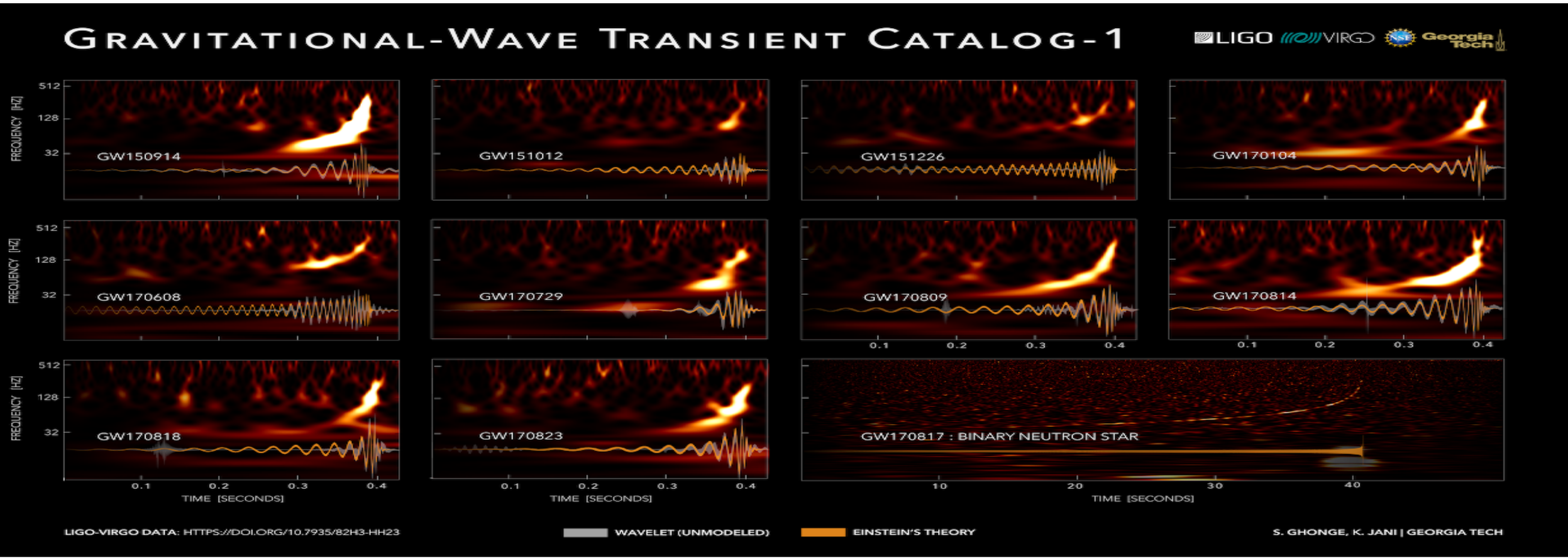

Ed Porter
APC/CNRS

Cosmic Explosions 19, Cargese, Corsica, 27/05-05/06

Topics Covered

- Part 1
  - Matched Filtering
  - CBC waveform modelling
  - Data treatment
  - CBC searches and parameter estimation
- Part 2
  - 01/02 detections
  - Fundamental physics and extreme matter
  - Astrophysics and Cosmology

Part 1

What is matched filtering?

- GWs are analogous to 1D sound waves
- Optimal linear filter for weak signals buried in random Gaussian noise
- Also known as optimal or Wiener filtering
- Works by correlating a known signal model (template) with the data

Constructing the optimal linear filter

- Starting with data : $s(t) = h(t) + n(t) \quad , \; n(t) >> h(t)$
- Define the correlation between the data and a real filter as

$$C(\tau) = \int_{-\infty}^{\infty} dt\, s(t) F(t+\tau) = \int_{-\infty}^{\infty} df\, \tilde{s}(f) \tilde{F}^*(f) e^{2\pi i f \tau}$$

- To evaluate the signal-to-noise ratio (SNR), $\rho = \frac{S}{N}$
- we define the filtered signal

$$S = \langle C(\tau) \rangle = \int_{-\infty}^{\infty} df\, \langle \tilde{s}(f) \rangle \tilde{F}^*(f) e^{2\pi i f \tau} = \int_{-\infty}^{\infty} df\, \tilde{h}(f) \tilde{F}^*(f) e^{2\pi i f \tau}$$

- using $\langle n(t) \rangle = 0$

Constructing the optimal linear filter

- For stationary, Gaussian noise, the variance is

$$\left\langle N^2 \right\rangle = \left[\left\langle C^2(\tau) \right\rangle - \left\langle C(\tau) \right\rangle^2 \right]_{h(t)=0} = \int_{-\infty}^{\infty} df df' \, \left\langle \tilde{n}(f) \tilde{n}^*(f') \right\rangle \tilde{F}(f) \tilde{F}^*(f') e^{2\pi i \tau (f - f')}$$

- Defining a two-sided power spectral density $\left\langle \tilde{n}(f) \tilde{n}^*(f') \right\rangle = \delta(f - f') S_h(f)$

- we can now write $\left\langle N^2 \right\rangle = \int_{-\infty}^{\infty} df \, |\tilde{F}(f)|^2 S_h(f)$

- defining the SNR as $\rho = \frac{S}{N} = \frac{\int_{-\infty}^{\infty} df \, \tilde{h}(f) \tilde{F}^*(f) e^{2\pi i f \tau}}{\left[\int_{-\infty}^{\infty} df \, |\tilde{F}(f)|^2 S_h(f) \right]^{1/2}}$

Constructing the optimal linear filter

- Defining a noise-weighted inner product

$$\langle a \,|\, b \rangle = 2 \int_0^\infty \frac{df}{S_n(f)} \tilde{a}(f) \tilde{b}^*(f) + c\,.\,c\,.$$

- the SNR now becomes

$$\frac{S}{N} = \frac{\left\langle \tilde{h}(f) \,|\, S_n(f) \tilde{F}(f) e^{2\pi i f \tau} \right\rangle}{\left\langle S_n(f) \tilde{F}(f) \,|\, S_n(f) \tilde{F}(f) \right\rangle^{1/2}}$$

- To optimise the SNR, we require $\tilde{F}(f) \,||\, \tilde{h}(f)$
- allowing us to define the optimal linear filter as $\tilde{F}(f) = \frac{\tilde{h}(f)}{S_n(f)} e^{-2\pi i f \tau}$
- and the optimal SNR as $\rho_{opt} = \langle h \,|\, h \rangle^{1/2}$

Response to a GW

- The response at each detector is

$$h_i(t) = h_+(t+\tau_i)F_i^+ + h_\times(t+\tau_i)F_i^\times$$

- where $(h_+, h_\times)$ are the GW polarisations
- and $(F^+, F^\times)$ are the detector pattern response
- In general, the GWs are defined by 15-17 parameters that we can define as extrinsic and intrinsic

Extrinsic Parameters (Positional)

$$h_i(t) = h_+(t+\tau_i)F_i^+ + h_\times(t+\tau_i)F_i^\times$$

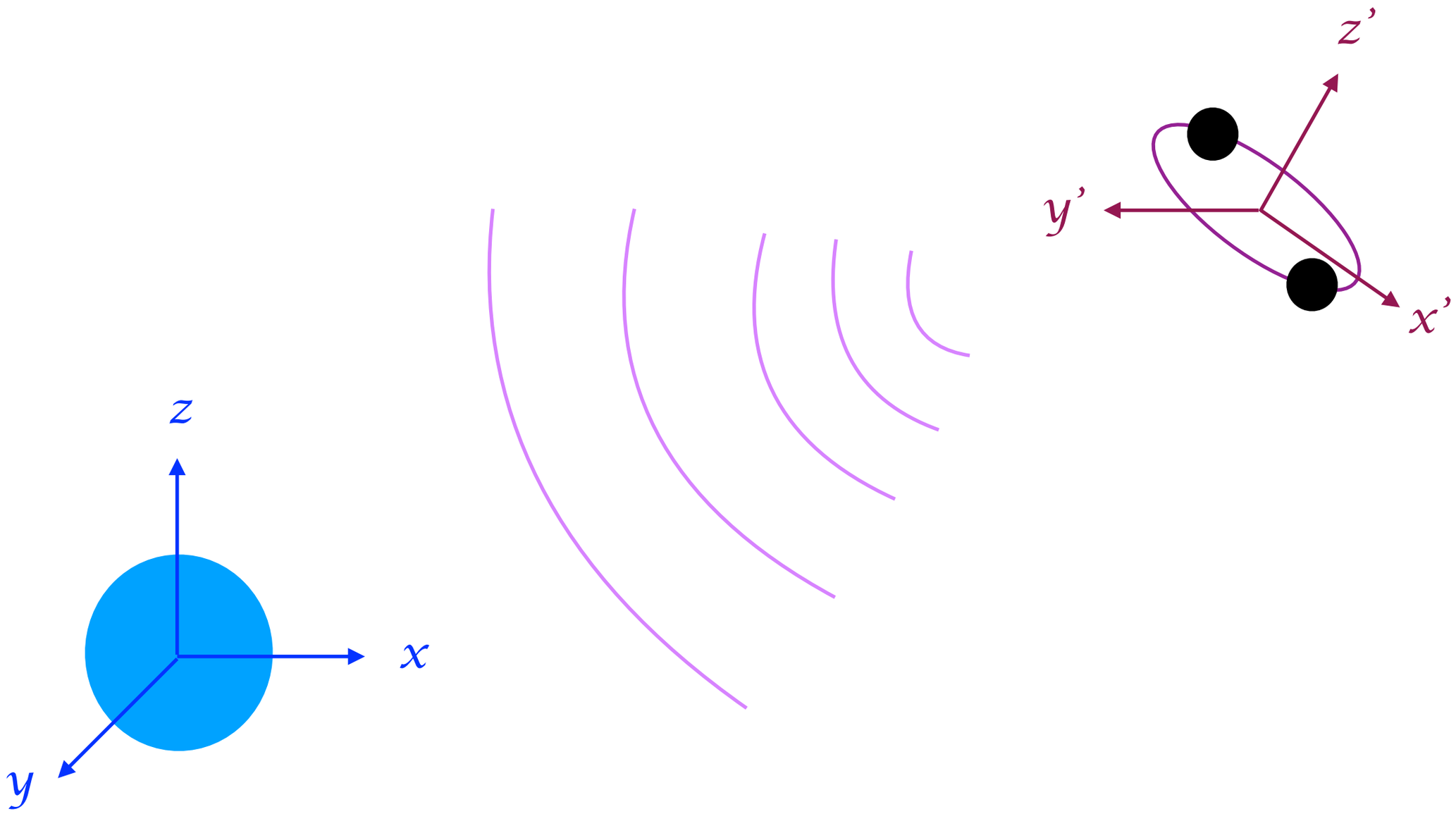

Luminosity Distance

$$h_i(t) = h_+(t+\tau_i)F_i^+ + h_\times(t+\tau_i)F_i^\times$$

Parameters

1

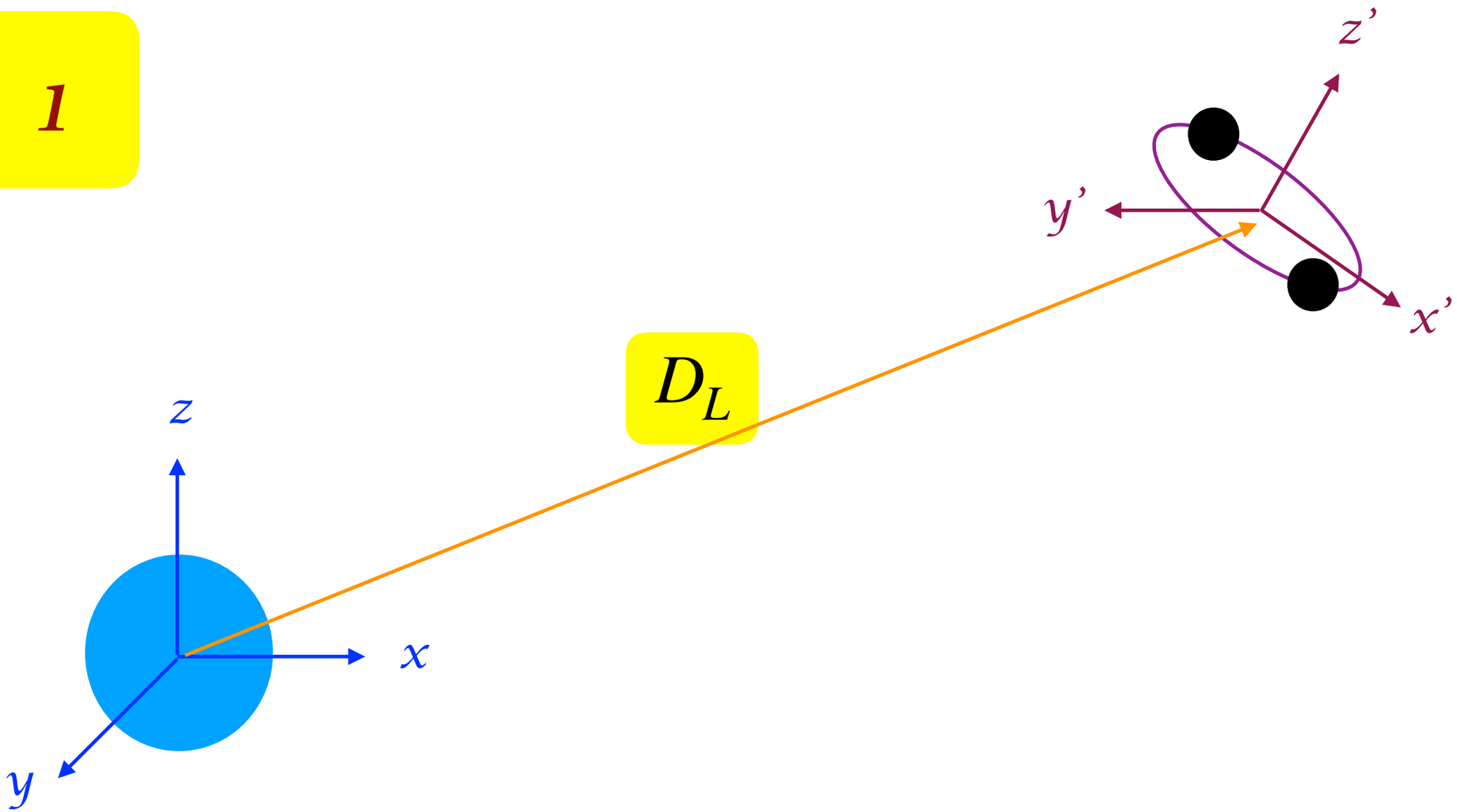

Sky Position

$$h_i(t) = h_+(t+\tau_i)F_i^+ + h_\times(t+\tau_i)F_i^\times$$

Parameters

3

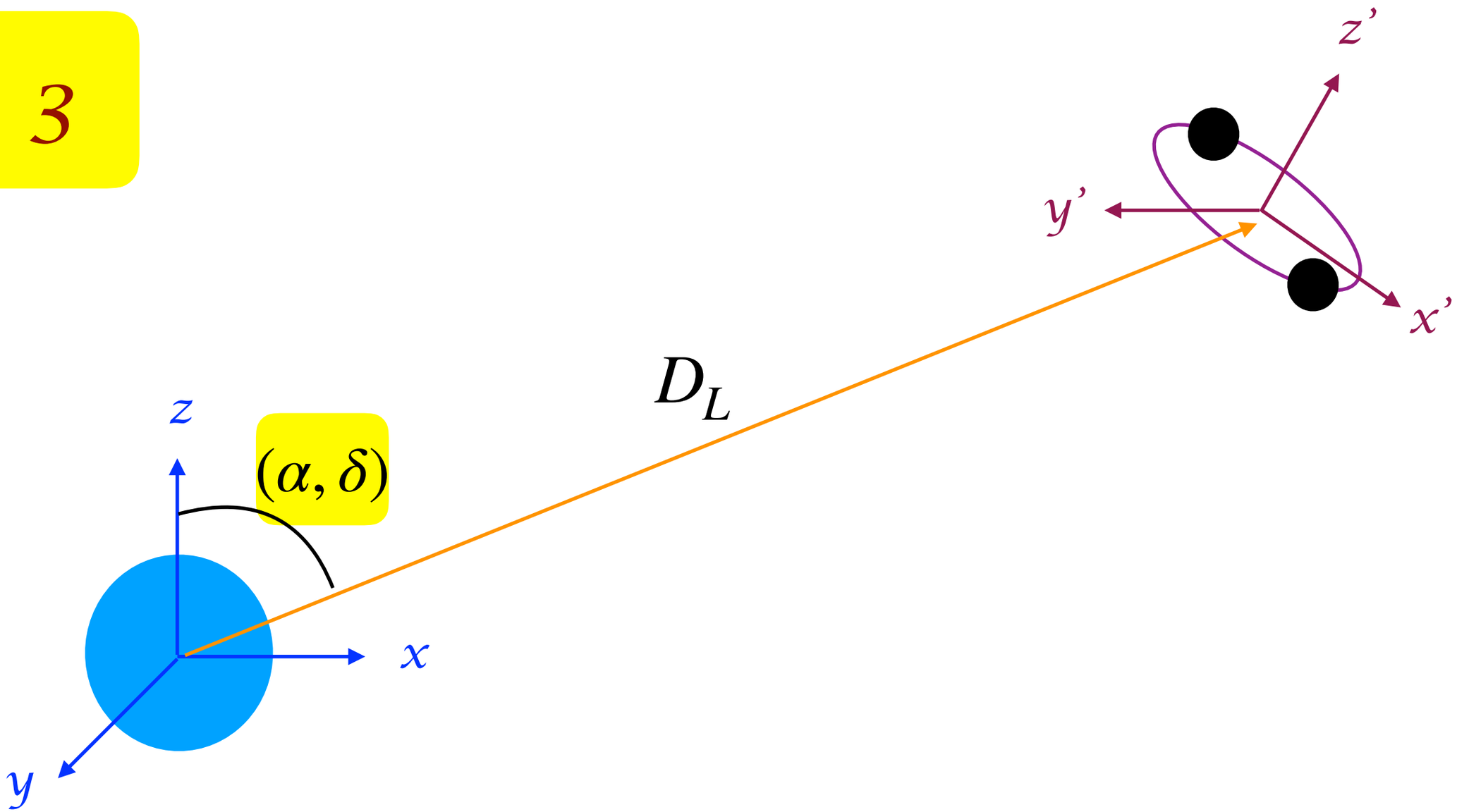

Inclination Angle

$$h_i(t) = h_+(t+\tau_i)F_i^+ + h_\times(t+\tau_i)F_i^\times$$

Parameters

4

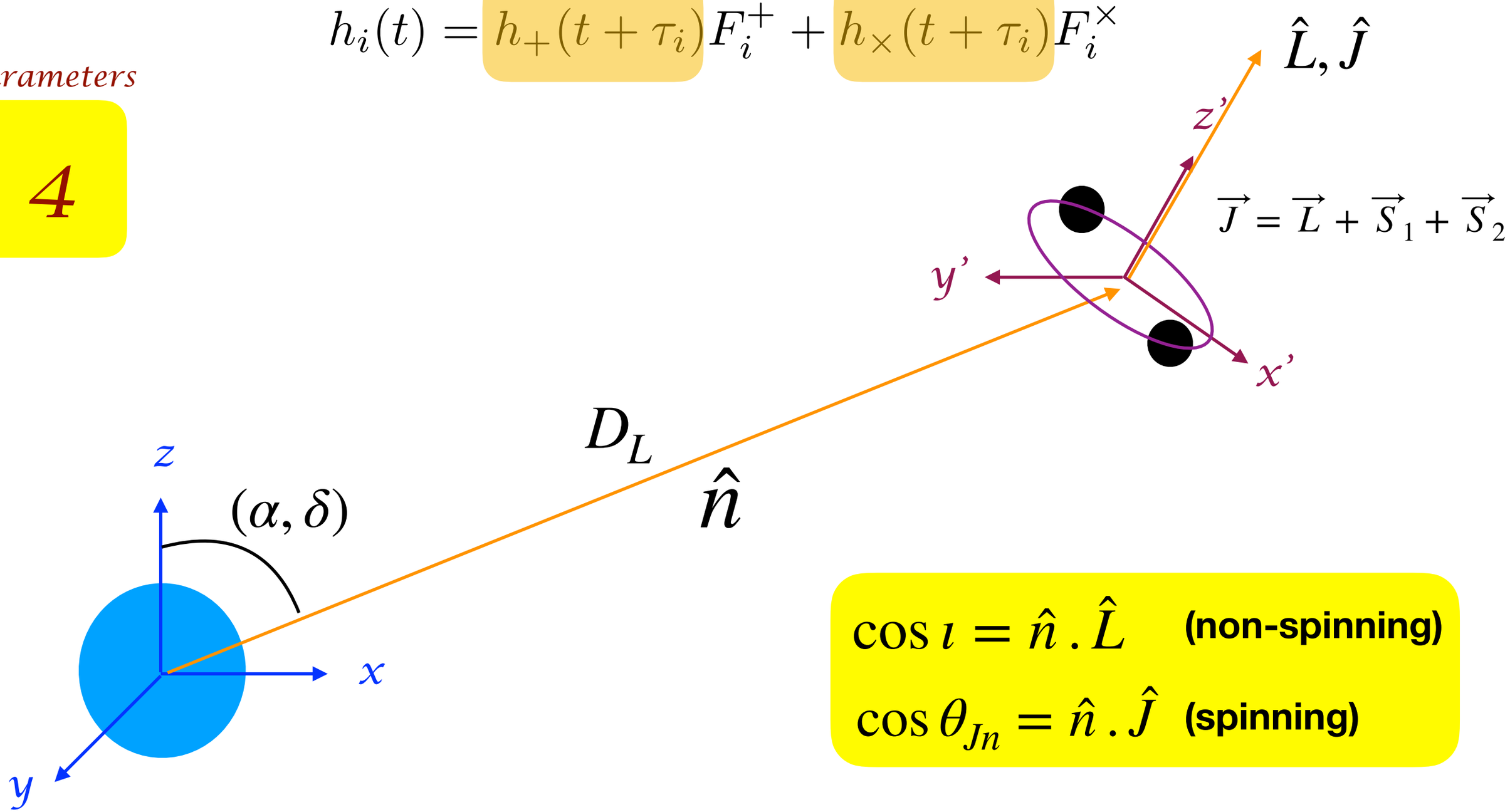

$\cos\iota = \hat{n}\,.\,\hat{L}$ **(non-spinning)**

$\cos\theta_{Jn} = \hat{n}\,.\,\hat{J}$ **(spinning)**

Polarisation Angle

$$h_i(t) = h_+(t+\tau_i)F_i^+ + h_\times(t+\tau_i)F_i^\times$$

Parameters

5

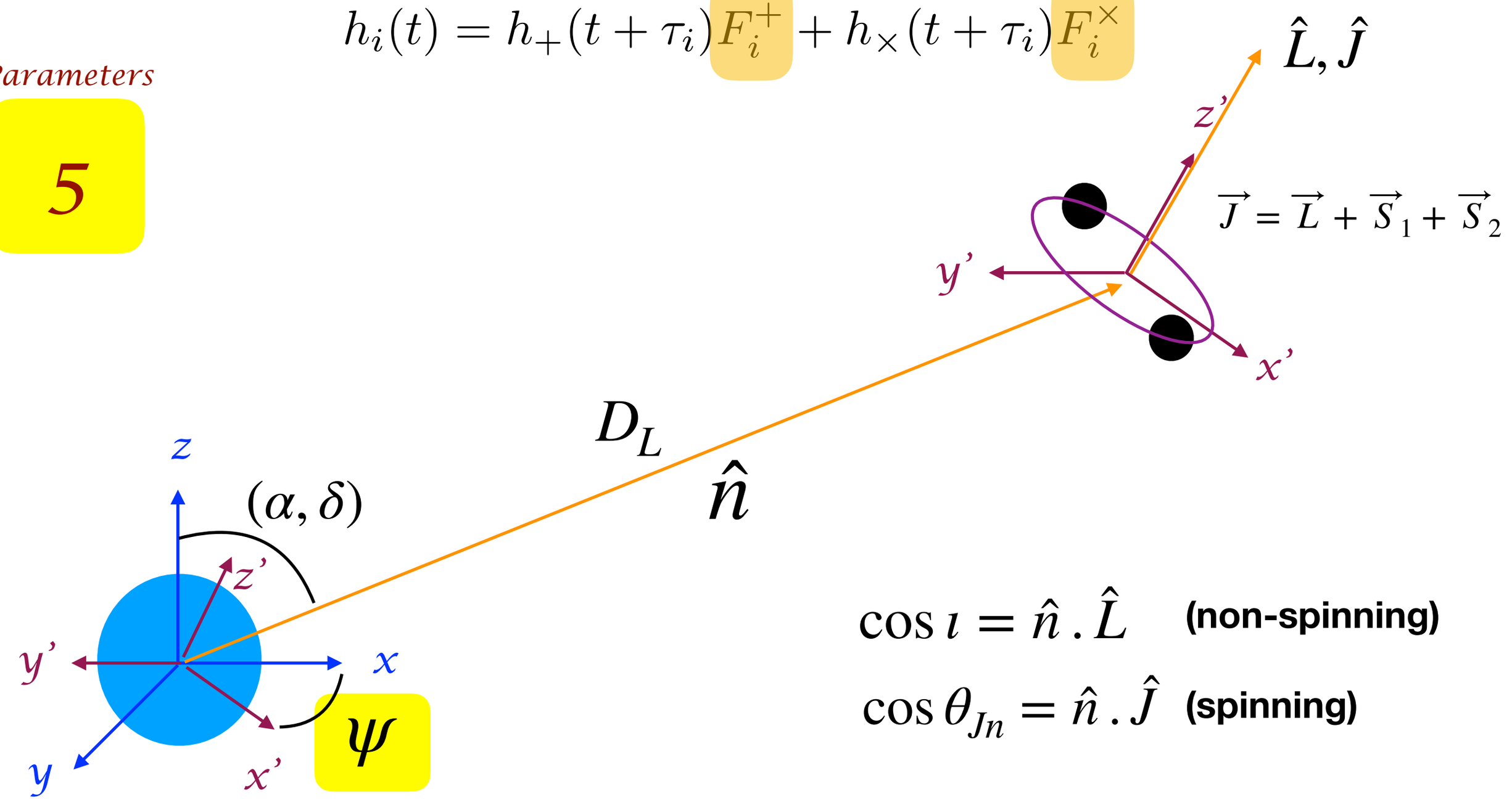

$$\cos\iota = \hat{n}\,.\,\hat{L} \quad \textbf{(non-spinning)}$$

$$\cos\theta_{Jn} = \hat{n}\,.\,\hat{J} \quad \textbf{(spinning)}$$

Reference Time and Phase

$$h_i(t) = h_+(t+\tau_i)F_i^+ + h_\times(t+\tau_i)F_i^\times$$

Parameters

7

(t_{ref}, ϕ_{ref})

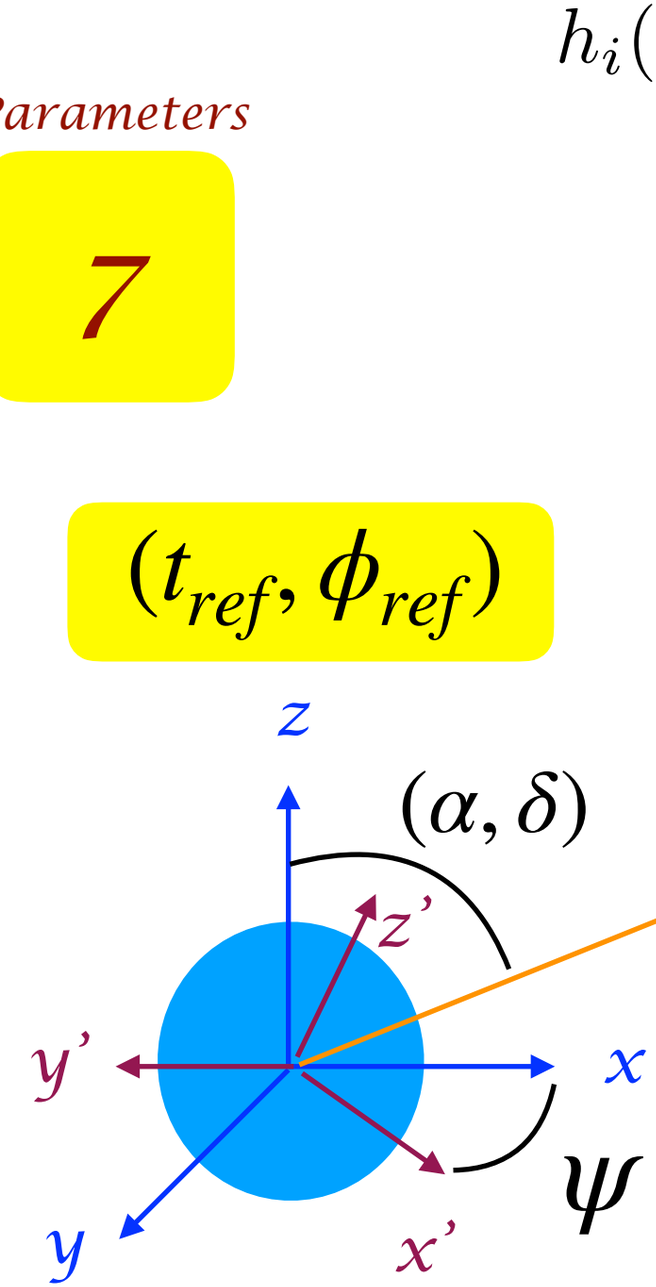

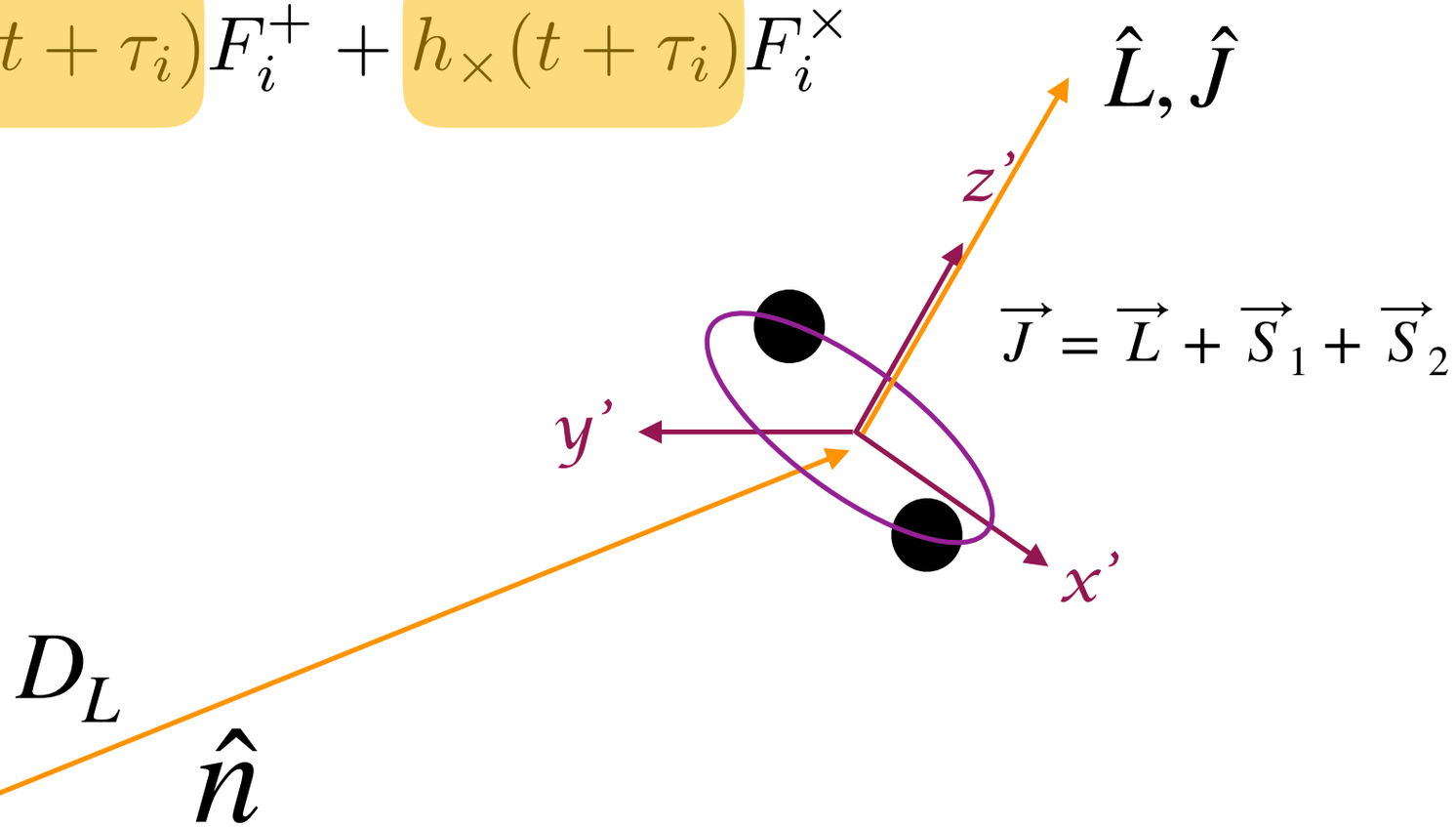

$$\cos\iota = \hat{n}\,.\,\hat{L} \quad \textbf{(non-spinning)}$$

$$\cos\theta_{Jn} = \hat{n}\,.\,\hat{J} \quad \textbf{(spinning)}$$

Intrinsic Parameters (Dynamical)

$$h_i(t) = h_+(t+\tau_i)F_i^+ + h_\times(t+\tau_i)F_i^\times$$

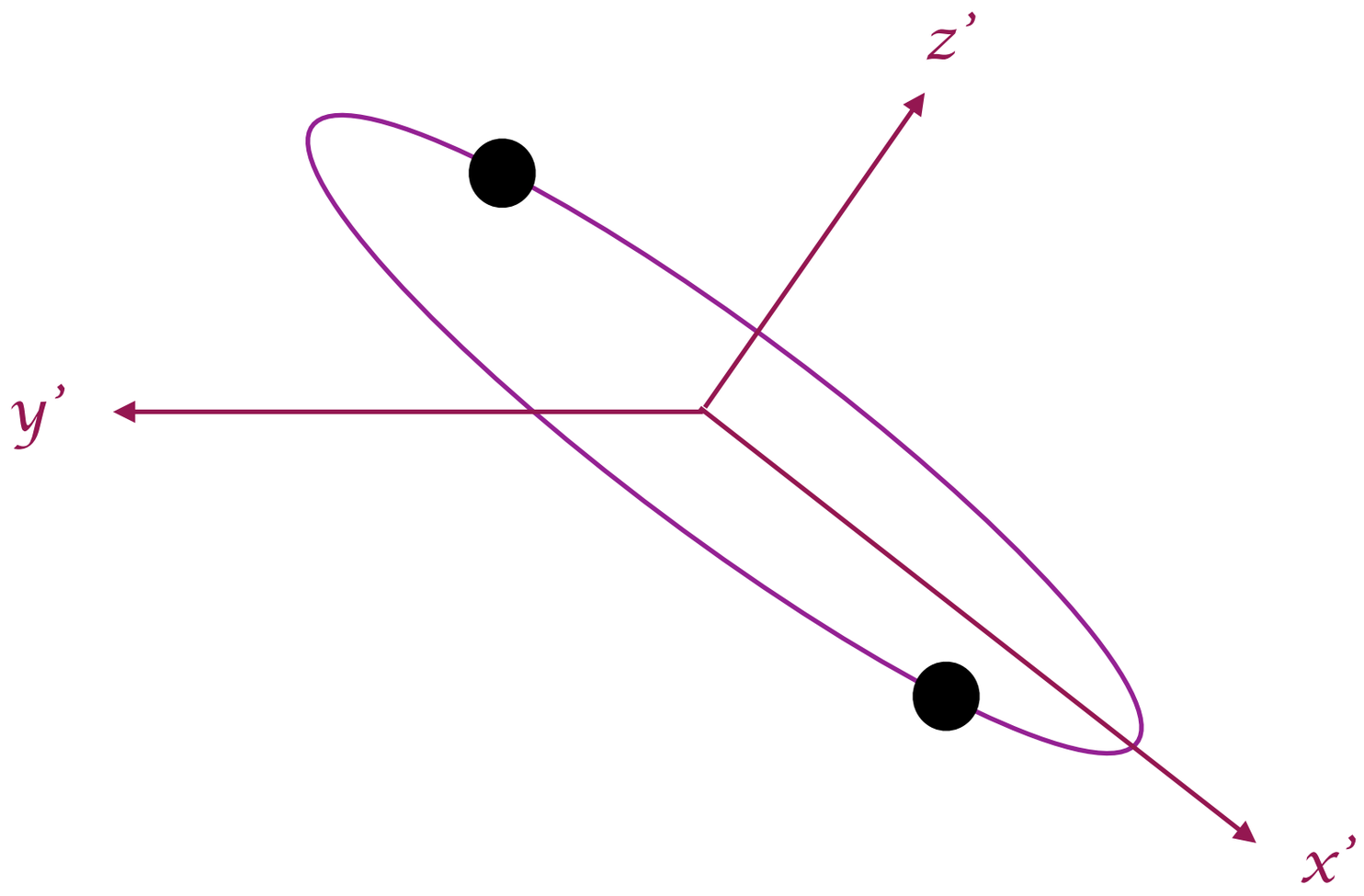

Intrinsic Parameters (Dynamical)

$$h_i(t) = h_+(t+\tau_i)F_i^+ + h_\times(t+\tau_i)F_i^\times$$

Parameters

9

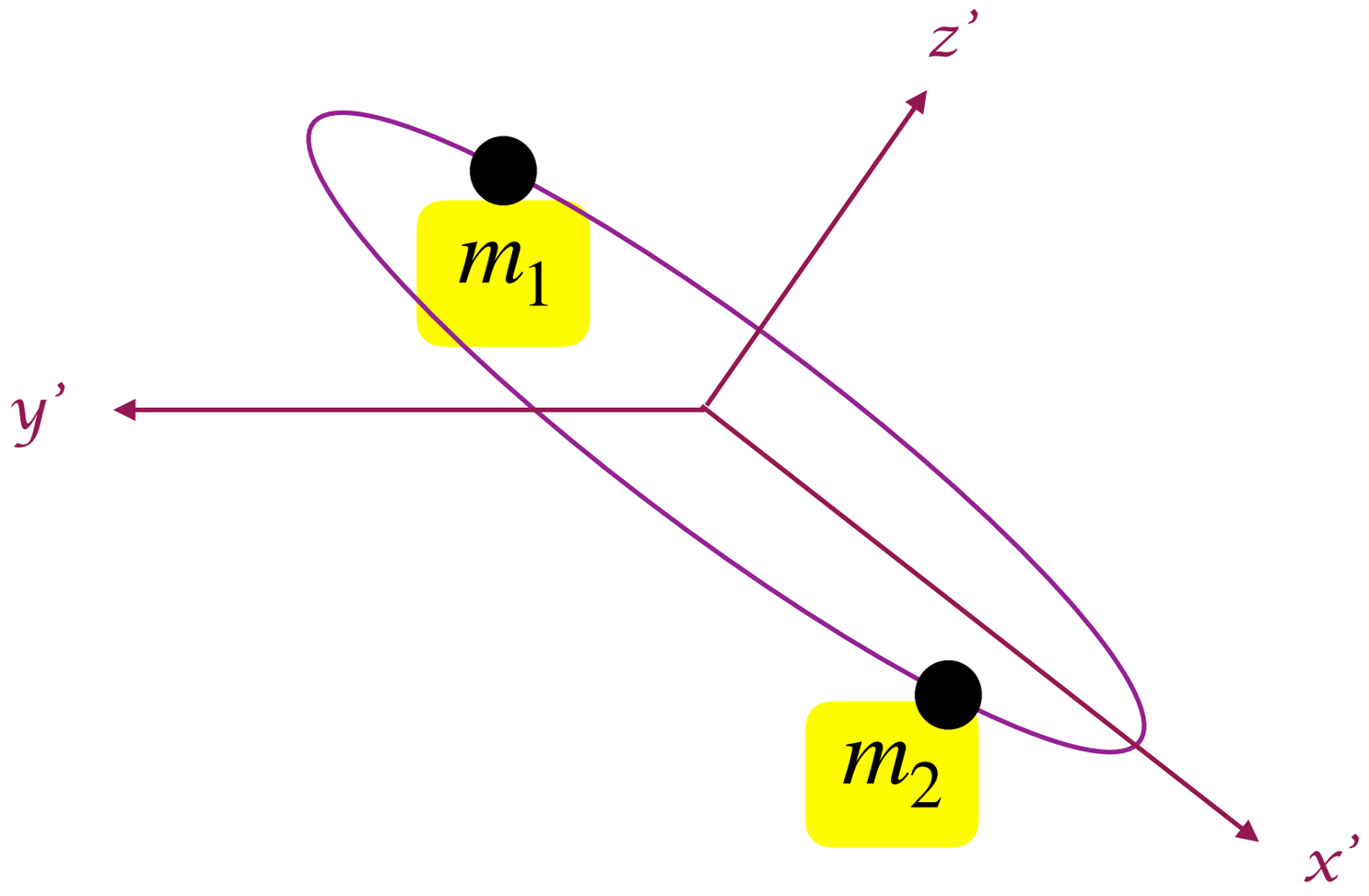

Intrinsic Parameters (Dynamical)

$$h_i(t) = h_+(t+\tau_i)F_i^+ + h_\times(t+\tau_i)F_i^\times$$

Parameters

9

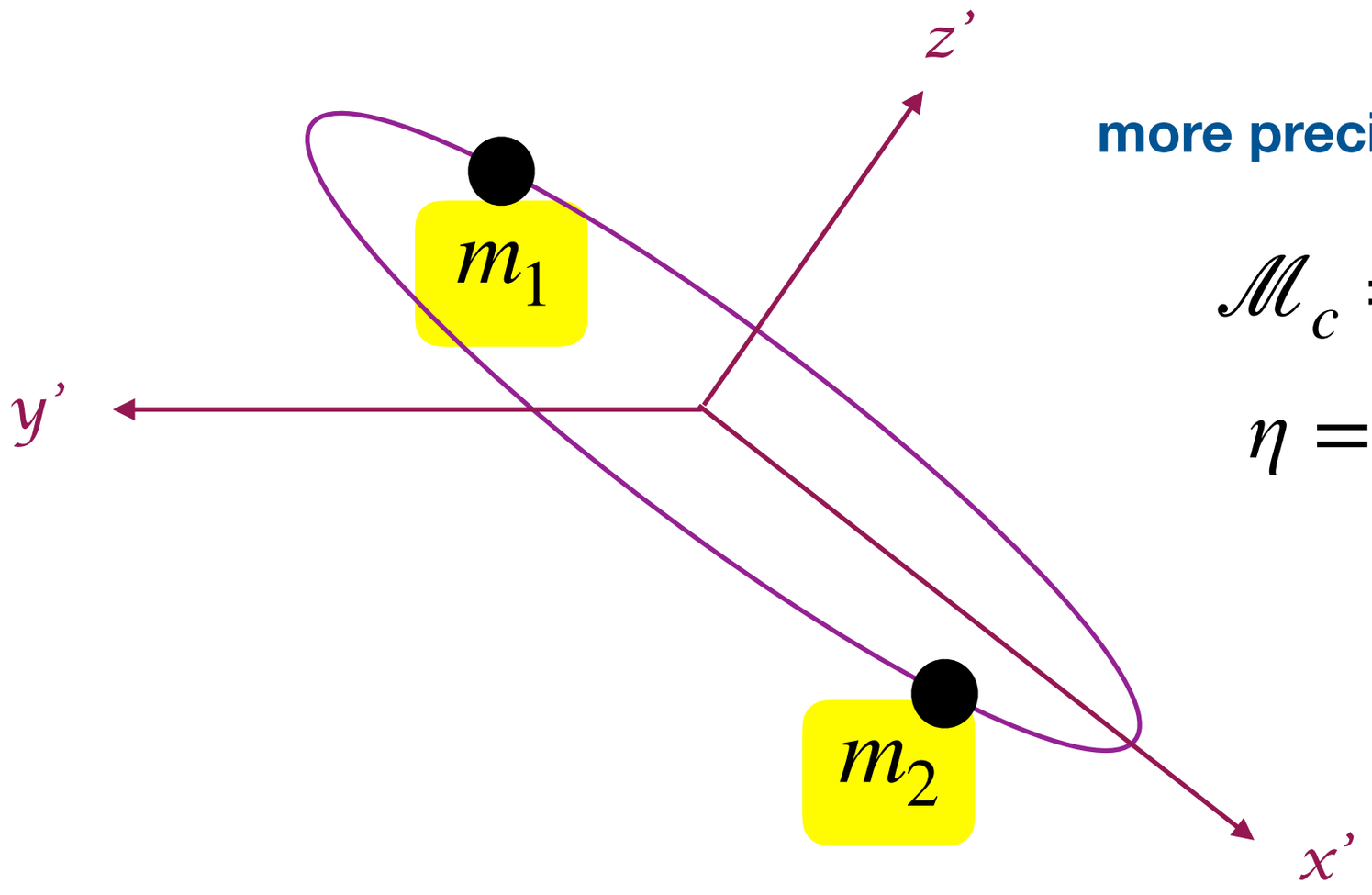

more precisely, we use

$$\mathscr{M}_c = m\eta^{3/5}$$

$$\eta = m_1 m_2 / m^2$$

Intrinsic Parameters (Dynamical)

$$h_i(t) = h_+(t+\tau_i)F_i^+ + h_\times(t+\tau_i)F_i^\times$$

Parameters

15

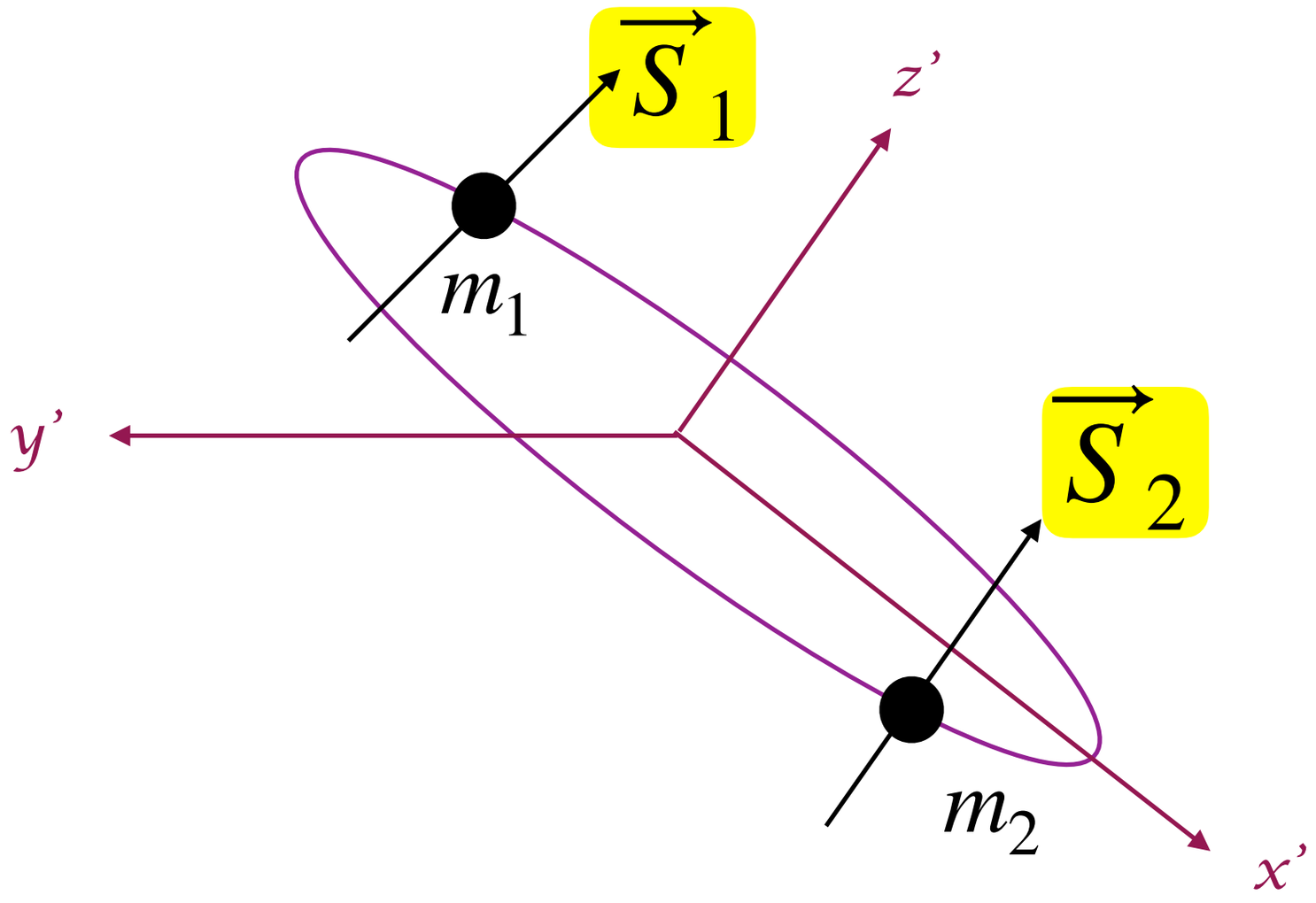

Intrinsic Parameters (Dynamical)

$$h_i(t) = h_+(t+\tau_i)F_i^+ + h_\times(t+\tau_i)F_i^\times$$

Parameters

17

For BNS systems

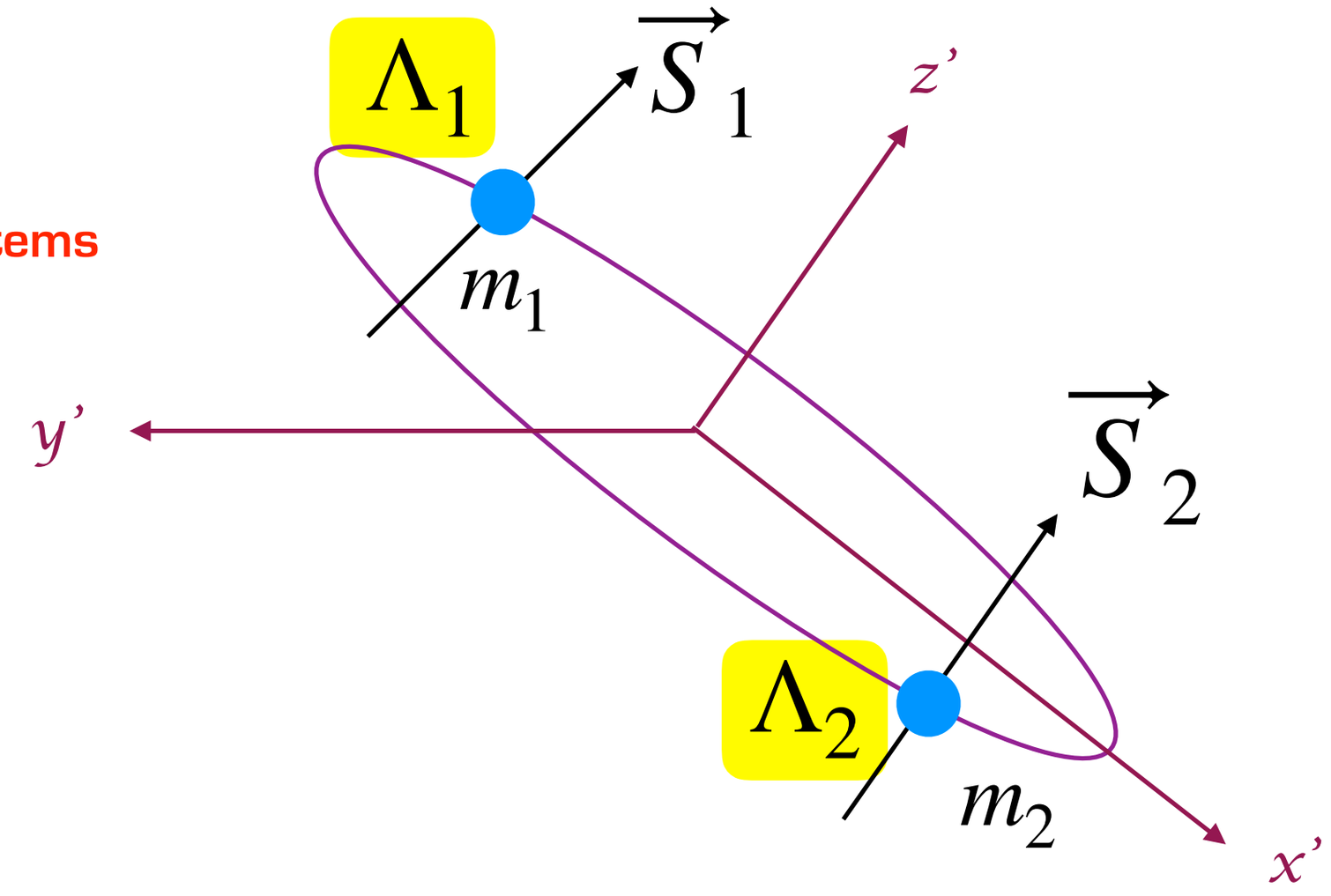

Modelling the Phase

- Remember, matched filtering needs phase coherence
- Newtonian mechanics : analytic solution to 2-body problem, no solution to the generic 3-body problem
- GR : no solution to the 2-body problem
- Modelling requires a combination of analytic and numerical relativity

Time-Domain Morphology of a CBC Signal

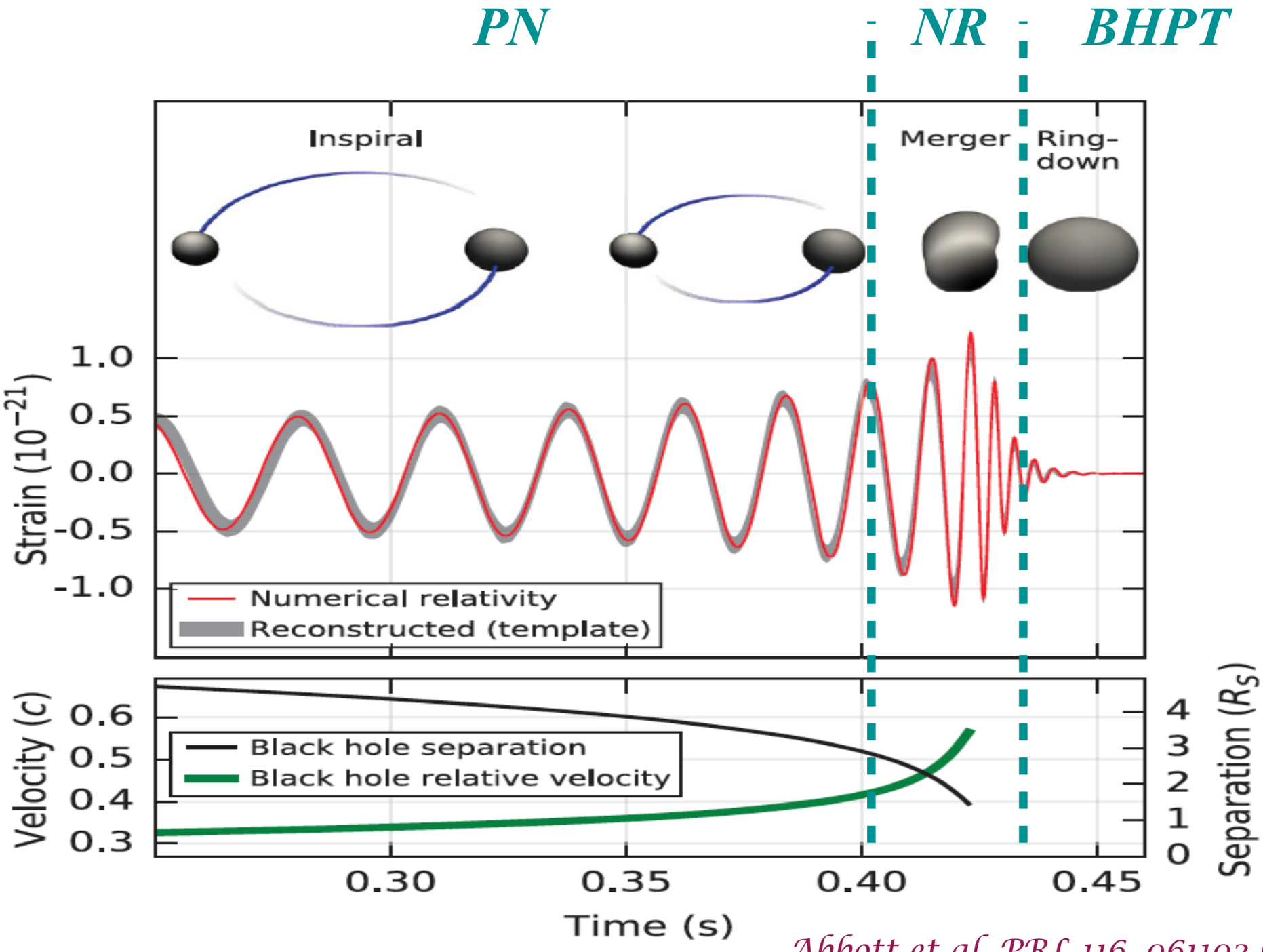

Abbott et al, PRL 116, 061102 (2016)

Inspiral

- Wide separation, i.e. $v_{orb} << c$
- To start we can write the TD polarisations as

$$h_+(t) = \frac{2(1+\cos^2(\iota))m\eta}{D_L}\cos\Phi(t) \;\;,\;\; h_\times(t) = -\frac{4\cos(\iota)m\eta}{D_L}\sin\Phi(t)$$

- where $\eta = m_1 m_2/m^2$, and $\Phi(t) \equiv \Phi_{GW}(t) = 2\Phi_{orb}(t)$
- We can then write the GW phase as a PN expansion

$$\Phi(t) = \phi_N(t) + \phi_2(t) + \phi_3(t) + \ldots.$$

- in terms of a small parameter $v = (\pi m f)^{1/3}$, where f is the GW frequency, and the sub-script corresponds to the power of (v/c) correction

Inspiral

- In the early inspiral, we can assume $\dot{f}_{orb}/f_{orb}^2 \ll 1$
- This allows us to use the energy balance equation $F(t) = -m\dfrac{dE(t)}{dt}$
- and calculate the phase evolution

$$\frac{d\phi}{dt} - \frac{v^3}{m} = 0 \qquad \Leftrightarrow \qquad t(v) = t_{ref} + m\int_v^{v_{ref}} dv\, \frac{E'(v)}{F(v)}$$

$$\frac{dv}{dt} + \frac{F(v)}{mE'(v)} = 0 \qquad \phi(v) = \phi_{ref} + \int_v^{v_{ref}} dv\, v^3 \frac{E'(v)}{F(v)}$$

Limits of the PN expansion

- Both $E'(v)$ and $F(v)$ have a PN (power) series solution
- How we treat the ratio $E'(v)/F(v)$ leads to different PN families
- Each PN series is asymptotically divergent, meaning…
  - …different families have differing levels of accuracy,
  - …a higher approximation does not guarantee higher accuracy,
  - …the PN approximation should break down at the LSO $(\sim R=6M)$
  - …but in fact, breaks down much sooner $(R\sim 12M)$

Late Inspiral / Merger

- Both the late inspiral and merger need to solved numerically
- A relatively small number of cycles can take months to generate on a supercomputer

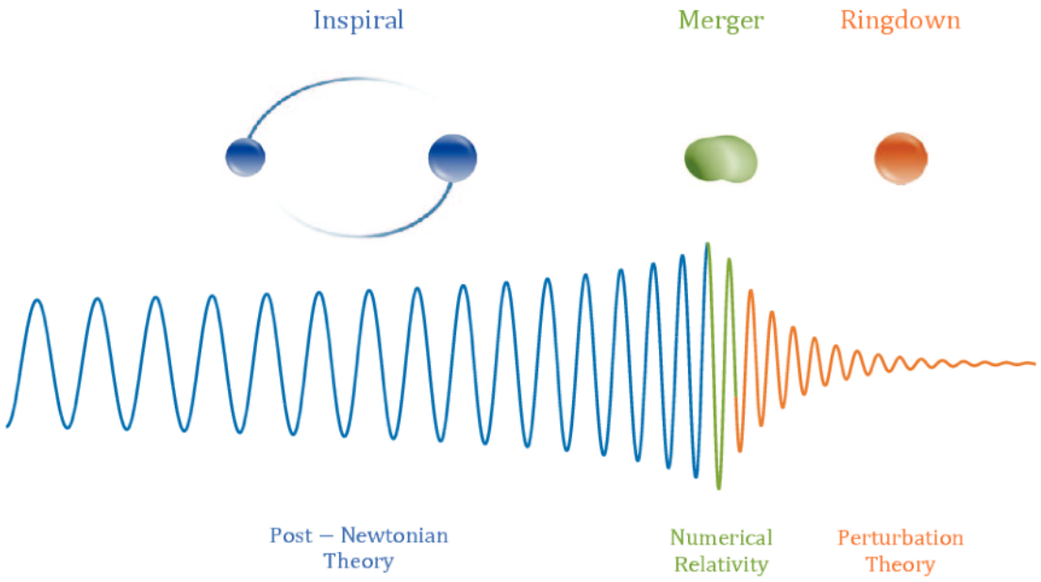

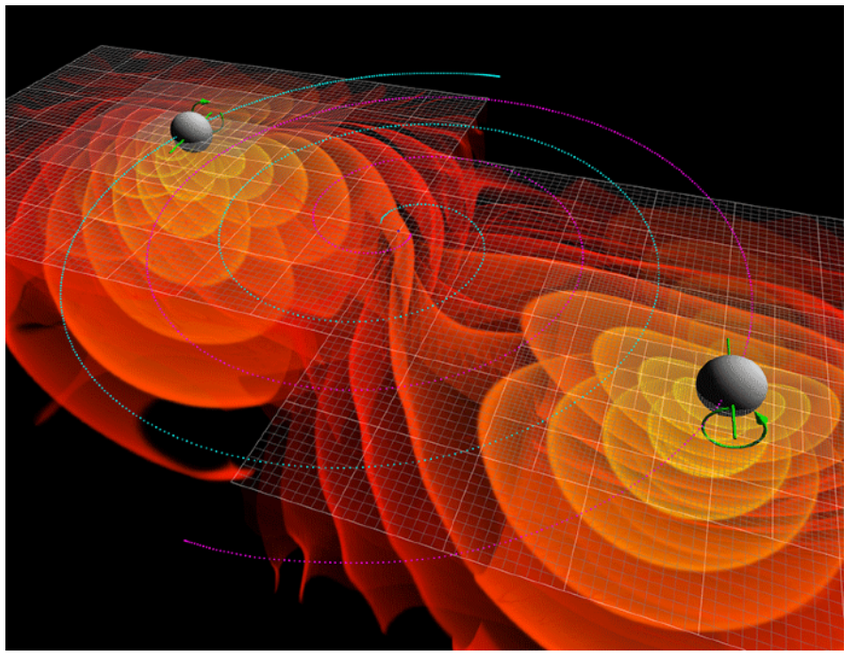

Late Inspiral / Merger

- NR becomes even more important as we try and simulate BNS and NSBH systems

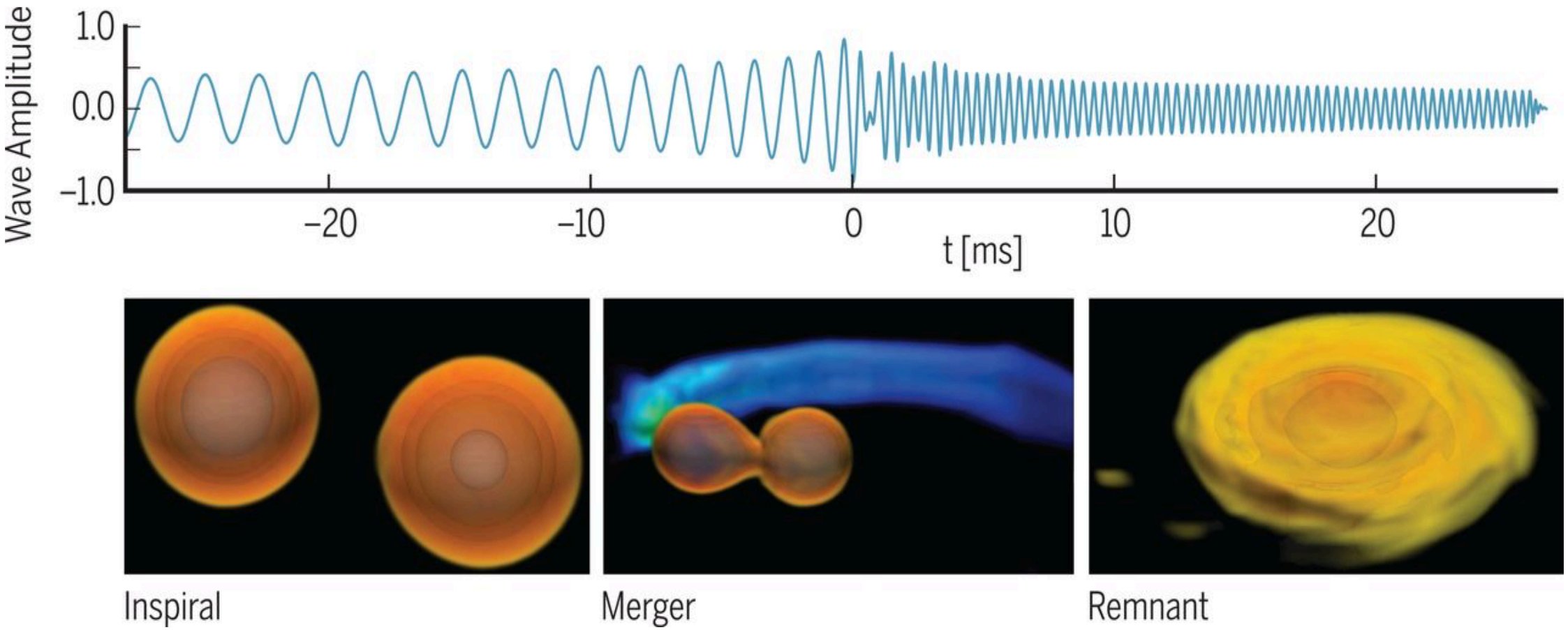

B. Brugmann, Science 361, 336 (2018)

Ringdown

- The final black hole rings like a bell that's been struck
- An analytic solution exists using black hole perturbation theory
- The energy is radiated in a series of quasi-normal modes
- These modes can be used to test the no-hair theorem
- No evidence of the QNMs as of yet

Hybrid Waveforms

- NR waveforms are expensive to generate and use
- For efficient data analysis, we use approximate analytical solutions
  - PN - Inspiral only
  - EOB - solves Hamilton's equations along the trajectory. Calibrated using NR waveforms
  - IMRPhenom - frequency domain analytic waveform, also calibrated using NR waveforms
- As we don't know if our waveforms are perfectly accurate, different families allow us to keep systematics under control
- New waveform families include eccentricity, tidal forces, precession etc.

Treating the Data

- Easiest to work in Fourier domain
- e.g. Sine-wave with f=50 Hz buried in random Gaussian noise

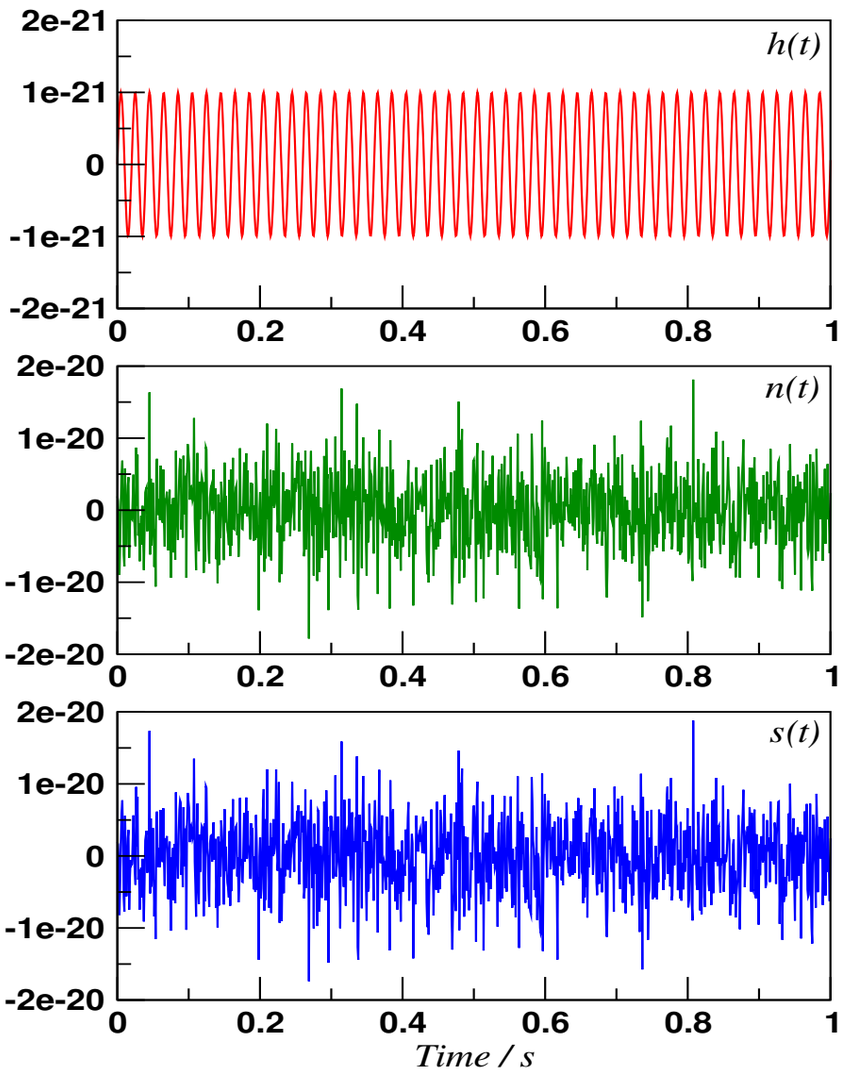

Signal Only

Noise Only

Signal + Noise

Treating the Data

- Easiest to work in Fourier domain
- e.g. Sine-wave with f=50 Hz buried in random Gaussian noise

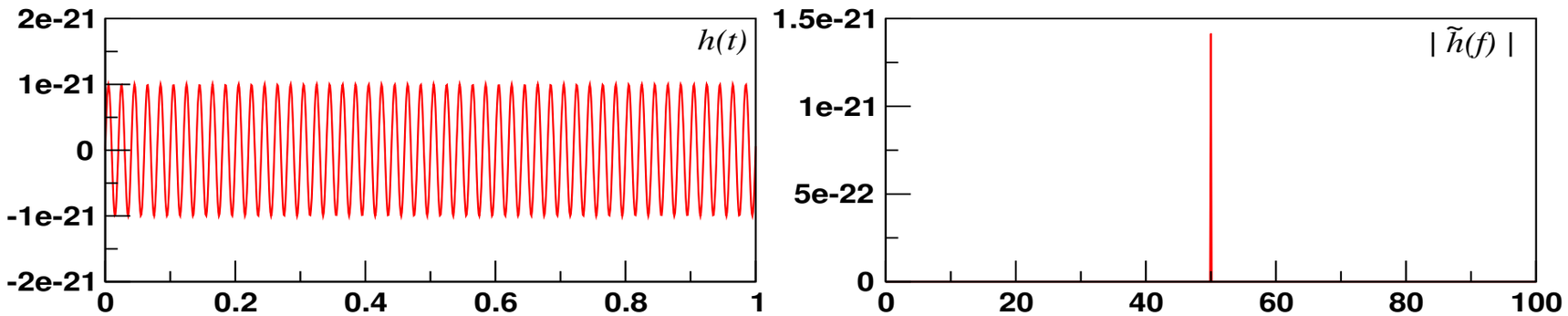

Signal Only

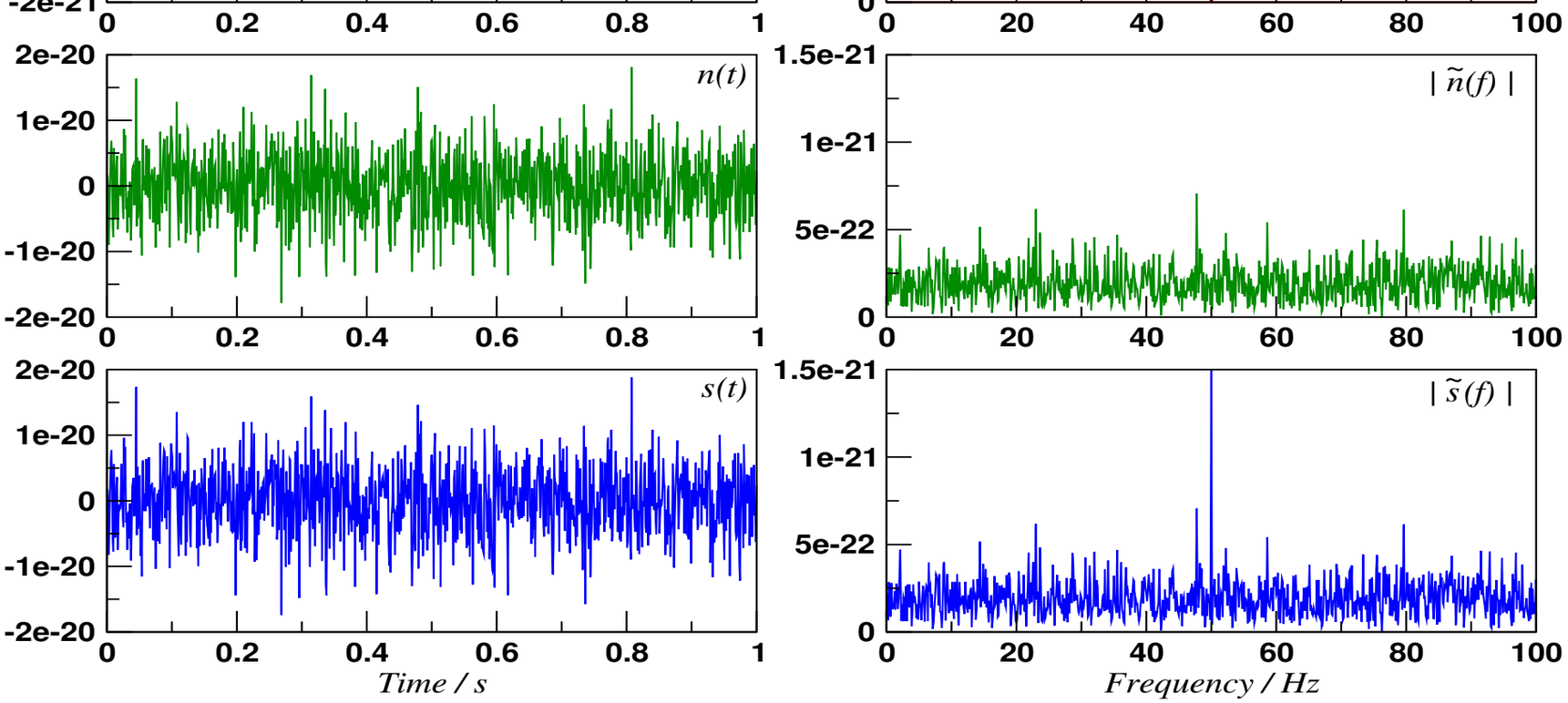

Noise Only

Signal + Noise

Fourier Domain Waveforms

- Stationary phase approximation
- Start with a generalised Fourier integral $I = \int F(\omega)\, e^{i\,\varphi(\omega)}\, d\omega$

- Assume $F(\omega)$ varies slowly compared to $\varphi(\omega)$ .As the phase rapidly varies, the integral averages to zero except where $\varphi(\omega)$ has an extremum

- So find points where $d\varphi/d\omega = 0$ and Taylor expand the phase

$$\varphi(\omega) = \varphi(\omega_{sp}) + \frac{1}{2}\varphi''(\omega - \omega_{sp})^2 + \ldots$$

- Evaluate the integral in the vicinity of extrema, and sum if more than one saddle point

$$I = F(\omega_{sp})\, e^{i\,\varphi(\omega_{sp})} \int e^{\frac{i}{2}\,\varphi(\omega-\omega_{sp})^2}\, d\omega$$

- Fresnel type integral with standard solution, leading to

$$\tilde{h}\left(f\right) = A\, f^{-7/6} e^{i\,\varphi\left(f\right)}$$

Frequency Domain CBC Waveform Morphology

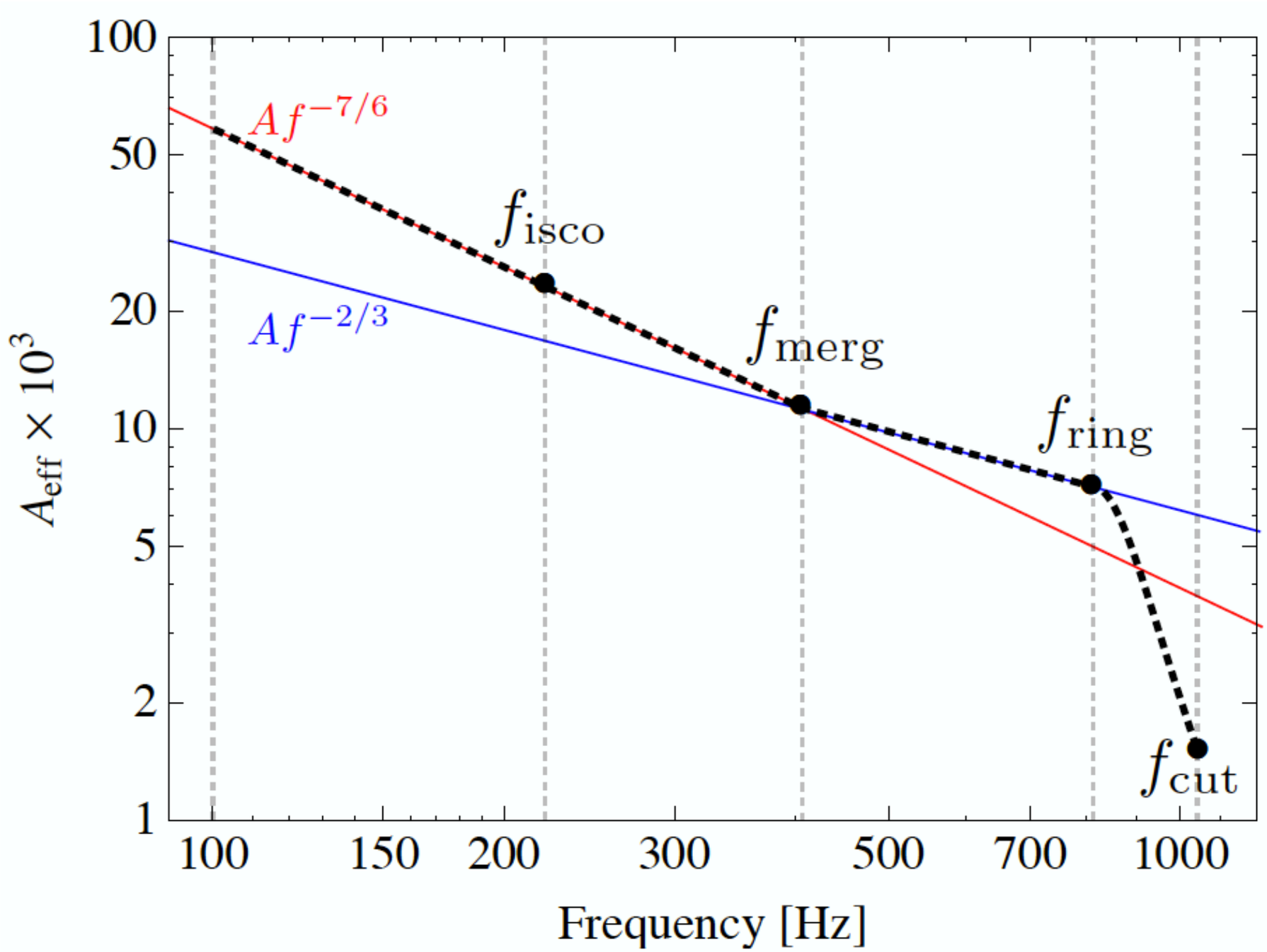

Waveform Comparisons

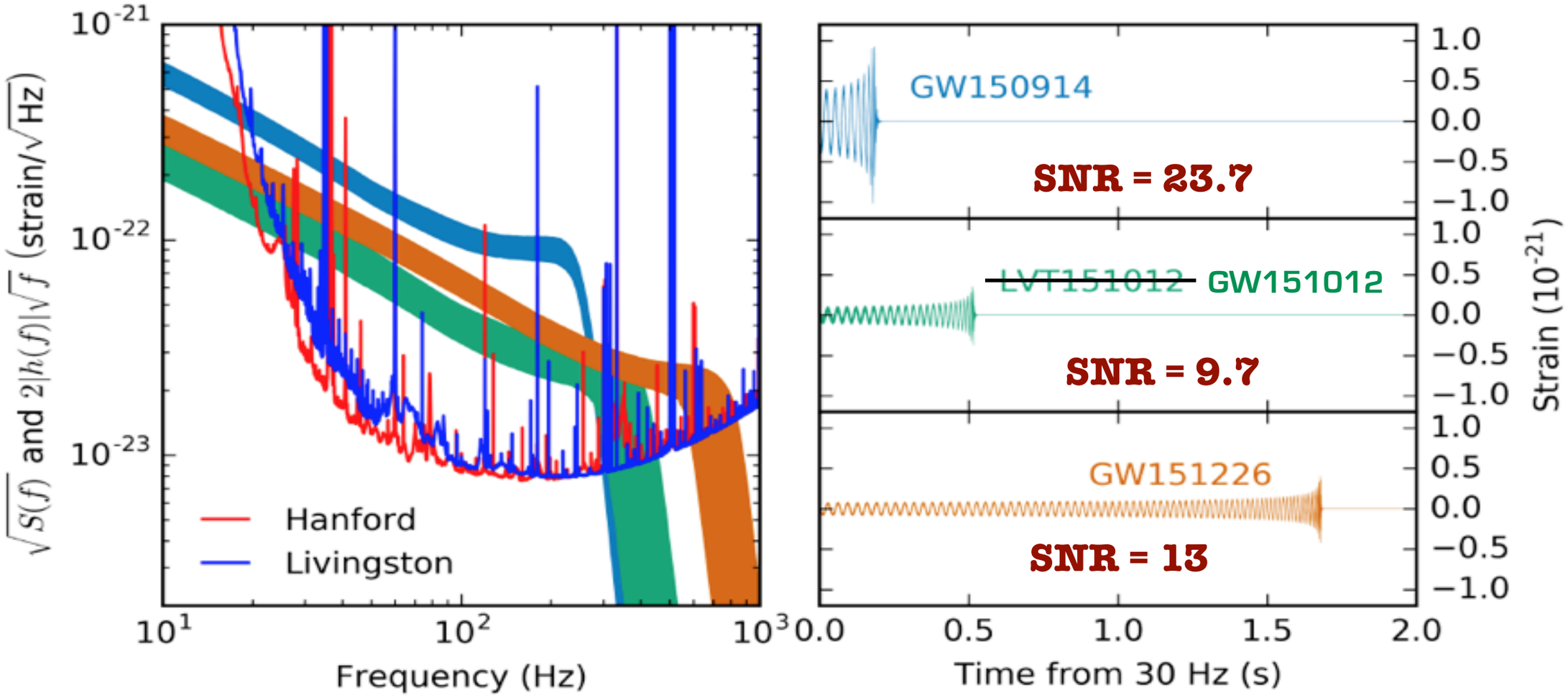

- Maximum frequency inversely proportional to total mass
- Most of the SNR comes from the merger - ringdown

Abbott et al, PRX 6, 041015 (2016)

Sampling the data

- Our analysis is best represented in the Fourier domain
- So given a continuous signal $h(t)$, the FT is $\tilde{h}(f) = \int_{-\infty}^{\infty} dt\, h(t) e^{-2\pi i f t}$
- However, we need a digital representation, i.e. $h(t) \Rightarrow h_j = h(t_j)$
- Given a sampling frequency f_s, we define $\Delta t = 1/f_s$
- With time domain data of N samples, total observation time $T_{obs} = N\,\Delta t$, the discrete FT is given by
- $\tilde{h}_k = \sum_{j=0}^{N-1} h_j e^{-2\pi i j k/N}$ where each sample has a frequency $f_k = k / T_{obs}$
- But how do we choose f_s ?

Sampling the data

- Nyquist theorem prescribes how to digitally represent a continuous signal
- It defines a critical or Nyquist frequency taken to be the highest frequency content of the signal
- Define:
  - Nyquist frequency - $f_{Nyq} \equiv f_{max}$
  - Sampling frequency - $f_s \geq 2f_{Nyq}$
  - Sampling period - $\Delta t = 1/f_s$
- Sampling at less than twice the Nyquist frequency leads to “aliasing”
- For GWs, if the sampling frequency is $f_s = 4096\ Hz$, the highest frequency signal we can model is $f_{max} = 2048\ Hz$

Sampling the data

- Example : sine-wave with $f = 10\ Hz$, $T_{obs} = 1\ sec$, $dt = 1/f_s$

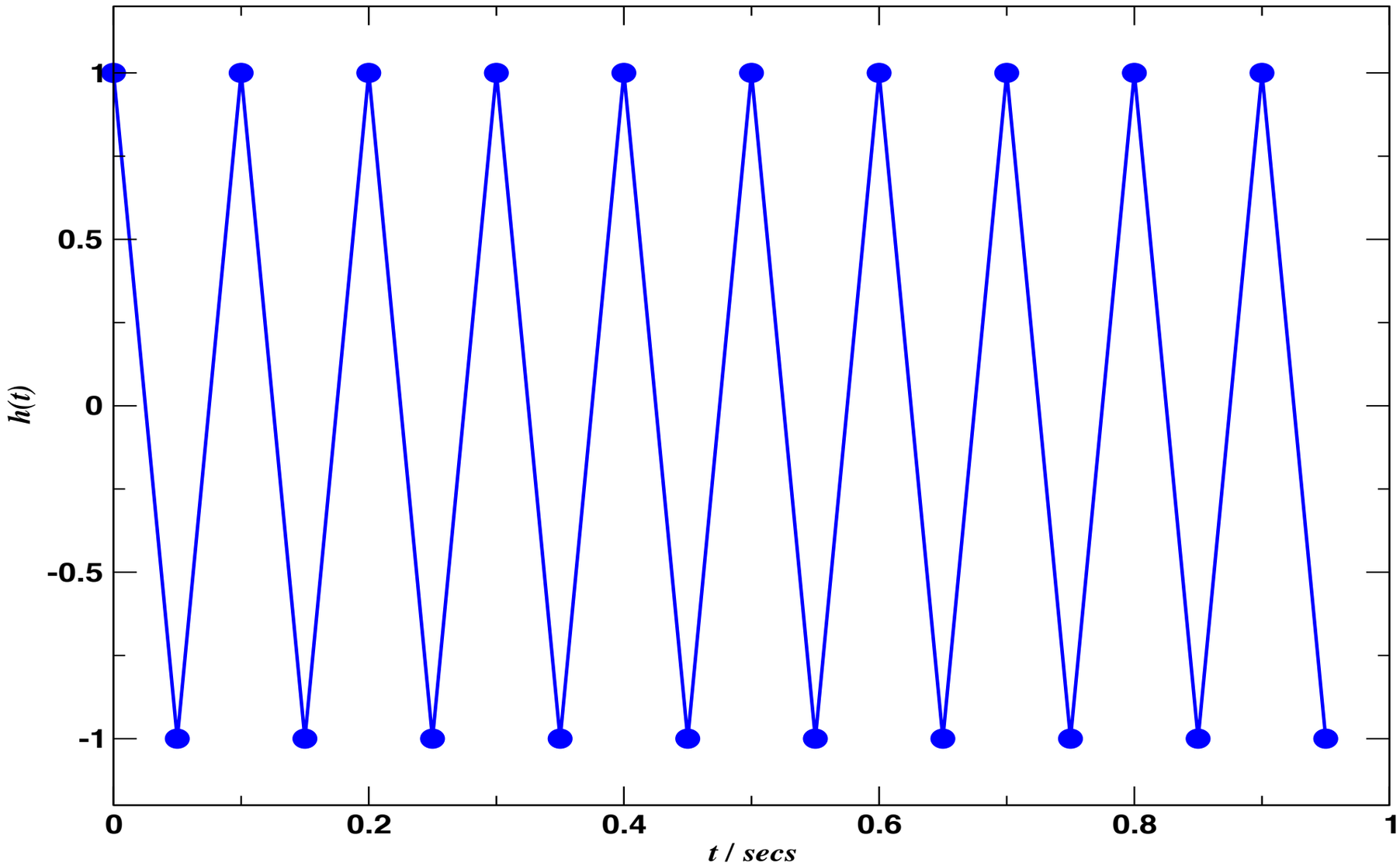

$$f_s = 2f_{Nyq}$$

Sampling the data

- If I oversample…?

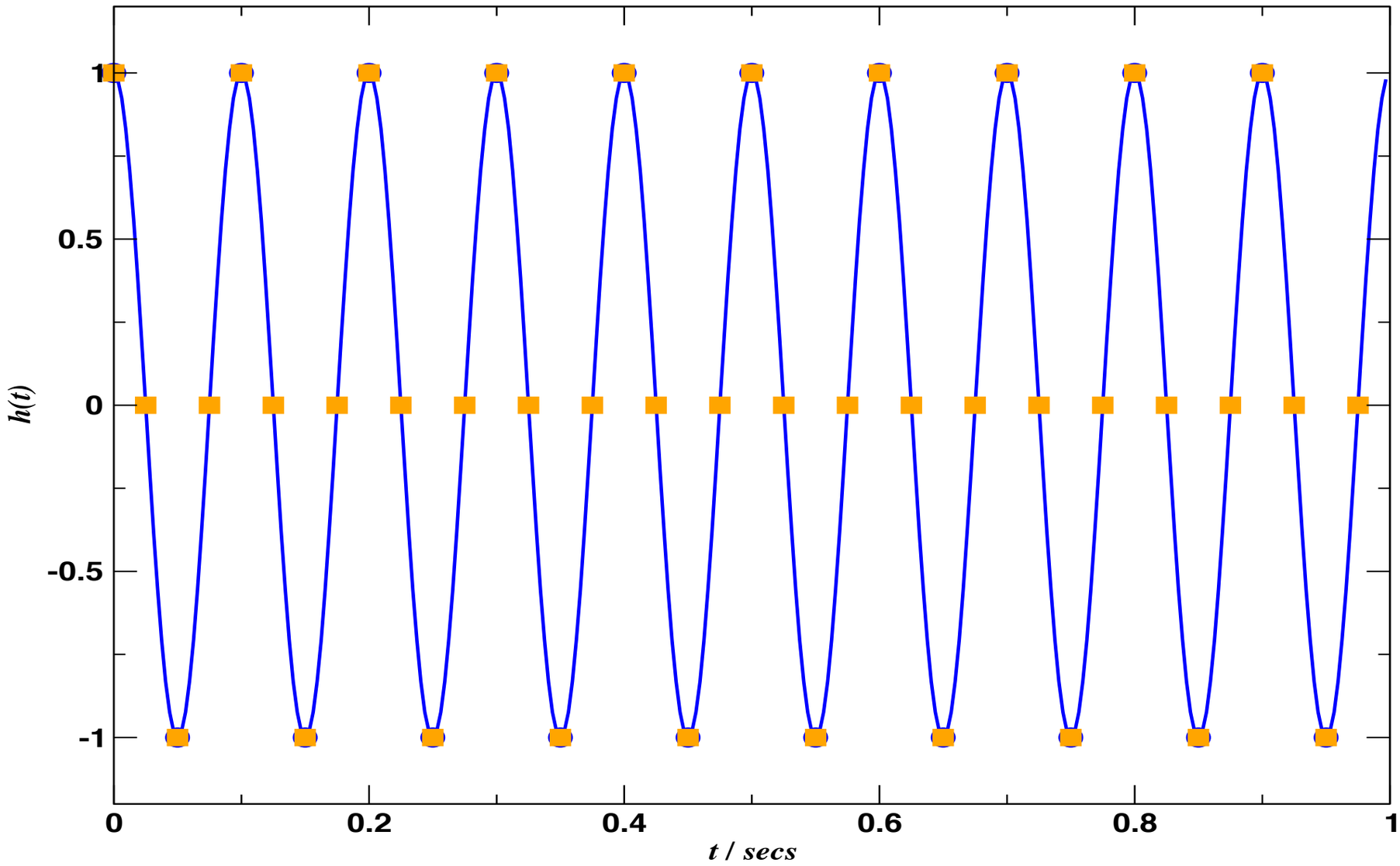

$$f_s = 4f_{Nyq}$$

Sampling the data

- and if I undersample…?

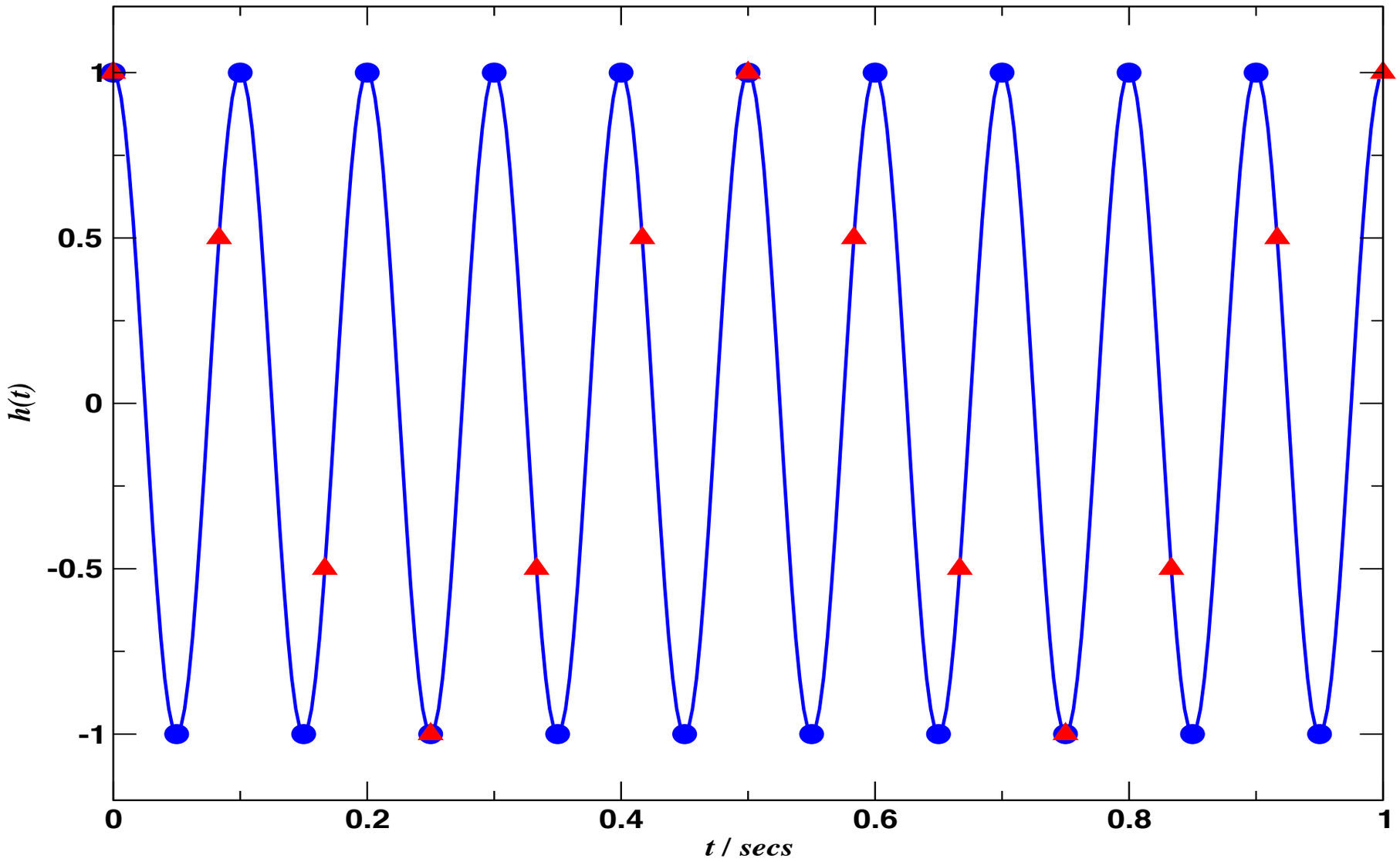

$f_s = 1.2 f_{Nyq}$

Sampling the data

- I get aliasing!!

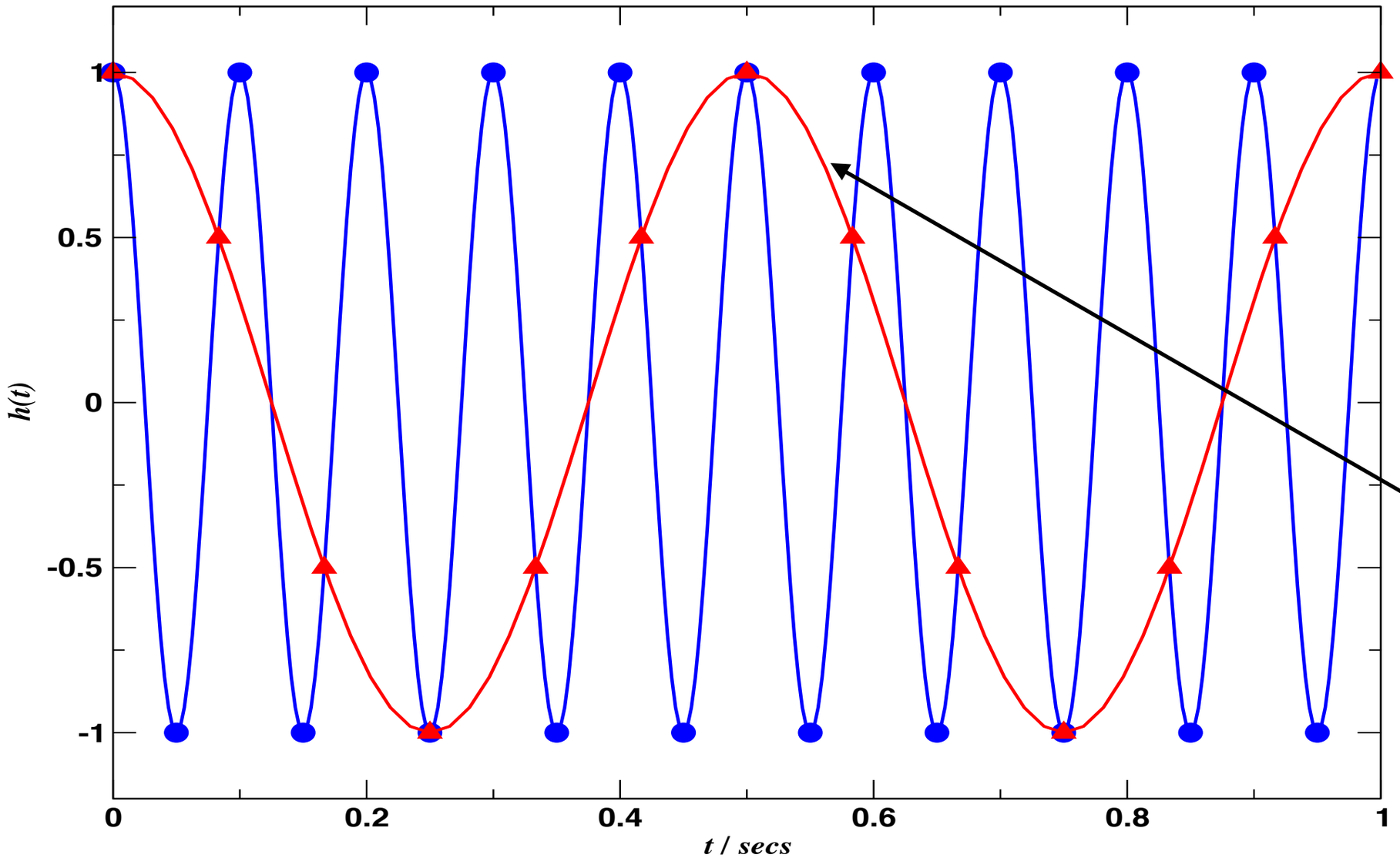

$$f_s = 1.2 f_{Nyq}$$

Corresponds to a wave at 2 Hz

Low and High-band pass filtering

- Detectors very noisy below 20Hz and above 2kHz
- High pass filter > 20Hz
- Low pass filter < 2kHz

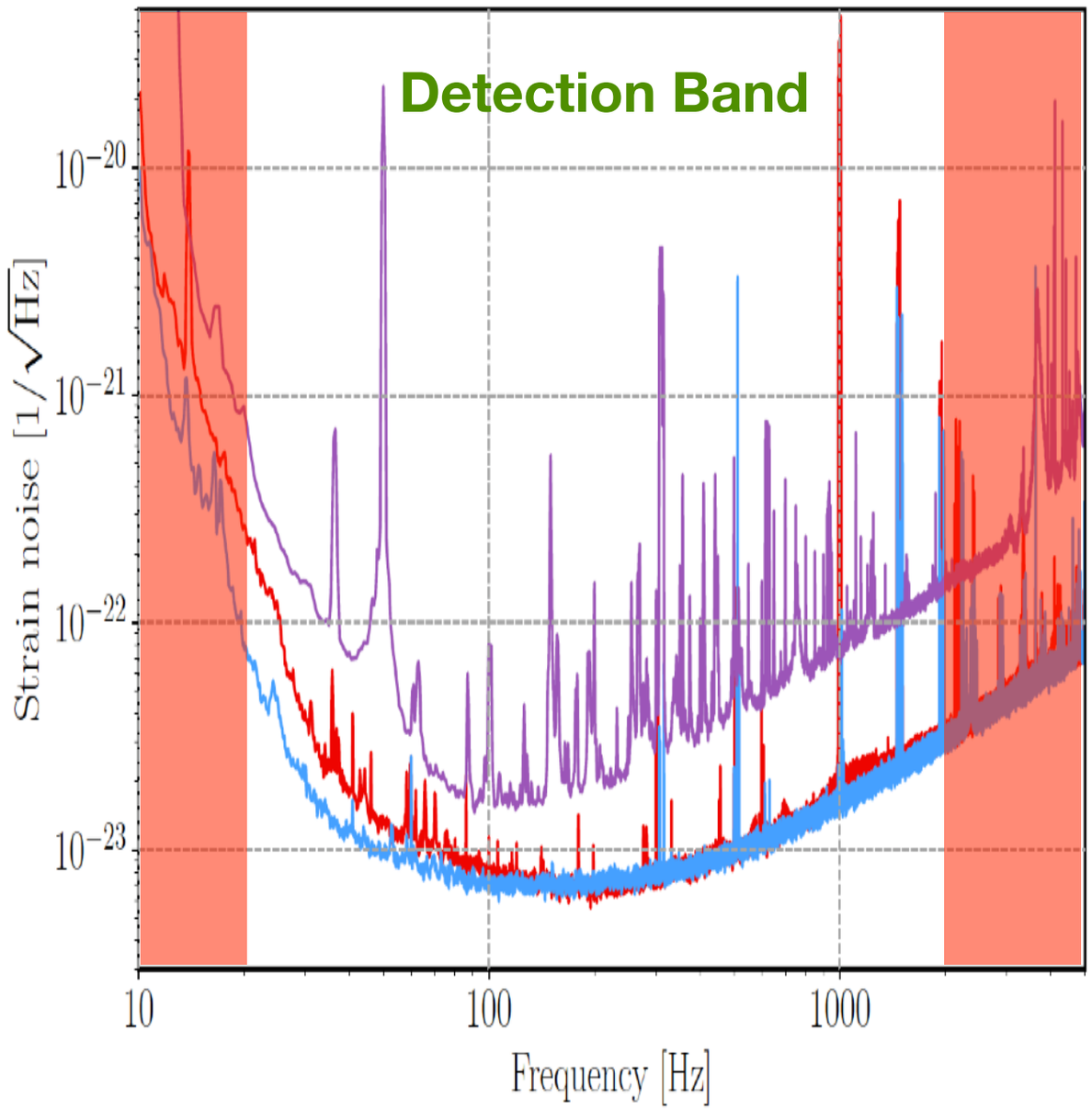

Windowing the data

“Newtonian” inspiral chirp for a (10,10) solar mass system

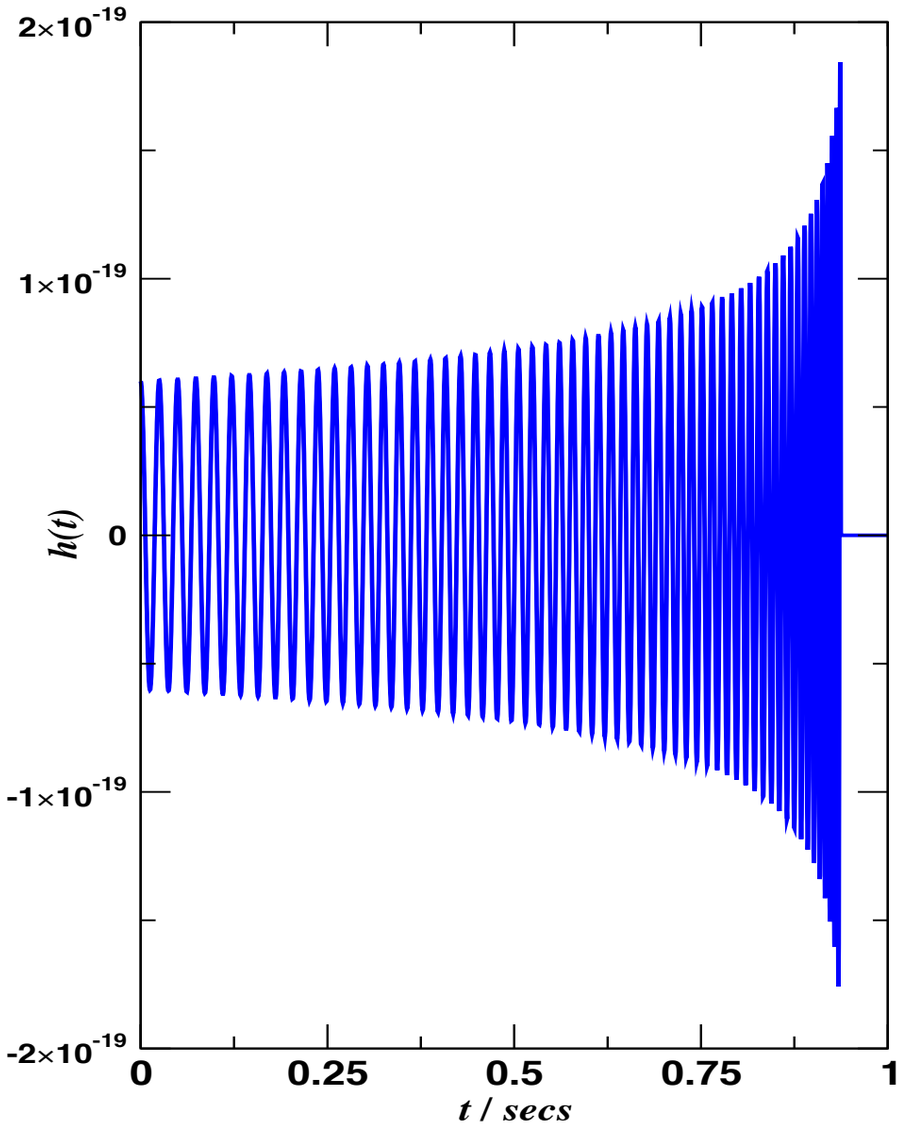

Windowing the data

large oscillations, spectral leakage…what's going on?

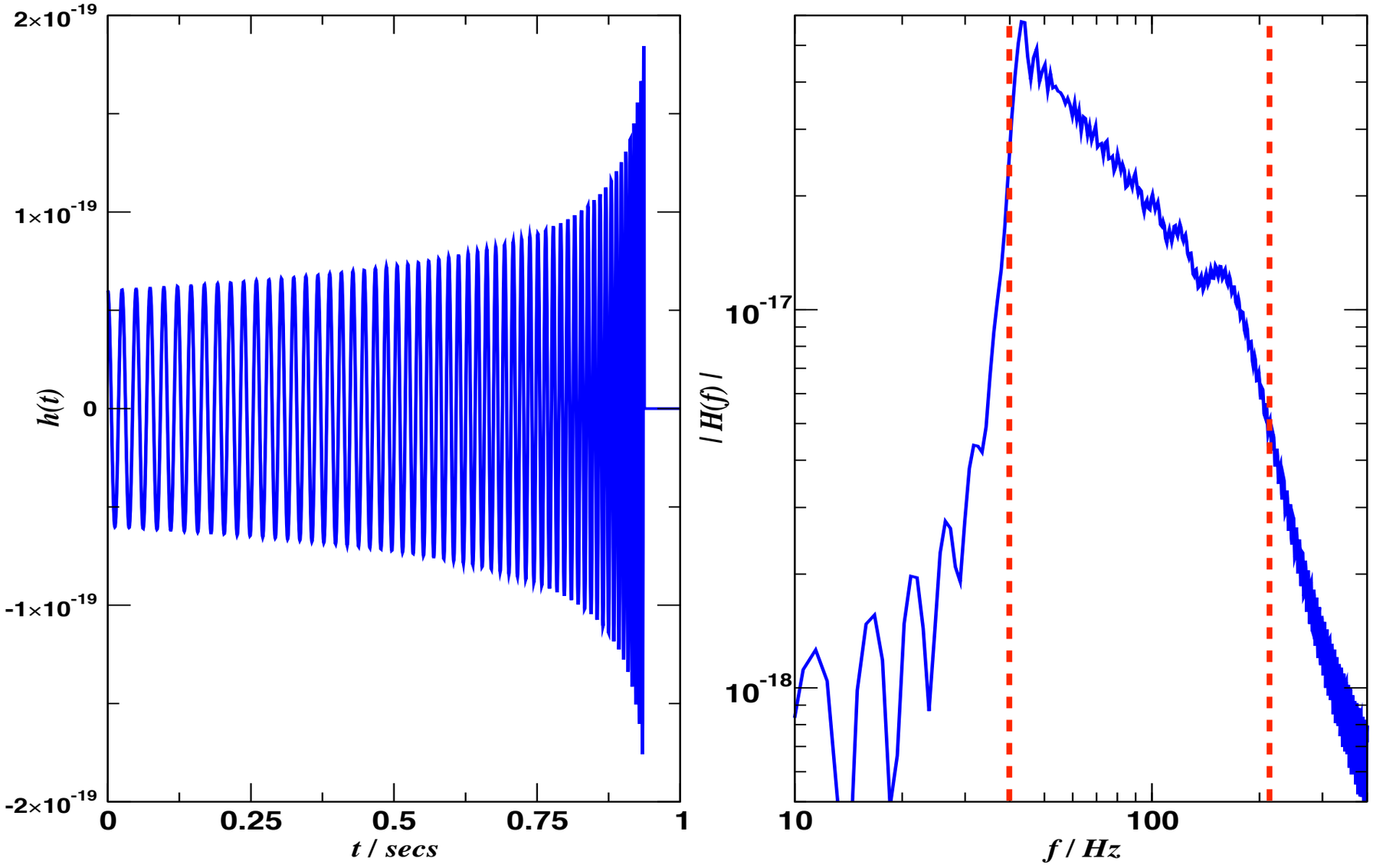

Windowing the data

- Our signal starts abruptly at t = 0, and finishes abruptly at t = 0.973 secs
- Equivalent to multiplying the signal with a rectangular window function
- and.....?

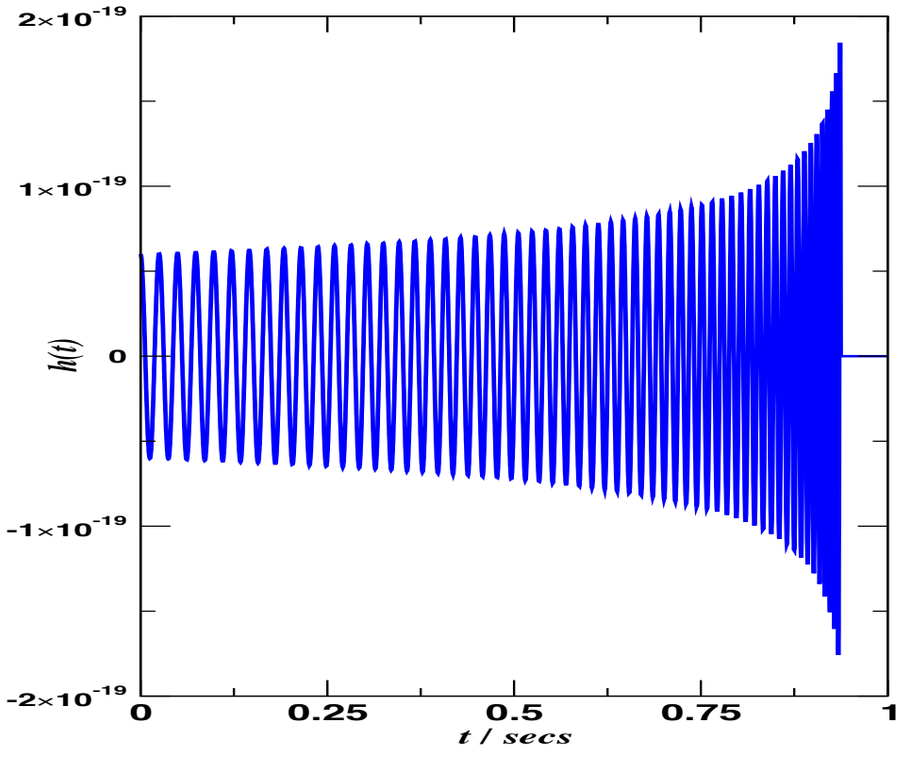

*

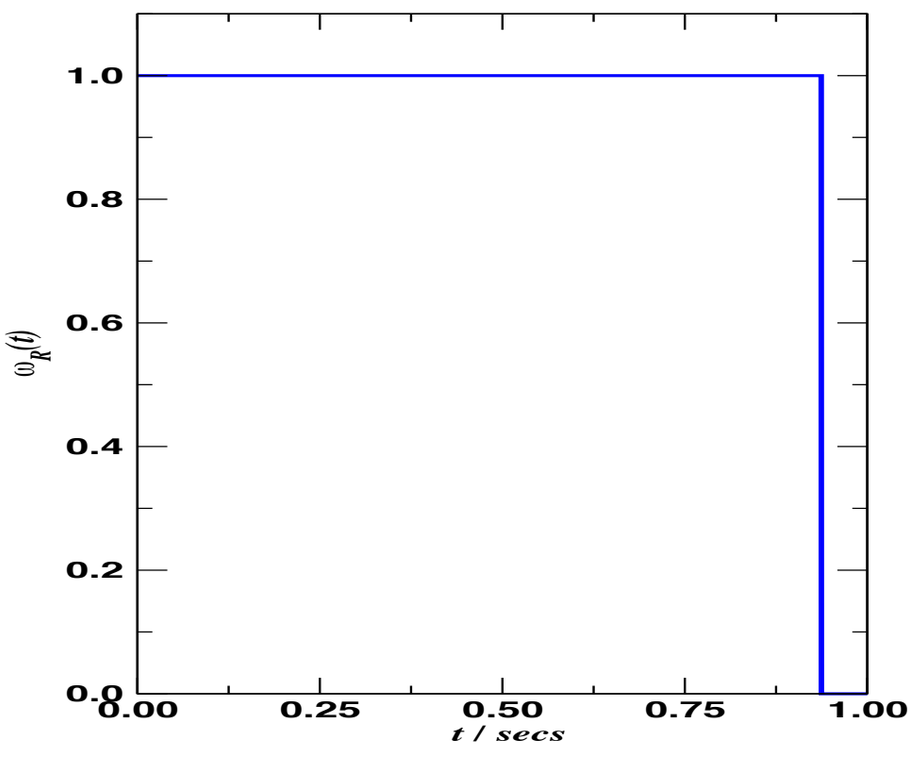

Windowing the data

FT of a rectangular window function

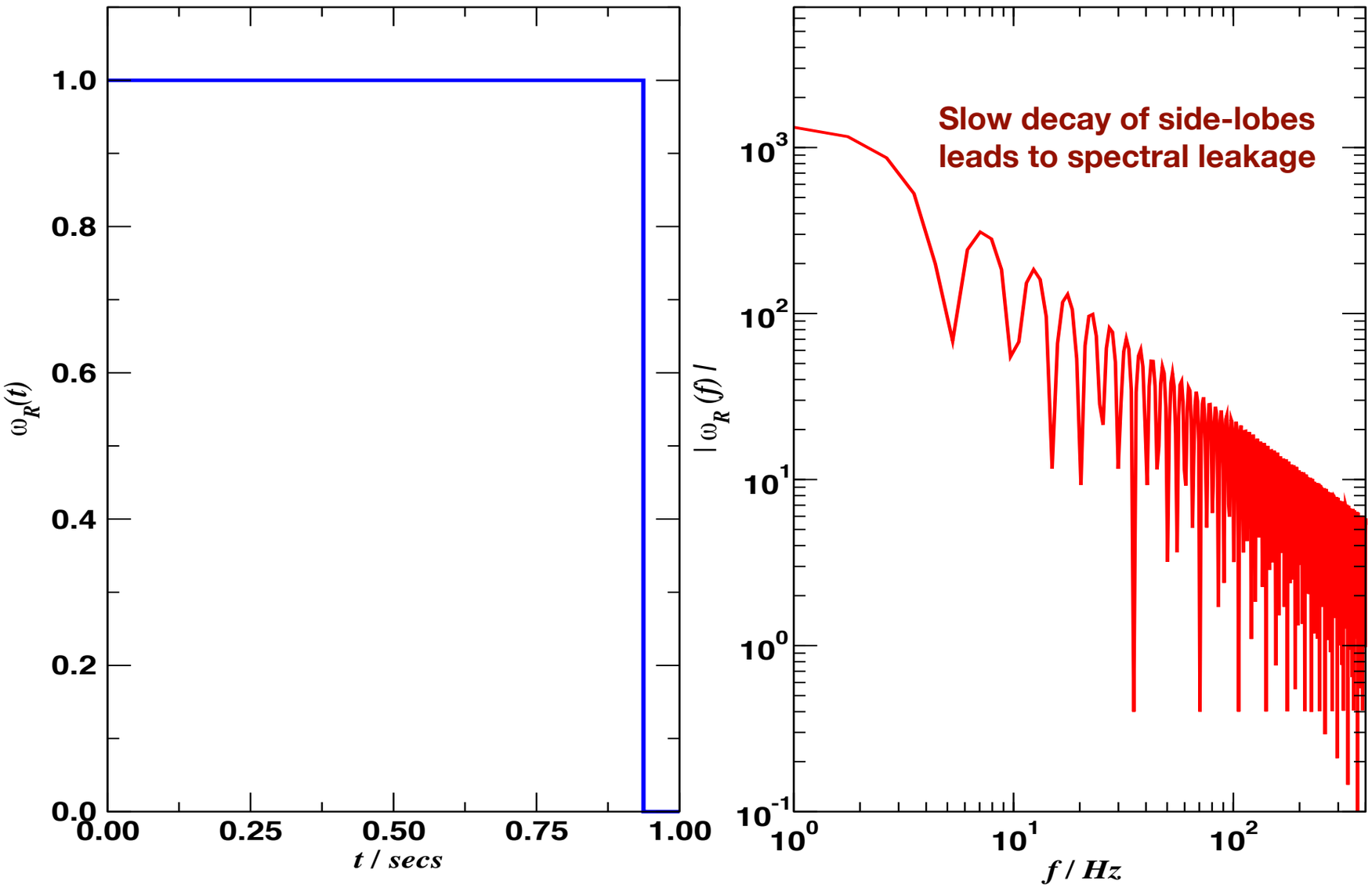

Windowing the data

FT of a 1/2-Hann window function

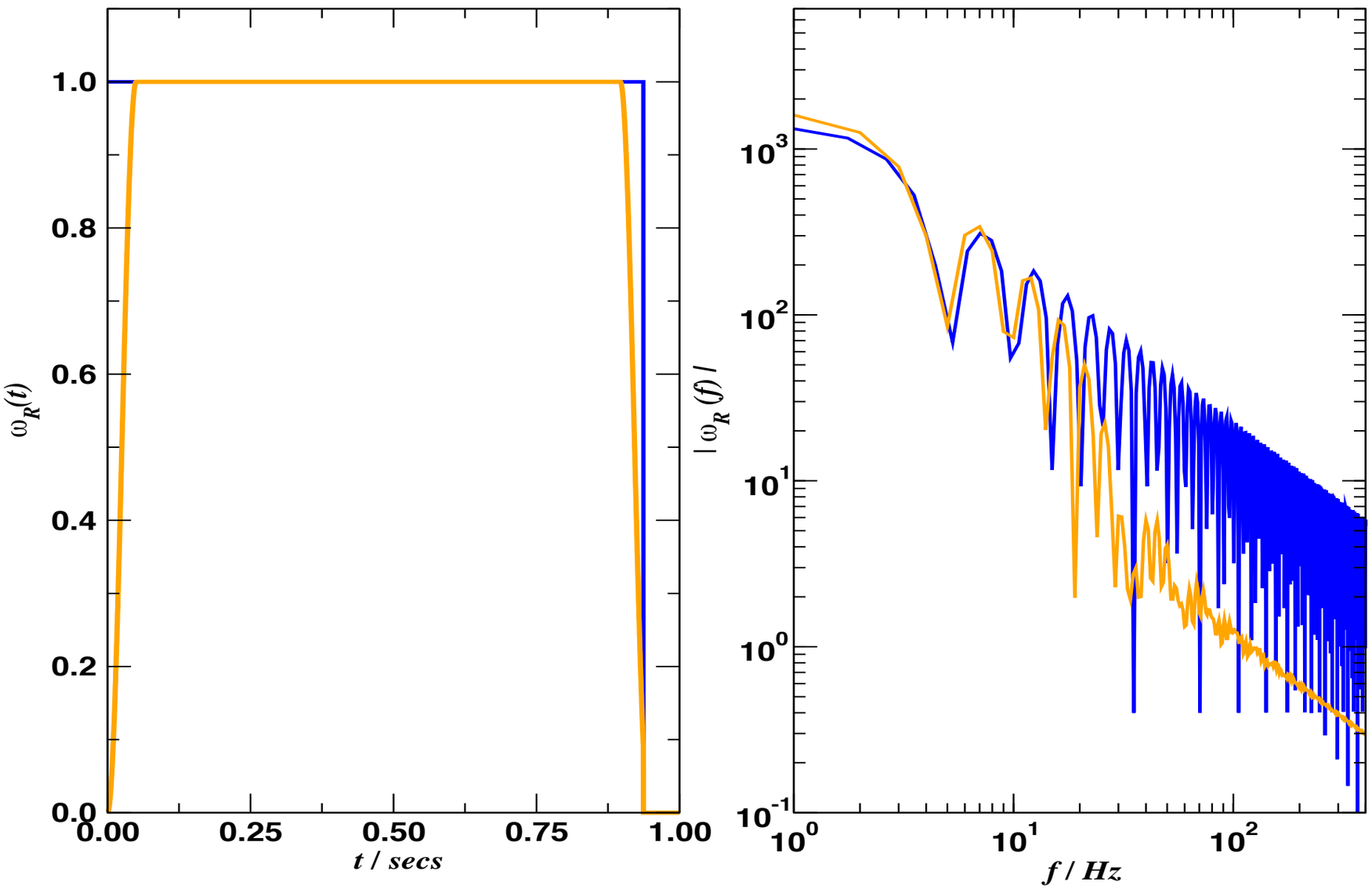

Windowing the data

FT of a chirp waveform using a 1/2-Hann window function

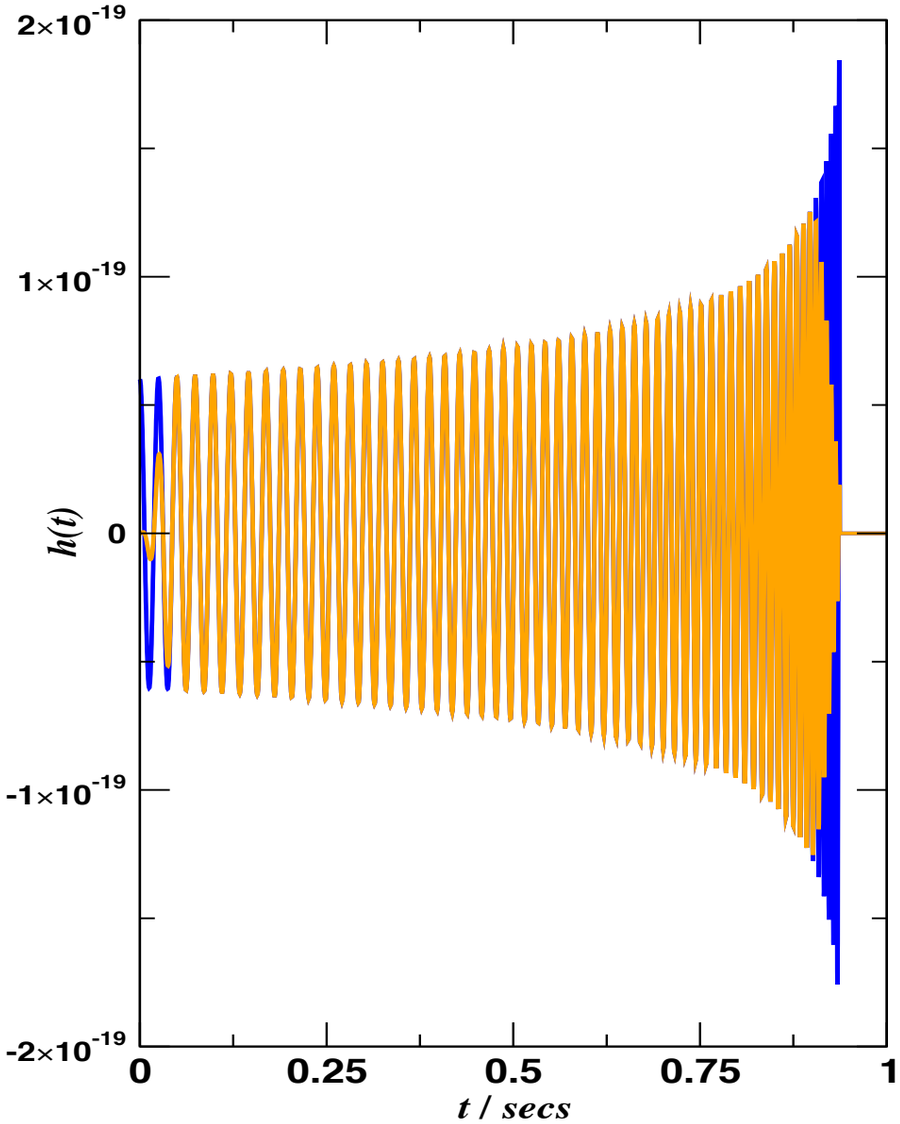

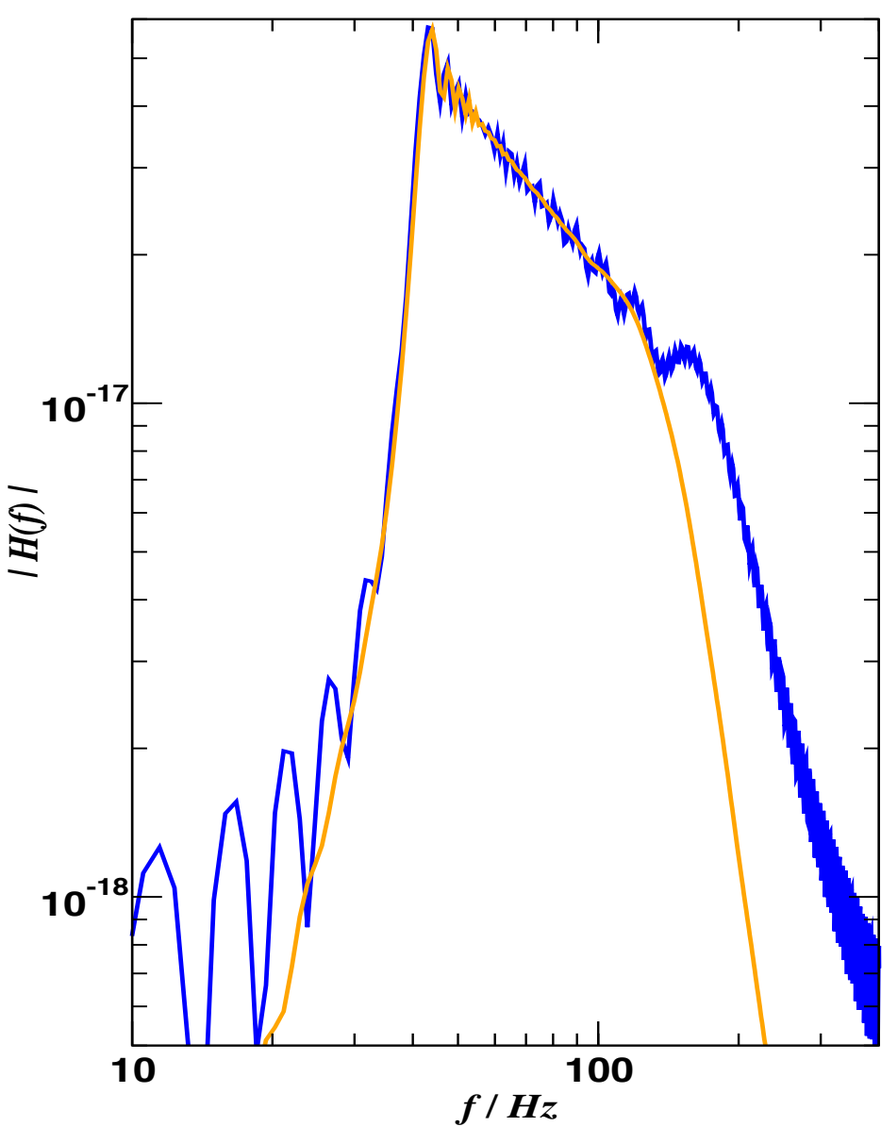

Application to real data

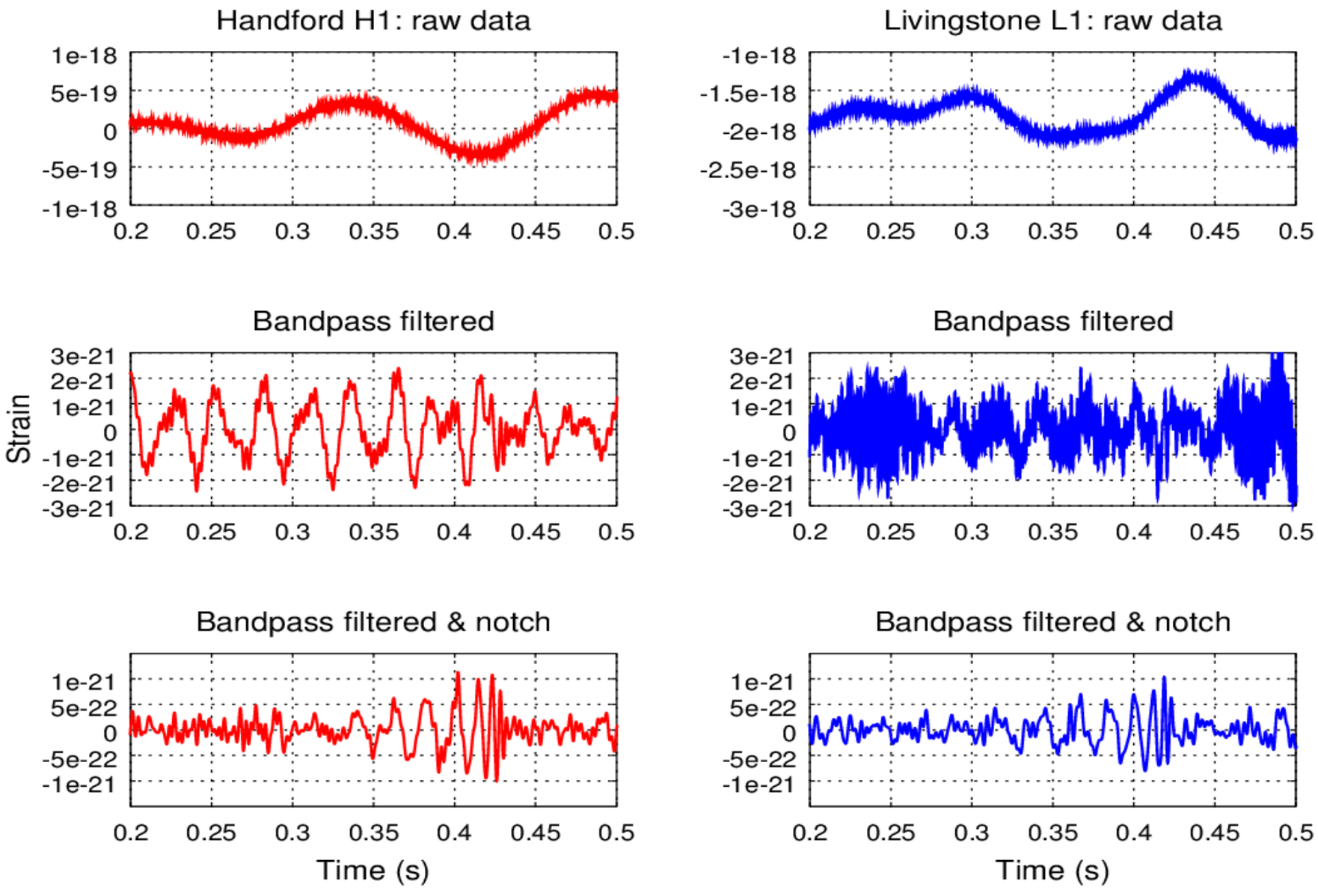

Primer on GW data analysis

- Two parts:
  - Detection
  - Parameter estimation (Bayesian inference)

Time-Frequency Analysis

GW150914 *Abbott et al, PRL 116, 061102 (2016)*

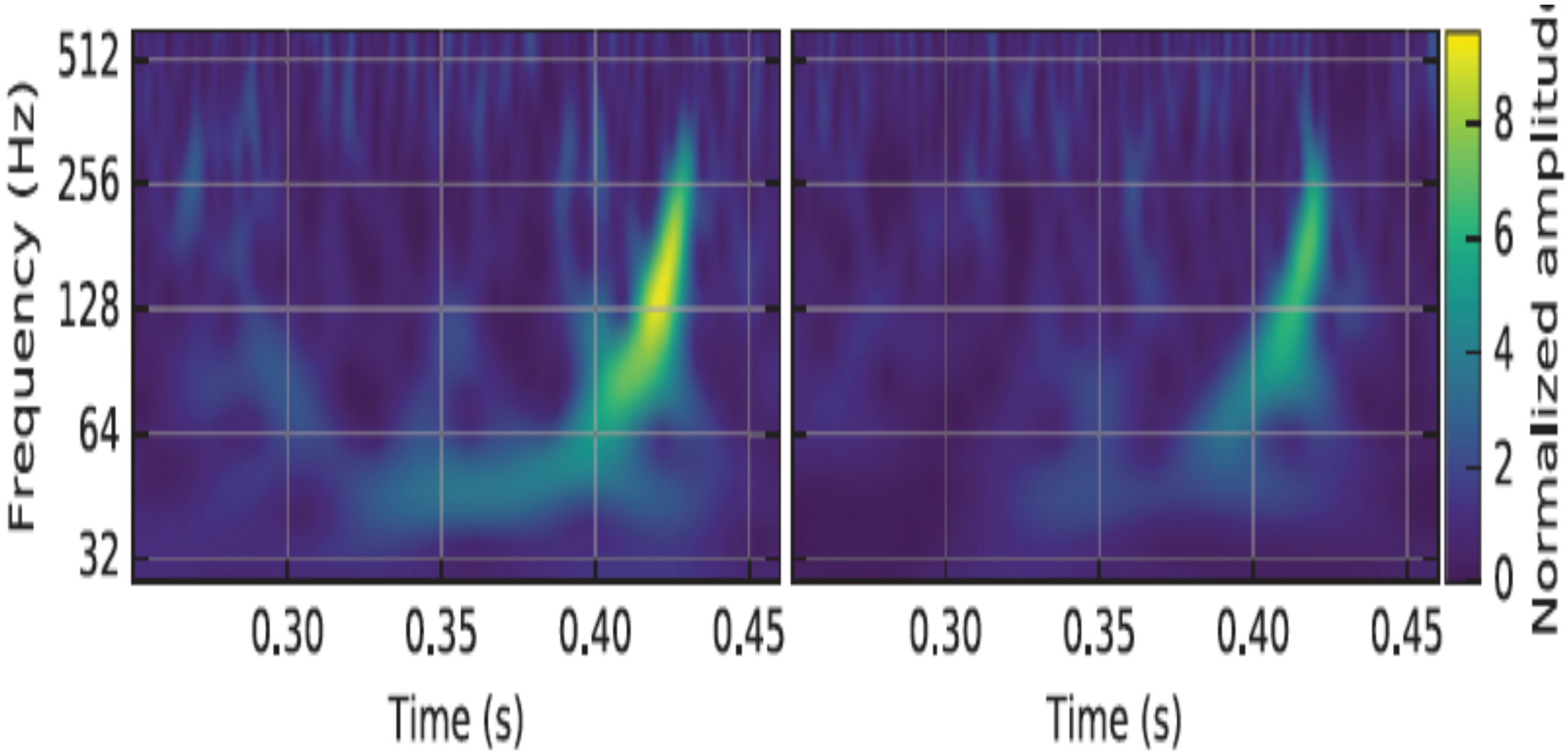

First GW detection was made by the cWB pipeline

Time-Frequency Analysis

GW170817+glitch

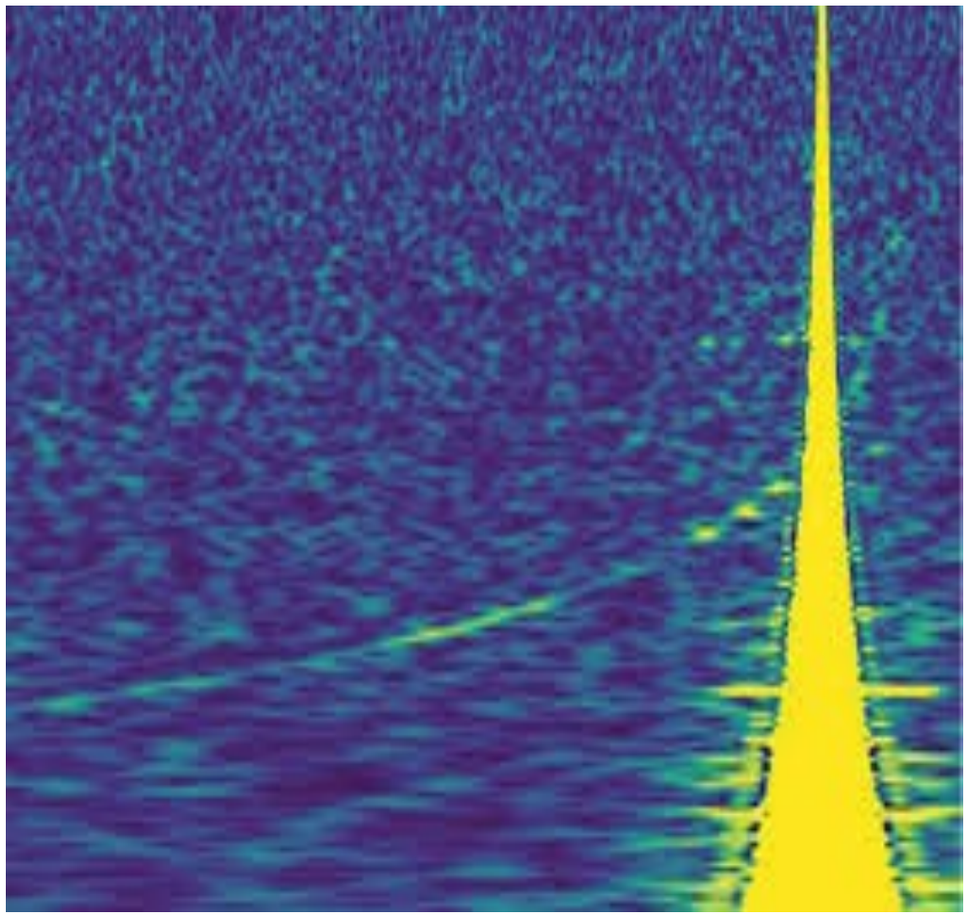

GW170817+glitch removed

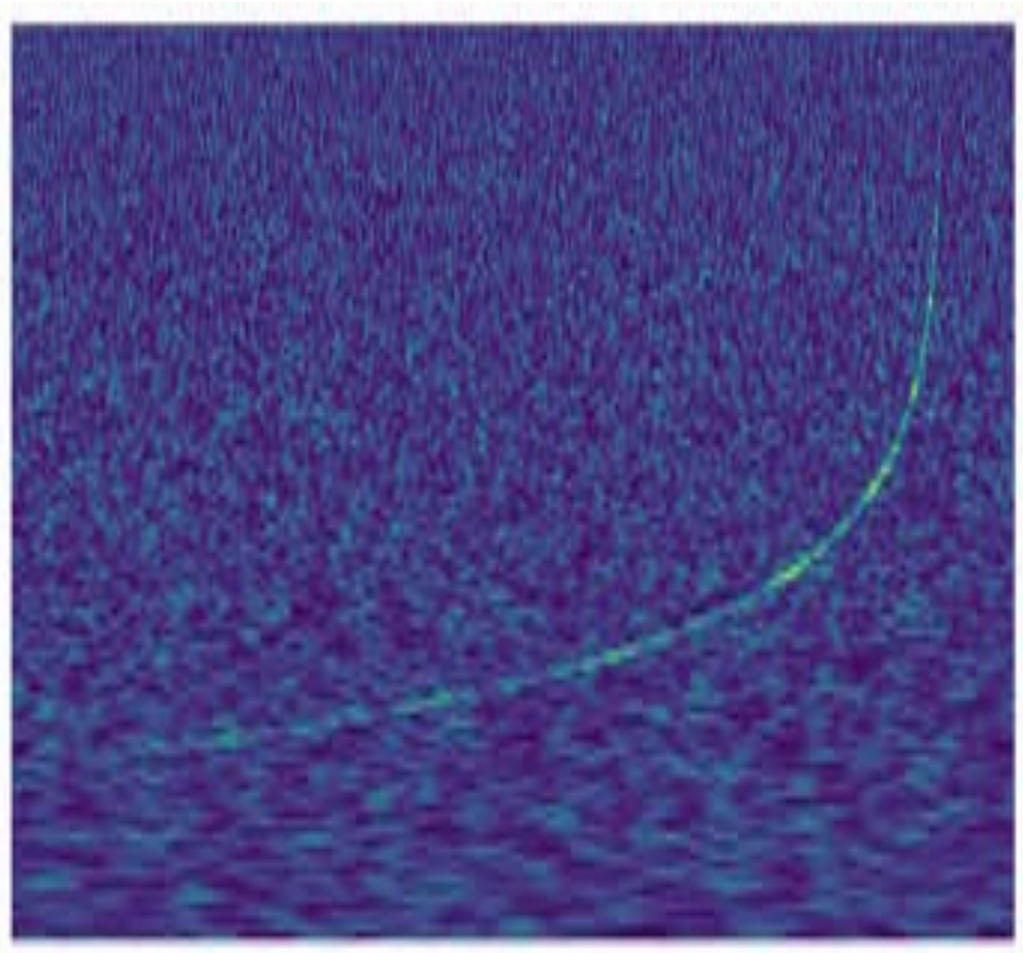

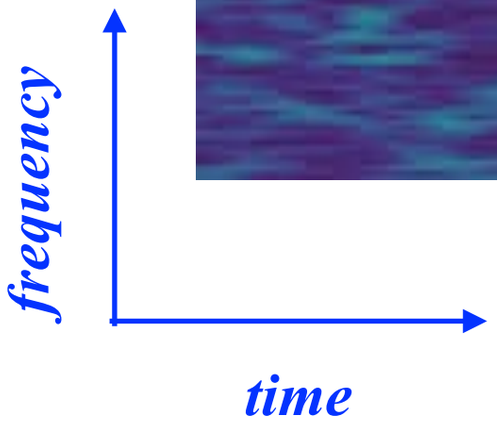

Abbott et al, PRL 116, 061102 (2016)

Glitches

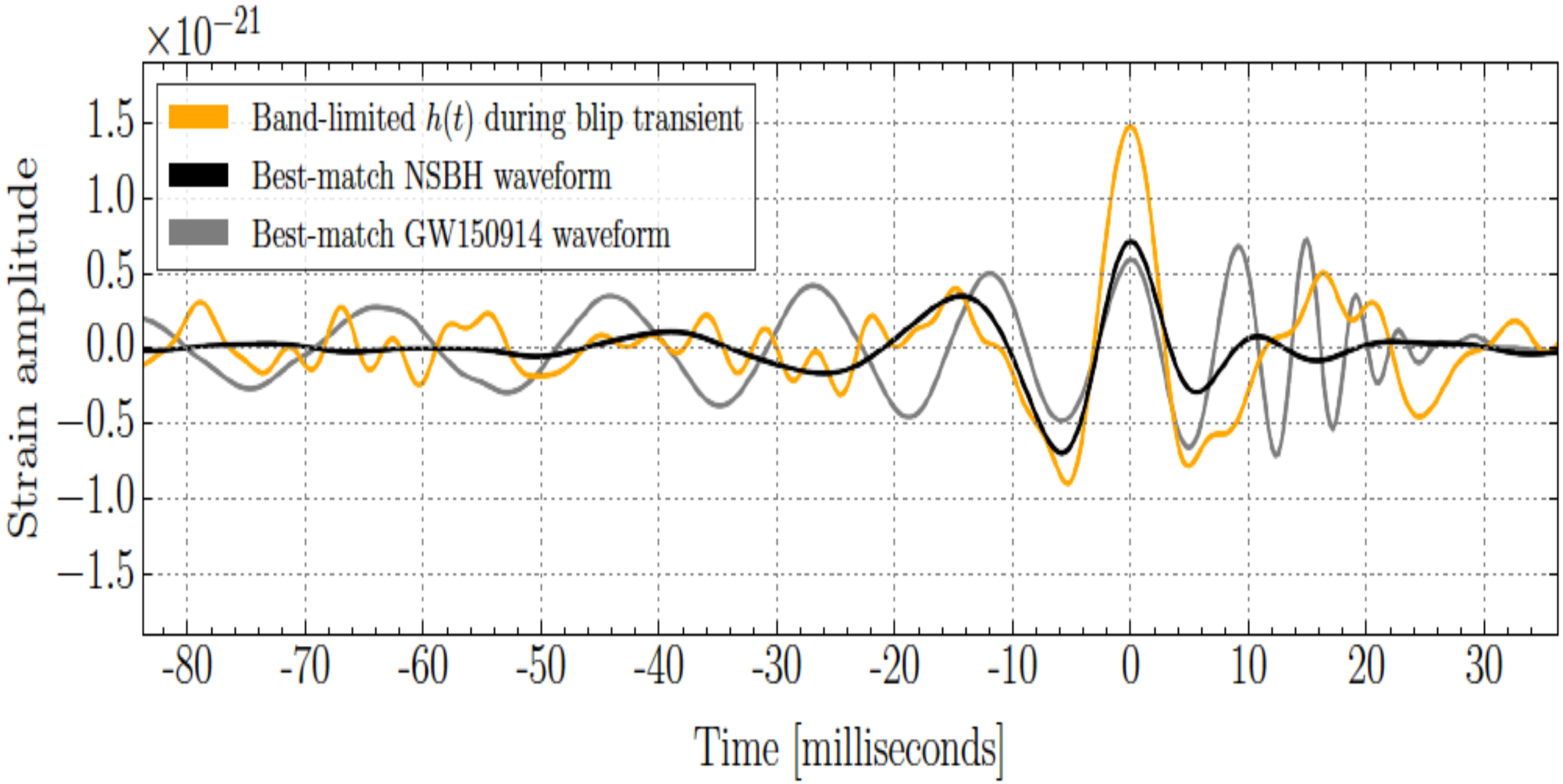
×10−21
Band-limited h(t) during blip transient
Best-match NSBH waveform
Best-match GW150914 waveform
Strain amplitude
1.5
1.0
0.5
0.0
−0.5
−1.0
−1.5
-80
-70
-60
-50
-40
-30
-20
-10
0
10
20
30
Time [milliseconds]

Detection

- Template Grid : assume 2D

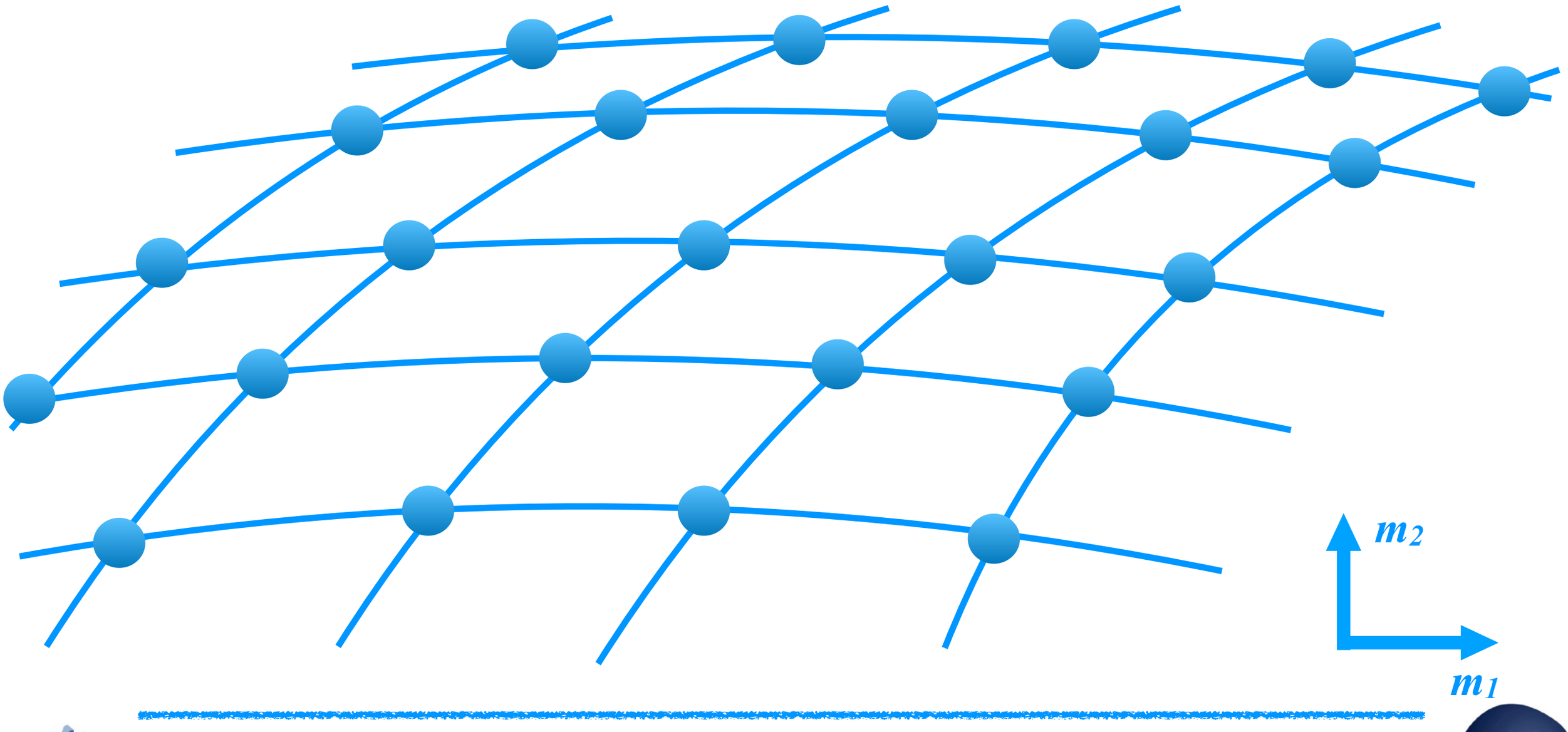

Detection

- Template Grid

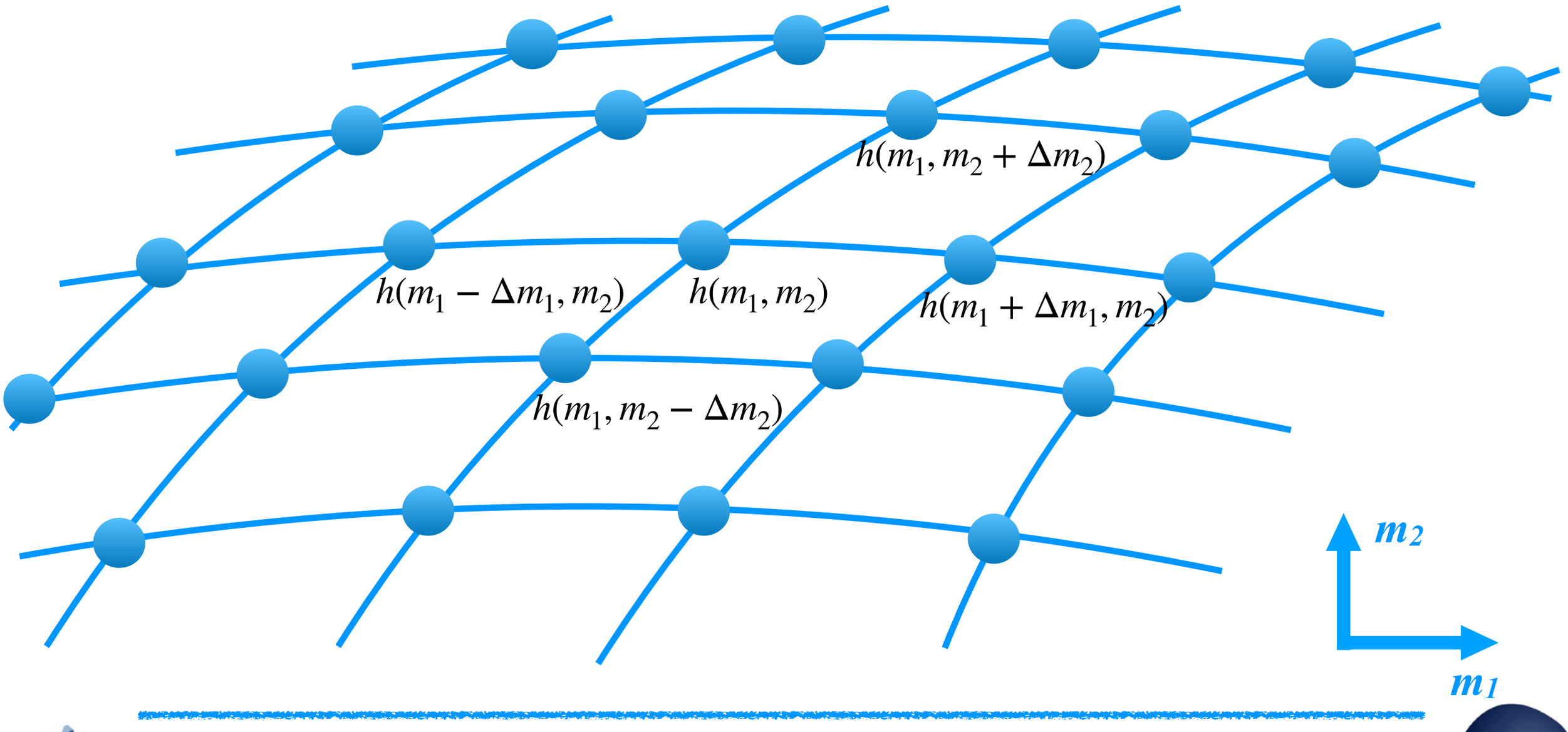

Detection

- Template Grid

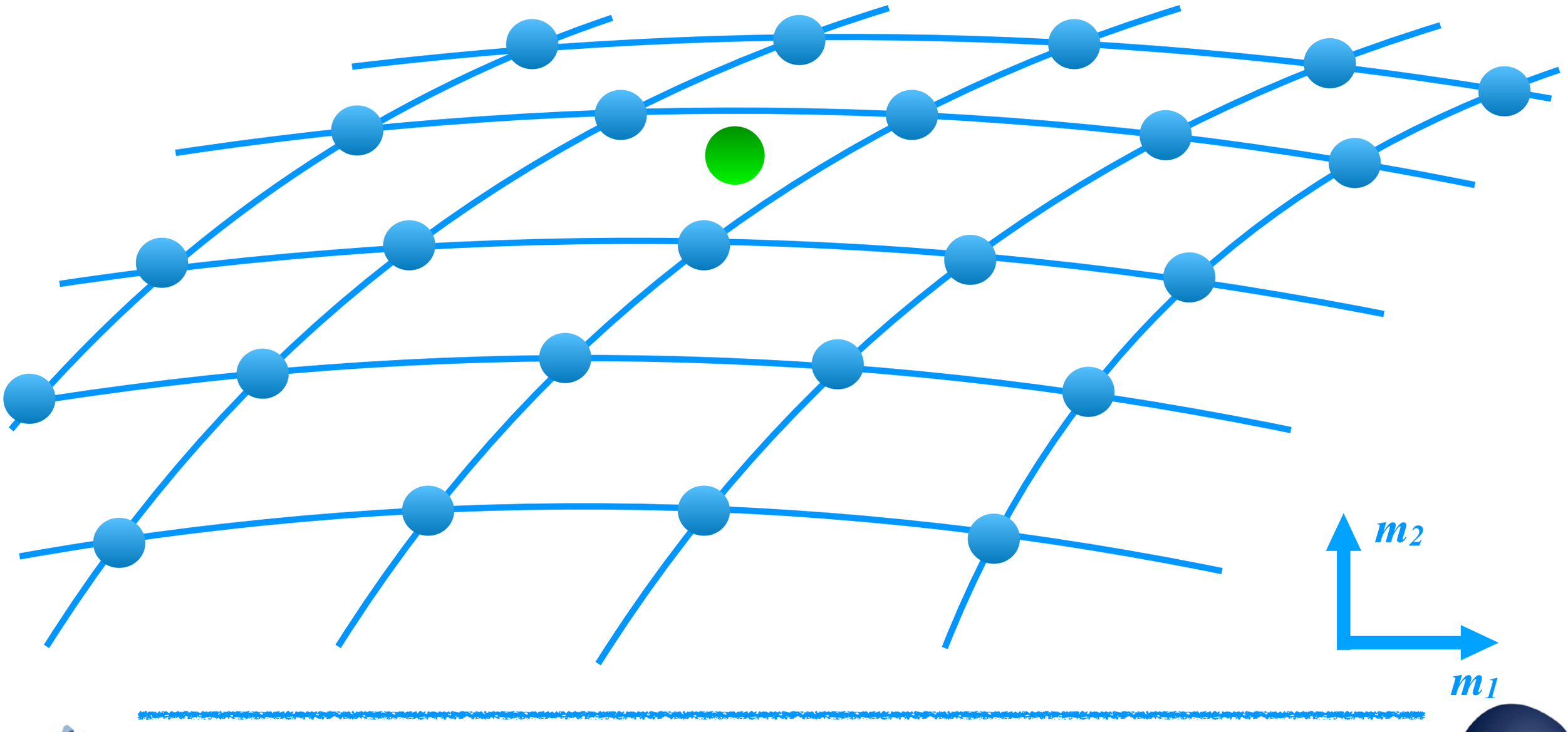

Detection

- Template Grid

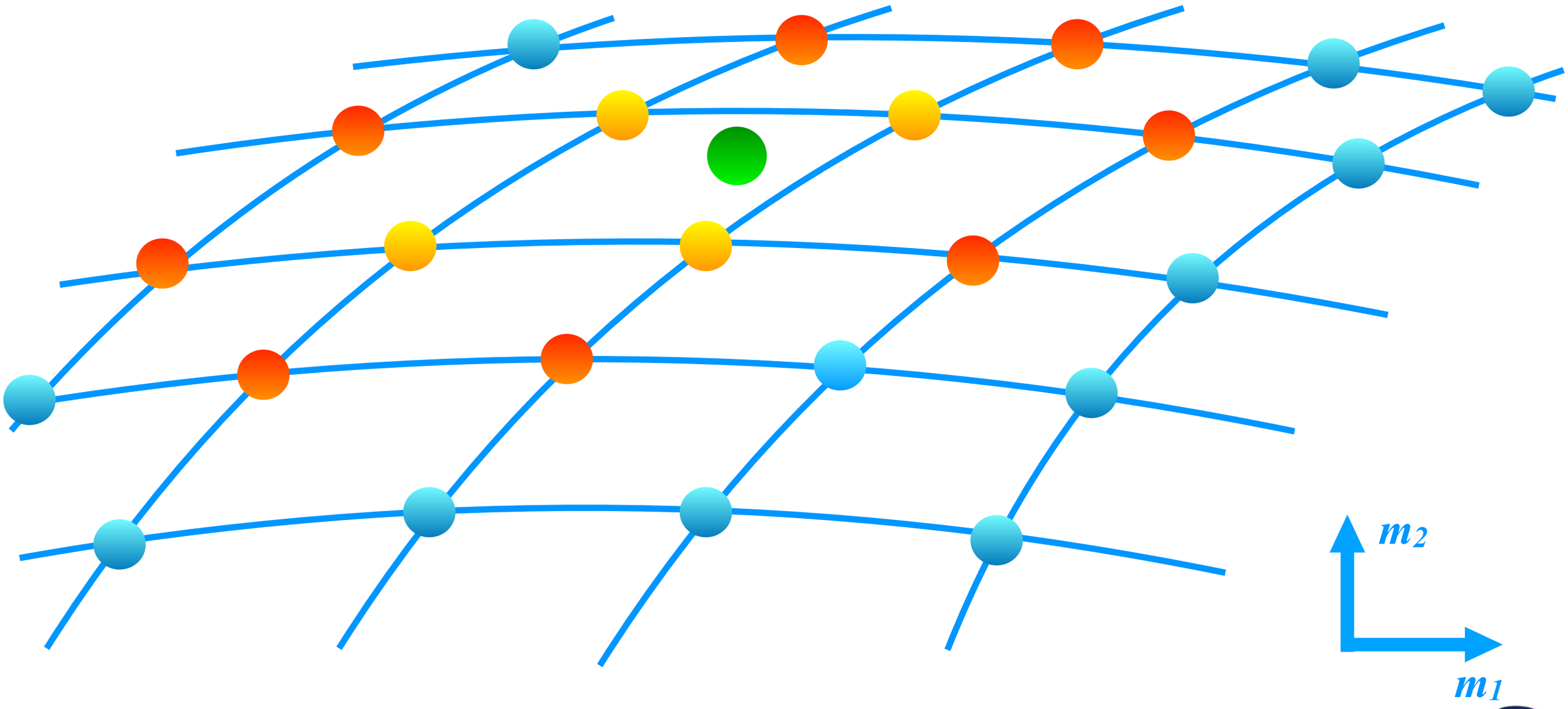

Data Quality & Detector Characterisation

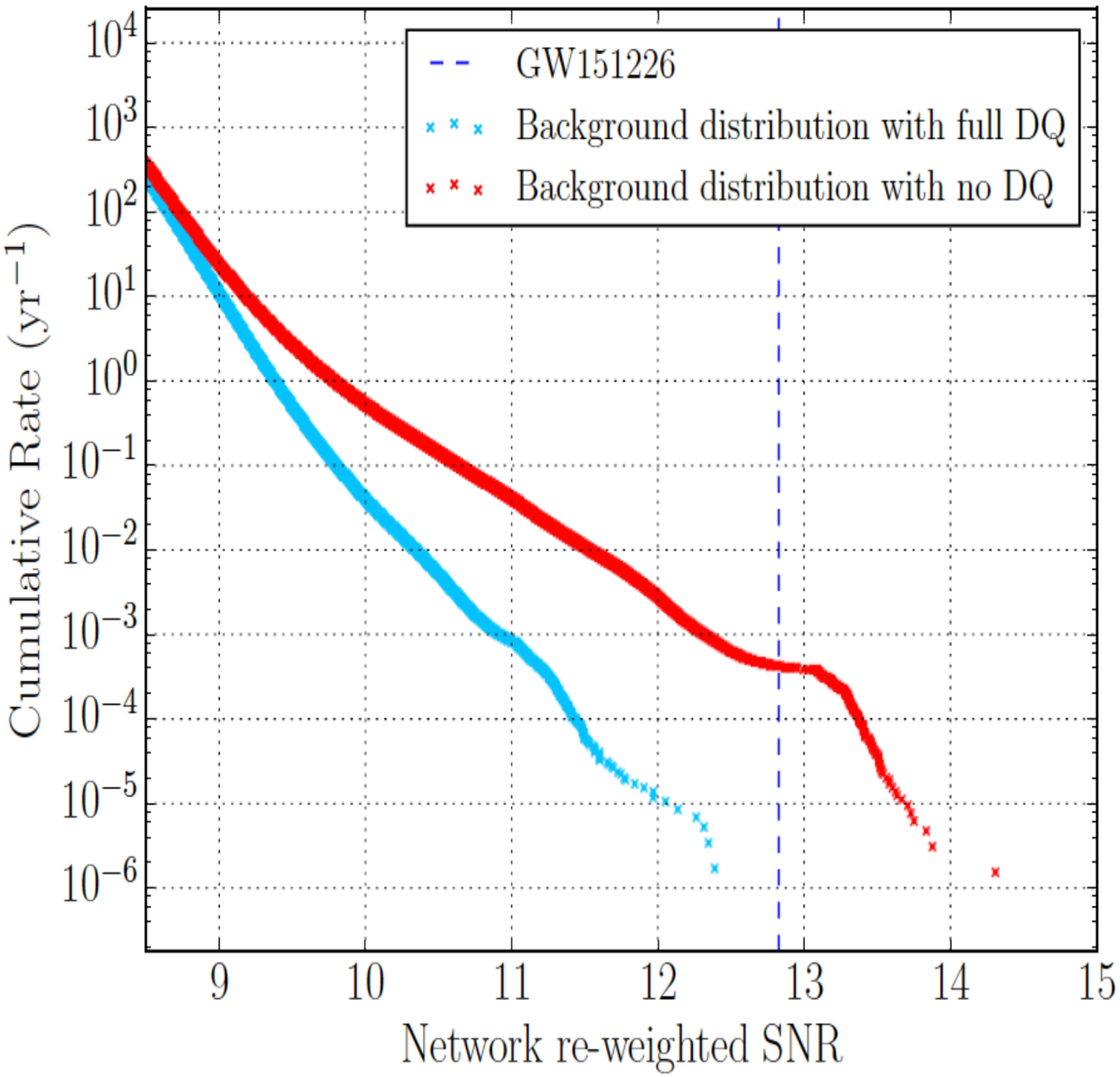

Detector Characterisation improved the FAR of GW151226 by a factor of 500: from 1/320 years to 1/183000 years

Also need to calibrate the time series: reduce the error in amplitude and phase measurement

B. Abbott, CQG 2018

False Alarm Rates

PyCBC

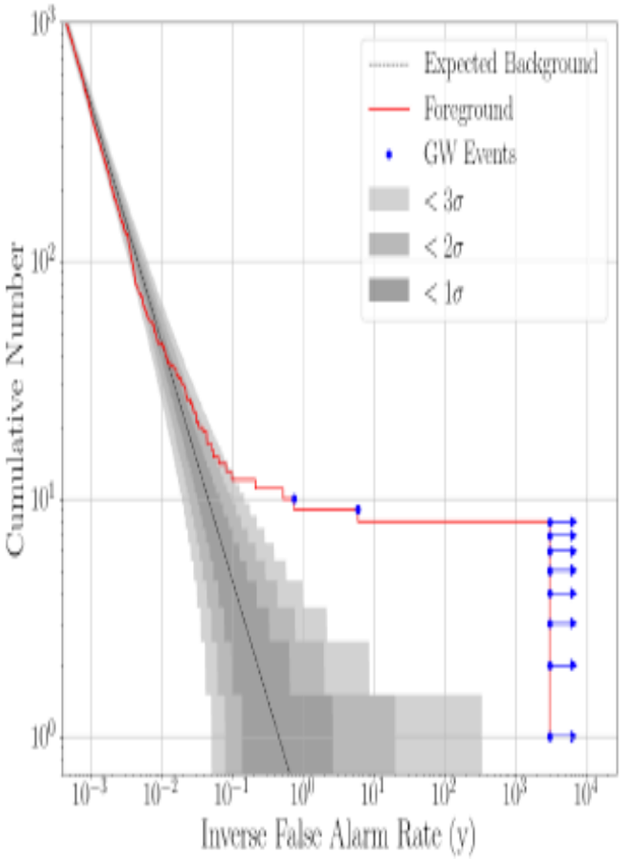

GstLAL

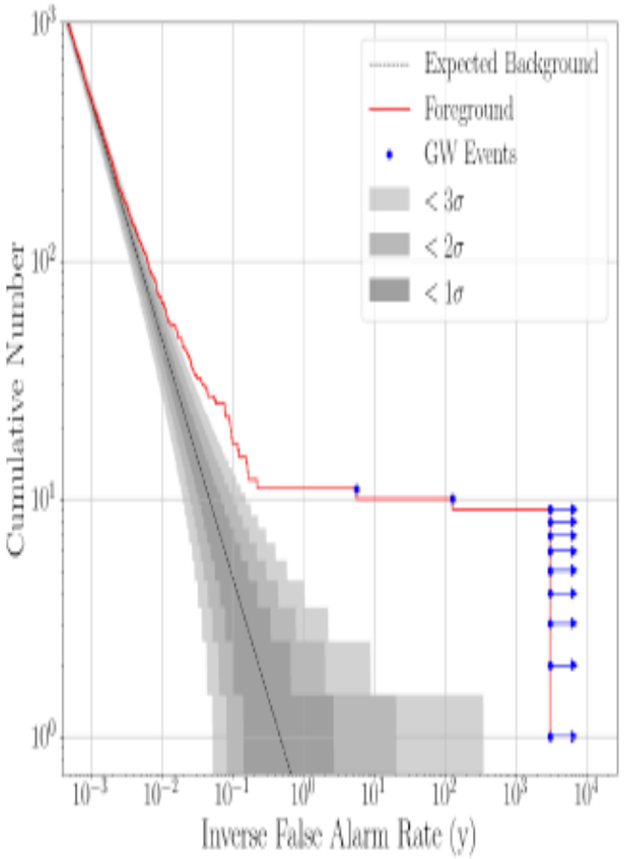

cWB

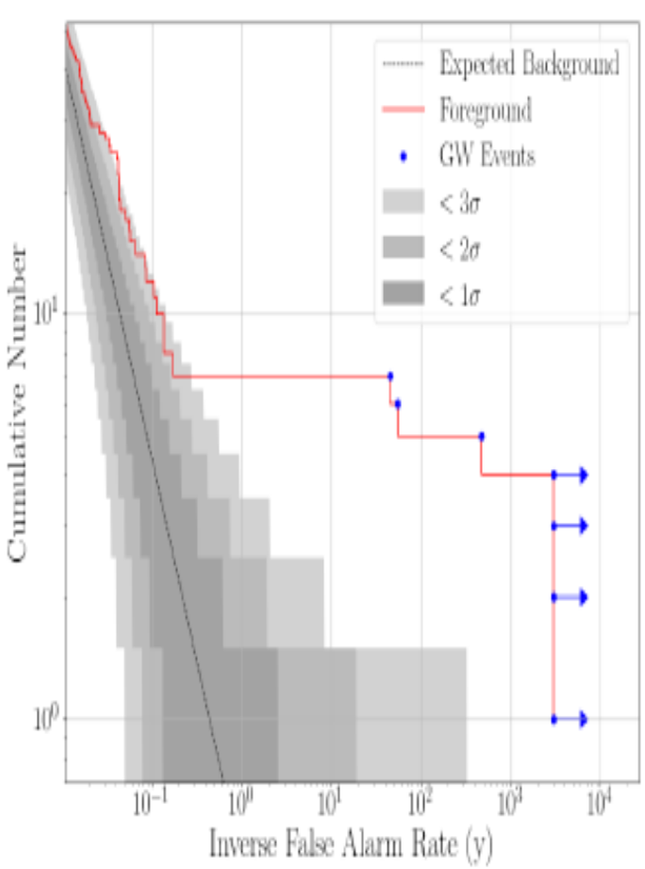

Abbott et al, arXiv:1811.12907 (2018)

Low-latency Analysis

- First alert goes out to the astronomical community within minutes
- Alert contains a 3D sky-map, an “EM-bright” flag, and for O3 a data quality statement
- Further circulars are sent as data comes in
- Updated sky-maps sent to external community until an EM counterpart has been found, or there is no improvement in the map.

EM Follow-up

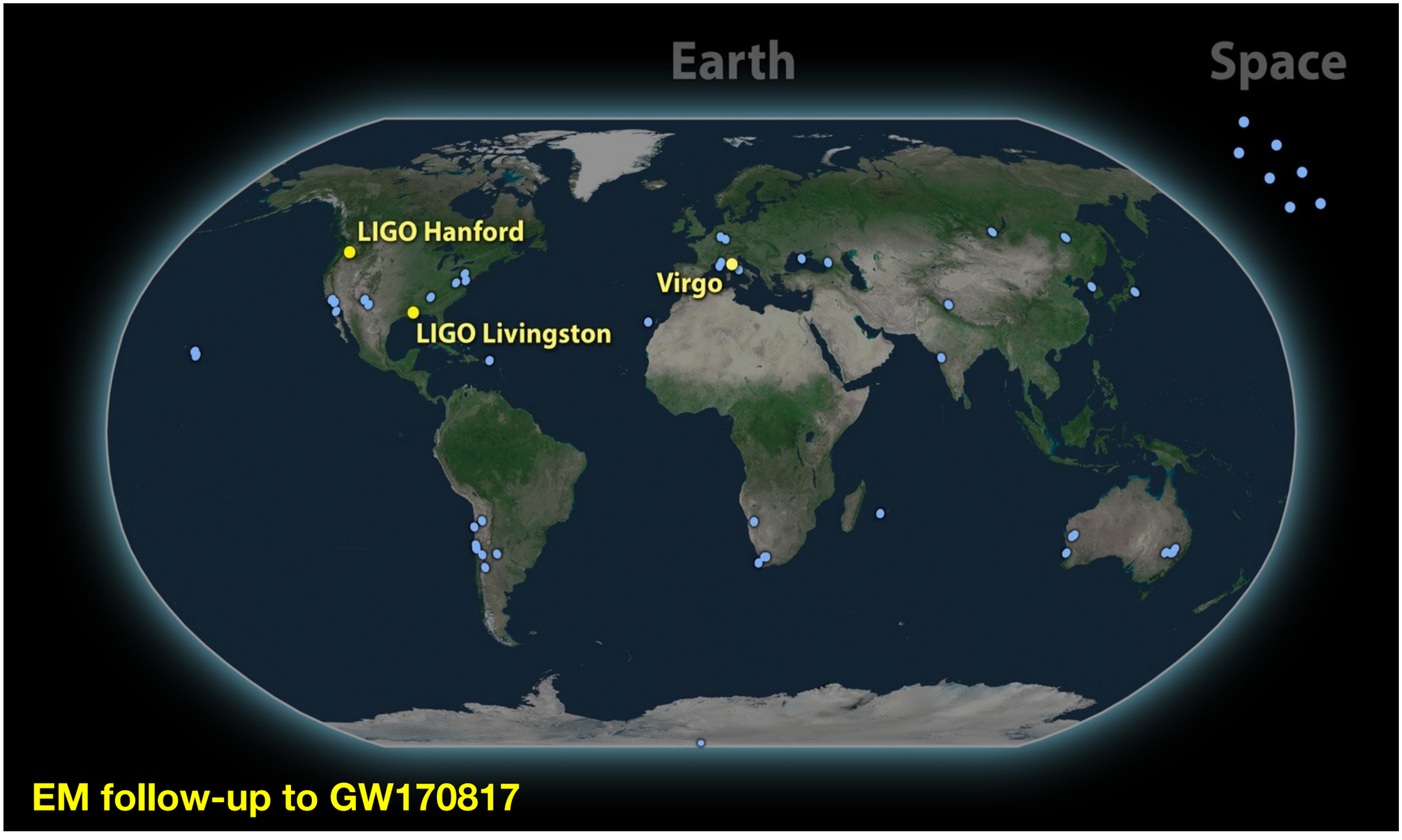

www.ligo.caltech.edu/images

Sky Localisation

$$h_i(t) = h_+(t+\tau_i)F_i^+ + h_\times(t+\tau_i)F_i^\times$$

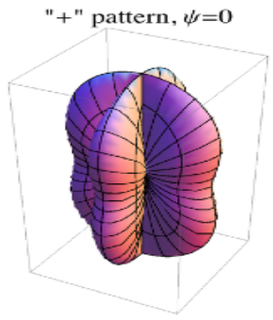

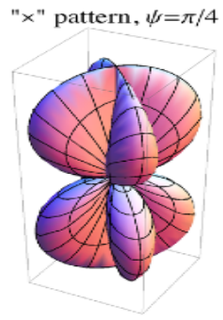

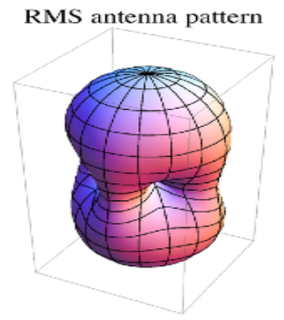

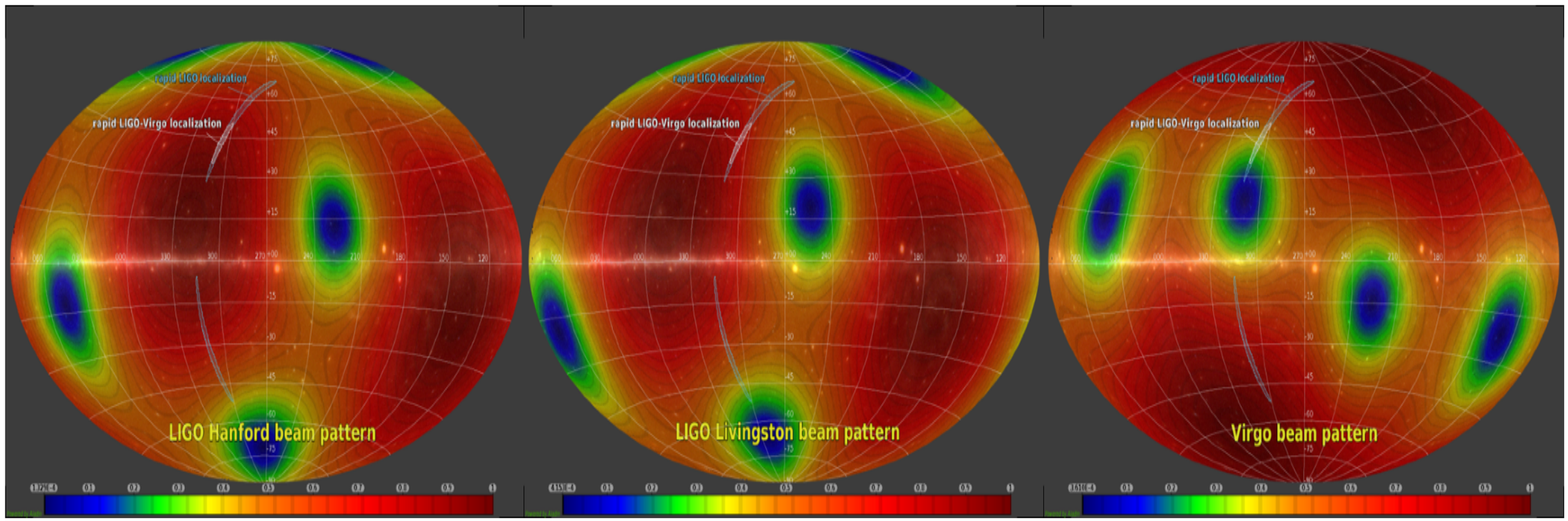

Bayesian Inference

- Use stochastic samplers
- Extract astrophysical parameters

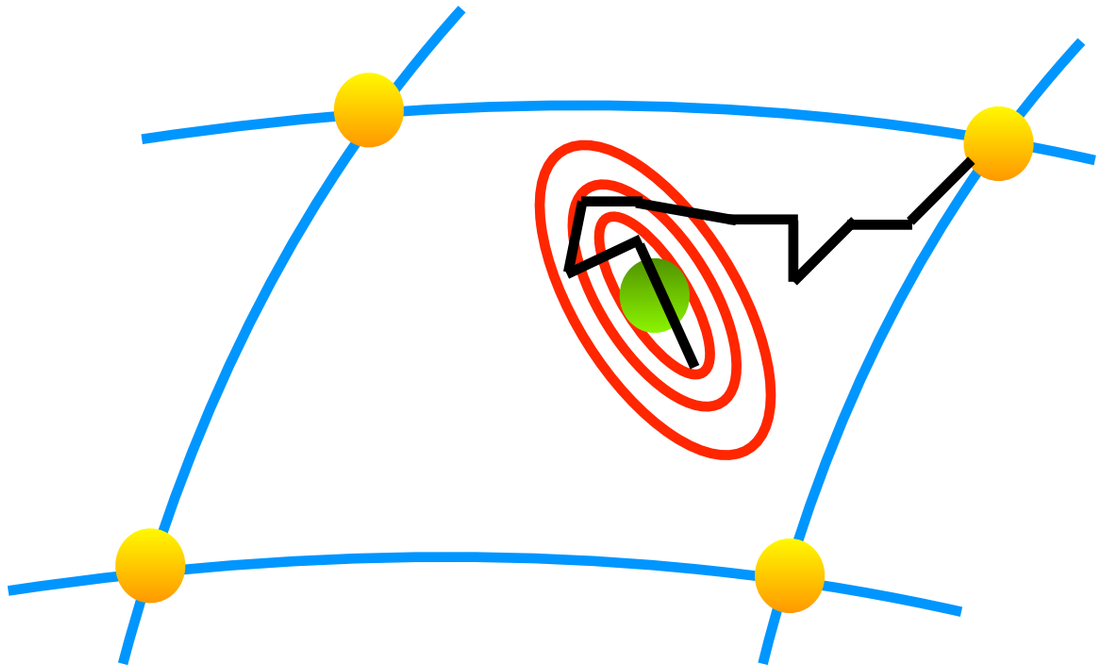

- Provide posterior distributions…
- …and confidence intervals

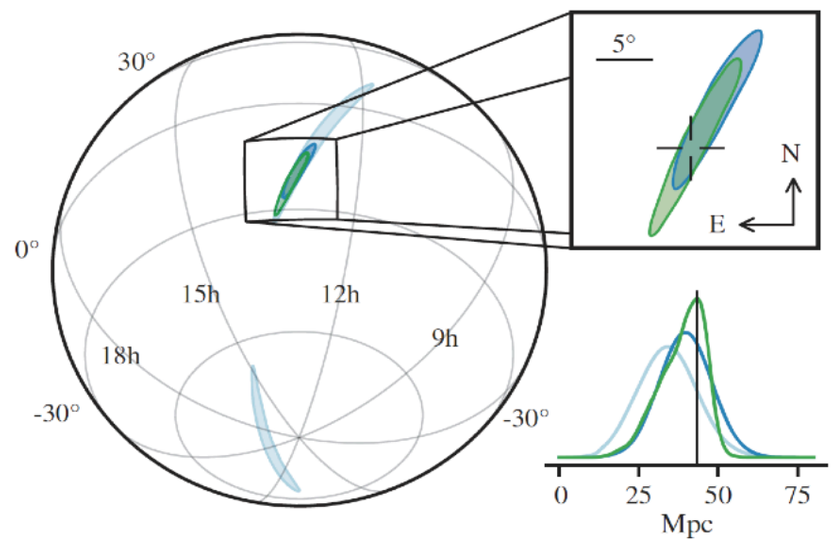

GW170817, B. Abbott et al, PRL 119, 161101 (2017)

Part 2

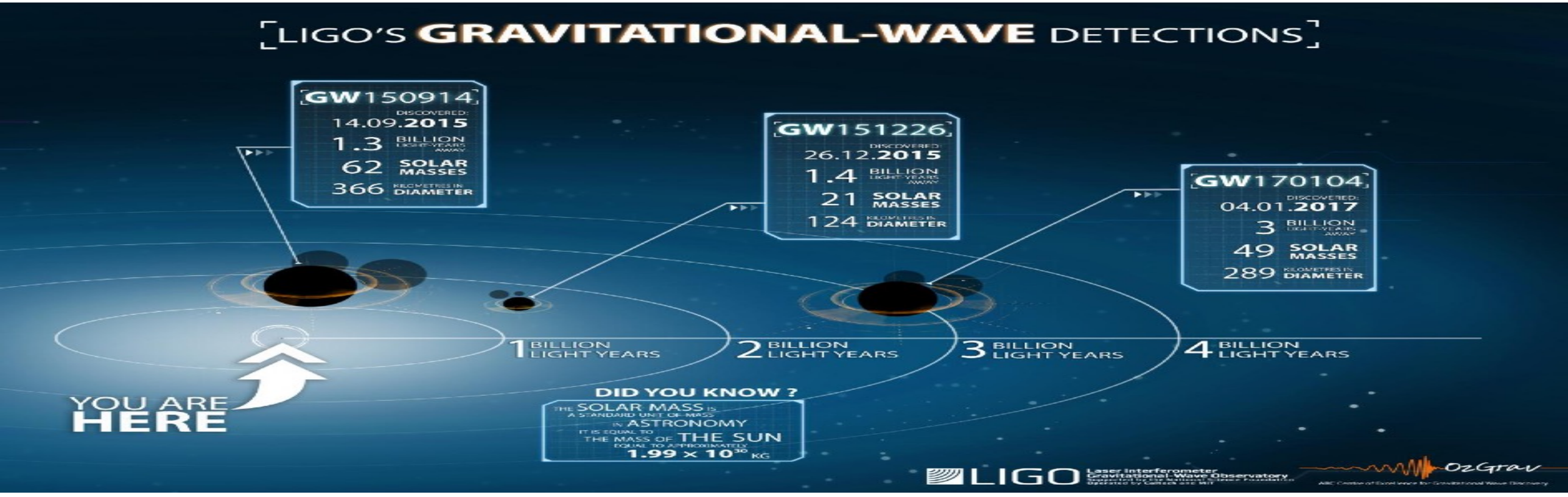
LIGO'S GRAVITATIONAL-WAVE DETECTIONS
GW150914
DISCOVERED: 14.09.2015
1.3 BILLION LIGHT-YEARS AWAY
62 SOLAR MASSES
366 KILOMETRES IN DIAMETER
GW151226
DISCOVERED: 26.12.2015
1.4 BILLION LIGHT-YEARS AWAY
21 SOLAR MASSES
124 KILOMETRES IN DIAMETER
GW170104
DISCOVERED: 04.01.2017
3 BILLION LIGHT-YEARS AWAY
49 SOLAR MASSES
289 KILOMETRES IN DIAMETER
1 BILLION LIGHT YEARS
2 BILLION LIGHT YEARS
3 BILLION LIGHT YEARS
4 BILLION LIGHT YEARS
YOU ARE HERE
DID YOU KNOW ?
THE SOLAR MASS IS A STANDARD UNIT OF MASS IN ASTRONOMY
IT IS EQUAL TO THE MASS OF THE SUN
EQUAL TO APPROXIMATELY 1.99 x 10^30 KG
LIGO Laser Interferometer Gravitational-Wave Observatory
OzGrav

O1/O2

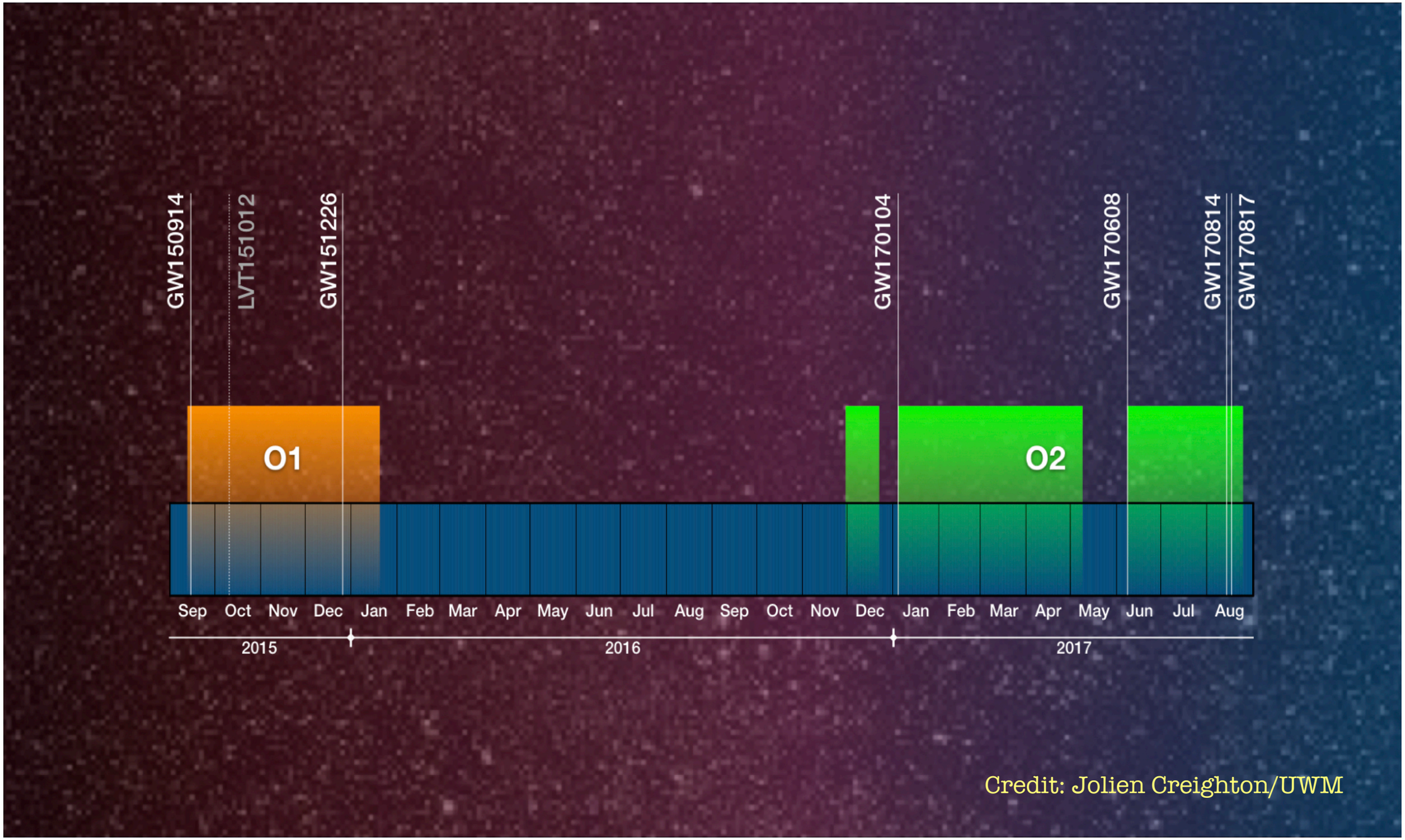
GW150914
LVT151012
GW151226
GW170104
GW170608
GW170814
GW170817
O1
O2
Sep Oct Nov Dec Jan Feb Mar Apr May Jun Jul Aug Sep Oct Nov Dec Jan Feb Mar Apr May Jun Jul Aug
2015
2016
2017
Credit: Jolien Creighton/UWM

O2

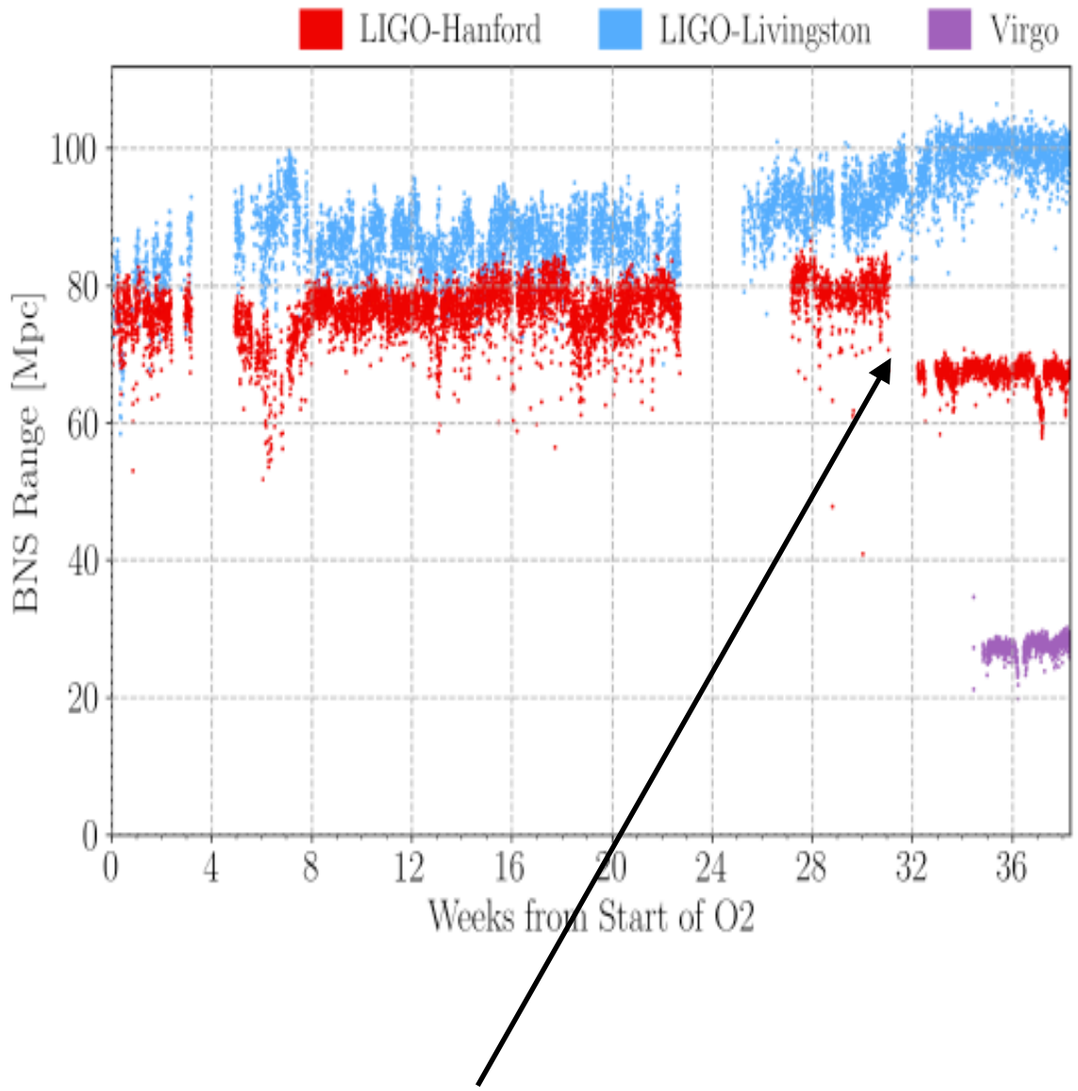

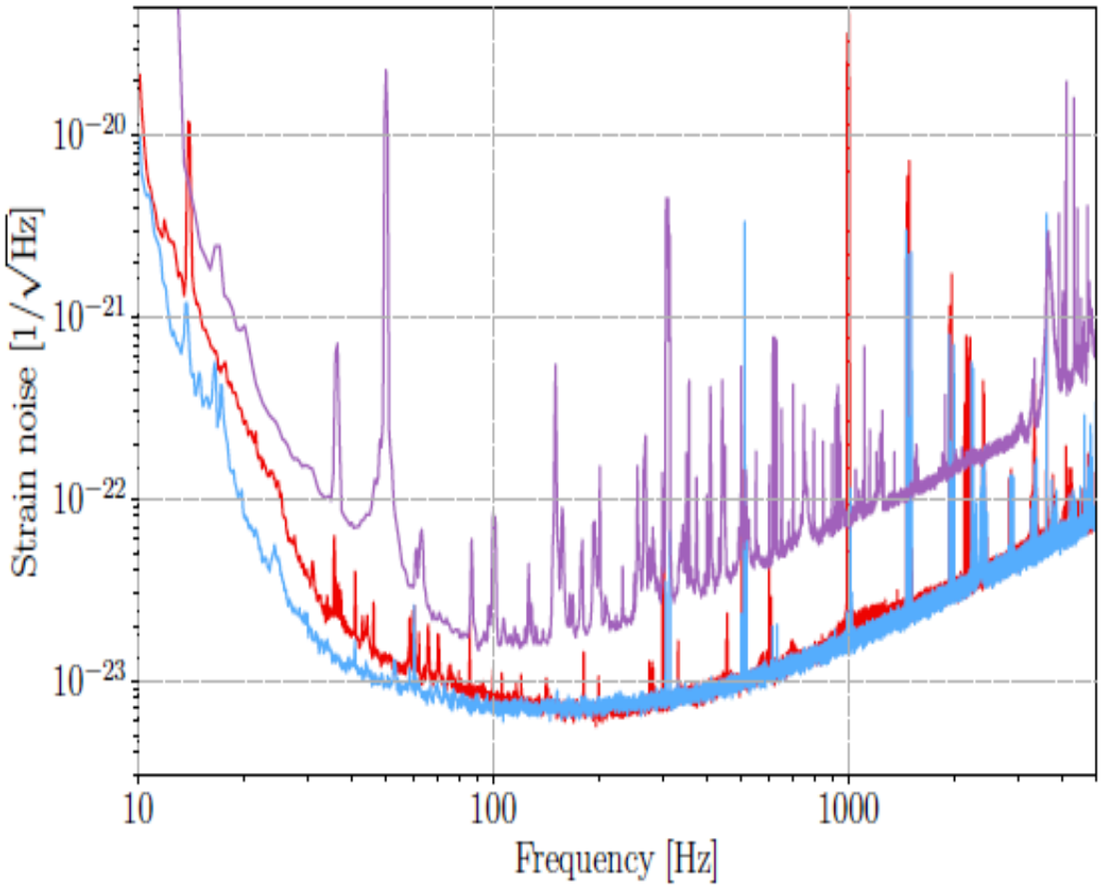

Earthquake in Montana (~700kms)

What do we measure with GWs?

- Redshift masses - need an EM counterpart or assume a cosmology to get detector frame masses, i.e. $m_i{}^{det} = (1+z)m_i$
- Direct measure of luminosity distance, D_L
- Spins
- All sky detector - sky position and orientation via triangulation / time delays
- inclination - highly correlated with luminosity distance
- tidal deformation (NSs)

GWTC-1 results

Event	$m_1/M_\odot$	$m_2/M_\odot$	$\mathcal{M}/M_\odot$	$\chi_{\rm eff}$	$M_{\rm f}/M_\odot$	$a_{\rm f}$	$E_{\rm rad}/(M_\odot c^2)$	$\ell_{\rm peak}/({\rm erg\,s^{-1}})$	$d_L/{\rm Mpc}$	z	$\Delta\Omega/{\rm deg}^2$
GW150914	$35.6^{+4.8}_{-3.0}$	$30.6^{+3.0}_{-4.4}$	$28.6^{+1.6}_{-1.5}$	$-0.01^{+0.12}_{-0.13}$	$63.1^{+3.3}_{-3.0}$	$0.69^{+0.05}_{-0.04}$	$3.1^{+0.4}_{-0.4}$	$3.6^{+0.4}_{-0.4}\times10^{56}$	430^{+150}_{-170}	$0.09^{+0.03}_{-0.03}$	180
GW151012	$23.3^{+14.0}_{-5.5}$	$13.6^{+4.1}_{-4.8}$	$15.2^{+2.0}_{-1.1}$	$0.04^{+0.28}_{-0.19}$	$35.7^{+9.9}_{-3.8}$	$0.67^{+0.13}_{-0.11}$	$1.5^{+0.5}_{-0.5}$	$3.2^{+0.8}_{-1.7}\times10^{56}$	1060^{+540}_{-480}	$0.21^{+0.09}_{-0.09}$	1555
GW151226	$13.7^{+8.8}_{-3.2}$	$7.7^{+2.2}_{-2.6}$	$8.9^{+0.3}_{-0.3}$	$0.18^{+0.20}_{-0.12}$	$20.5^{+6.4}_{-1.5}$	$0.74^{+0.07}_{-0.05}$	$1.0^{+0.1}_{-0.2}$	$3.4^{+0.7}_{-1.7}\times10^{56}$	440^{+180}_{-190}	$0.09^{+0.04}_{-0.04}$	1033
GW170104	$31.0^{+7.2}_{-5.6}$	$20.1^{+4.9}_{-4.5}$	$21.5^{+2.1}_{-1.7}$	$-0.04^{+0.17}_{-0.20}$	$49.1^{+5.2}_{-3.9}$	$0.66^{+0.08}_{-0.10}$	$2.2^{+0.5}_{-0.5}$	$3.3^{+0.6}_{-0.9}\times10^{56}$	960^{+430}_{-410}	$0.19^{+0.07}_{-0.08}$	924
GW170608	$10.9^{+5.3}_{-1.7}$	$7.6^{+1.3}_{-2.1}$	$7.9^{+0.2}_{-0.2}$	$0.03^{+0.19}_{-0.07}$	$17.8^{+3.2}_{-0.7}$	$0.69^{+0.04}_{-0.04}$	$0.9^{+0.05}_{-0.1}$	$3.5^{+0.4}_{-1.3}\times10^{56}$	320^{+120}_{-110}	$0.07^{+0.02}_{-0.02}$	396
GW170729	$50.6^{+16.6}_{-10.2}$	$34.3^{+9.1}_{-10.1}$	$35.7^{+6.5}_{-4.7}$	$0.36^{+0.21}_{-0.25}$	$80.3^{+14.6}_{-10.2}$	$0.81^{+0.07}_{-0.13}$	$4.8^{+1.7}_{-1.7}$	$4.2^{+0.9}_{-1.5}\times10^{56}$	2750^{+1350}_{-1320}	$0.48^{+0.19}_{-0.20}$	1033
GW170809	$35.2^{+8.3}_{-6.0}$	$23.8^{+5.2}_{-5.1}$	$25.0^{+2.1}_{-1.6}$	$0.07^{+0.16}_{-0.16}$	$56.4^{+5.2}_{-3.7}$	$0.70^{+0.08}_{-0.09}$	$2.7^{+0.6}_{-0.6}$	$3.5^{+0.6}_{-0.9}\times10^{56}$	990^{+320}_{-380}	$0.20^{+0.05}_{-0.07}$	340
GW170814	$30.7^{+5.7}_{-3.0}$	$25.3^{+2.9}_{-4.1}$	$24.2^{+1.4}_{-1.1}$	$0.07^{+0.12}_{-0.11}$	$53.4^{+3.2}_{-2.4}$	$0.72^{+0.07}_{-0.05}$	$2.7^{+0.4}_{-0.3}$	$3.7^{+0.4}_{-0.5}\times10^{56}$	580^{+160}_{-210}	$0.12^{+0.03}_{-0.04}$	87
GW170817	$1.46^{+0.12}_{-0.10}$	$1.27^{+0.09}_{-0.09}$	$1.186^{+0.001}_{-0.001}$	$0.00^{+0.02}_{-0.01}$	≤ 2.8	≤ 0.89	≥ 0.04	$\geq 0.1\times10^{56}$	40^{+10}_{-10}	$0.01^{+0.00}_{-0.00}$	16
GW170818	$35.5^{+7.5}_{-4.7}$	$26.8^{+4.3}_{-5.2}$	$26.7^{+2.1}_{-1.7}$	$-0.09^{+0.18}_{-0.21}$	$59.8^{+4.8}_{-3.8}$	$0.67^{+0.07}_{-0.08}$	$2.7^{+0.5}_{-0.5}$	$3.4^{+0.5}_{-0.7}\times10^{56}$	1020^{+430}_{-360}	$0.20^{+0.07}_{-0.07}$	39
GW170823	$39.6^{+10.0}_{-6.6}$	$29.4^{+6.3}_{-7.1}$	$29.3^{+4.2}_{-3.2}$	$0.08^{+0.20}_{-0.22}$	$65.6^{+9.4}_{-6.6}$	$0.71^{+0.08}_{-0.10}$	$3.3^{+0.9}_{-0.8}$	$3.6^{+0.6}_{-0.9}\times10^{56}$	1850^{+840}_{-840}	$0.34^{+0.13}_{-0.14}$	1651

- 10 BBHs

Abbott et al, arXiv:1811.12907 (2018)

GWTC-1 results

Event	$m_1/M_\odot$	$m_2/M_\odot$	$\mathcal{M}/M_\odot$	$\chi_{\rm eff}$	$M_{\rm f}/M_\odot$	$a_{\rm f}$	$E_{\rm rad}/(M_\odot c^2)$	$\ell_{\rm peak}/({\rm erg\,s^{-1}})$	$d_L/{\rm Mpc}$	z	$\Delta\Omega/{\rm deg}^2$
GW150914	$35.6^{+4.8}_{-3.0}$	$30.6^{+3.0}_{-4.4}$	$28.6^{+1.6}_{-1.5}$	$-0.01^{+0.12}_{-0.13}$	$63.1^{+3.3}_{-3.0}$	$0.69^{+0.05}_{-0.04}$	$3.1^{+0.4}_{-0.4}$	$3.6^{+0.4}_{-0.4}\times10^{56}$	430^{+150}_{-170}	$0.09^{+0.03}_{-0.03}$	180
GW151012	$23.3^{+14.0}_{-5.5}$	$13.6^{+4.1}_{-4.8}$	$15.2^{+2.0}_{-1.1}$	$0.04^{+0.28}_{-0.19}$	$35.7^{+9.9}_{-3.8}$	$0.67^{+0.13}_{-0.11}$	$1.5^{+0.5}_{-0.5}$	$3.2^{+0.8}_{-1.7}\times10^{56}$	1060^{+540}_{-480}	$0.21^{+0.09}_{-0.09}$	1555
GW151226	$13.7^{+8.8}_{-3.2}$	$7.7^{+2.2}_{-2.6}$	$8.9^{+0.3}_{-0.3}$	$0.18^{+0.20}_{-0.12}$	$20.5^{+6.4}_{-1.5}$	$0.74^{+0.07}_{-0.05}$	$1.0^{+0.1}_{-0.2}$	$3.4^{+0.7}_{-1.7}\times10^{56}$	440^{+180}_{-190}	$0.09^{+0.04}_{-0.04}$	1033
GW170104	$31.0^{+7.2}_{-5.6}$	$20.1^{+4.9}_{-4.5}$	$21.5^{+2.1}_{-1.7}$	$-0.04^{+0.17}_{-0.20}$	$49.1^{+5.2}_{-3.9}$	$0.66^{+0.08}_{-0.10}$	$2.2^{+0.5}_{-0.5}$	$3.3^{+0.6}_{-0.9}\times10^{56}$	960^{+430}_{-410}	$0.19^{+0.07}_{-0.08}$	924
GW170608	$10.9^{+5.3}_{-1.7}$	$7.6^{+1.3}_{-2.1}$	$7.9^{+0.2}_{-0.2}$	$0.03^{+0.19}_{-0.07}$	$17.8^{+3.2}_{-0.7}$	$0.69^{+0.04}_{-0.04}$	$0.9^{+0.05}_{-0.1}$	$3.5^{+0.4}_{-1.3}\times10^{56}$	320^{+120}_{-110}	$0.07^{+0.02}_{-0.02}$	396
GW170729	$50.6^{+16.6}_{-10.2}$	$34.3^{+9.1}_{-10.1}$	$35.7^{+6.5}_{-4.7}$	$0.36^{+0.21}_{-0.25}$	$80.3^{+14.6}_{-10.2}$	$0.81^{+0.07}_{-0.13}$	$4.8^{+1.7}_{-1.7}$	$4.2^{+0.9}_{-1.5}\times10^{56}$	2750^{+1350}_{-1320}	$0.48^{+0.19}_{-0.20}$	1033
GW170809	$35.2^{+8.3}_{-6.0}$	$23.8^{+5.2}_{-5.1}$	$25.0^{+2.1}_{-1.6}$	$0.07^{+0.16}_{-0.16}$	$56.4^{+5.2}_{-3.7}$	$0.70^{+0.08}_{-0.09}$	$2.7^{+0.6}_{-0.6}$	$3.5^{+0.6}_{-0.9}\times10^{56}$	990^{+320}_{-380}	$0.20^{+0.05}_{-0.07}$	340
GW170814	$30.7^{+5.7}_{-3.0}$	$25.3^{+2.9}_{-4.1}$	$24.2^{+1.4}_{-1.1}$	$0.07^{+0.12}_{-0.11}$	$53.4^{+3.2}_{-2.4}$	$0.72^{+0.07}_{-0.05}$	$2.7^{+0.4}_{-0.3}$	$3.7^{+0.4}_{-0.5}\times10^{56}$	580^{+160}_{-210}	$0.12^{+0.03}_{-0.04}$	87
GW170817	$1.46^{+0.12}_{-0.10}$	$1.27^{+0.09}_{-0.09}$	$1.186^{+0.001}_{-0.001}$	$0.00^{+0.02}_{-0.01}$	≤ 2.8	≤ 0.89	≥ 0.04	$\geq 0.1\times10^{56}$	40^{+10}_{-10}	$0.01^{+0.00}_{-0.00}$	16
GW170818	$35.5^{+7.5}_{-4.7}$	$26.8^{+4.3}_{-5.2}$	$26.7^{+2.1}_{-1.7}$	$-0.09^{+0.18}_{-0.21}$	$59.8^{+4.8}_{-3.8}$	$0.67^{+0.07}_{-0.08}$	$2.7^{+0.5}_{-0.5}$	$3.4^{+0.5}_{-0.7}\times10^{56}$	1020^{+430}_{-360}	$0.20^{+0.07}_{-0.07}$	39
GW170823	$39.6^{+10.0}_{-6.6}$	$29.4^{+6.3}_{-7.1}$	$29.3^{+4.2}_{-3.2}$	$0.08^{+0.20}_{-0.22}$	$65.6^{+9.4}_{-6.6}$	$0.71^{+0.08}_{-0.10}$	$3.3^{+0.9}_{-0.8}$	$3.6^{+0.6}_{-0.9}\times10^{56}$	1850^{+840}_{-840}	$0.34^{+0.13}_{-0.14}$	1651

- Massive energy output

Abbott et al, arXiv:1811.12907 (2018)

GWTC-1 results

Event	$m_1/M_\odot$	$m_2/M_\odot$	$\mathcal{M}/M_\odot$	$\chi_{\rm eff}$	$M_{\rm f}/M_\odot$	$a_{\rm f}$	$E_{\rm rad}/(M_\odot c^2)$	$\ell_{\rm peak}/({\rm erg\,s^{-1}})$	$d_L/{\rm Mpc}$	z	$\Delta\Omega/{\rm deg}^2$
GW150914	$35.6^{+4.8}_{-3.0}$	$30.6^{+3.0}_{-4.4}$	$28.6^{+1.6}_{-1.5}$	$-0.01^{+0.12}_{-0.13}$	$63.1^{+3.3}_{-3.0}$	$0.69^{+0.05}_{-0.04}$	$3.1^{+0.4}_{-0.4}$	$3.6^{+0.4}_{-0.4}\times10^{56}$	430^{+150}_{-170}	$0.09^{+0.03}_{-0.03}$	180
GW151012	$23.3^{+14.0}_{-5.5}$	$13.6^{+4.1}_{-4.8}$	$15.2^{+2.0}_{-1.1}$	$0.04^{+0.28}_{-0.19}$	$35.7^{+9.9}_{-3.8}$	$0.67^{+0.13}_{-0.11}$	$1.5^{+0.5}_{-0.5}$	$3.2^{+0.8}_{-1.7}\times10^{56}$	1060^{+540}_{-480}	$0.21^{+0.09}_{-0.09}$	1555
GW151226	$13.7^{+8.8}_{-3.2}$	$7.7^{+2.2}_{-2.6}$	$8.9^{+0.3}_{-0.3}$	$0.18^{+0.20}_{-0.12}$	$20.5^{+6.4}_{-1.5}$	$0.74^{+0.07}_{-0.05}$	$1.0^{+0.1}_{-0.2}$	$3.4^{+0.7}_{-1.7}\times10^{56}$	440^{+180}_{-190}	$0.09^{+0.04}_{-0.04}$	1033
GW170104	$31.0^{+7.2}_{-5.6}$	$20.1^{+4.9}_{-4.5}$	$21.5^{+2.1}_{-1.7}$	$-0.04^{+0.17}_{-0.20}$	$49.1^{+5.2}_{-3.9}$	$0.66^{+0.08}_{-0.10}$	$2.2^{+0.5}_{-0.5}$	$3.3^{+0.6}_{-0.9}\times10^{56}$	960^{+430}_{-410}	$0.19^{+0.07}_{-0.08}$	924
GW170608	$10.9^{+5.3}_{-1.7}$	$7.6^{+1.3}_{-2.1}$	$7.9^{+0.2}_{-0.2}$	$0.03^{+0.19}_{-0.07}$	$17.8^{+3.2}_{-0.7}$	$0.69^{+0.04}_{-0.04}$	$0.9^{+0.05}_{-0.1}$	$3.5^{+0.4}_{-1.3}\times10^{56}$	320^{+120}_{-110}	$0.07^{+0.02}_{-0.02}$	396
GW170729	$50.6^{+16.6}_{-10.2}$	$34.3^{+9.1}_{-10.1}$	$35.7^{+6.5}_{-4.7}$	$0.36^{+0.21}_{-0.25}$	$80.3^{+14.6}_{-10.2}$	$0.81^{+0.07}_{-0.13}$	$4.8^{+1.7}_{-1.7}$	$4.2^{+0.9}_{-1.5}\times10^{56}$	2750^{+1350}_{-1320}	$0.48^{+0.19}_{-0.20}$	1033
GW170809	$35.2^{+8.3}_{-6.0}$	$23.8^{+5.2}_{-5.1}$	$25.0^{+2.1}_{-1.6}$	$0.07^{+0.16}_{-0.16}$	$56.4^{+5.2}_{-3.7}$	$0.70^{+0.08}_{-0.09}$	$2.7^{+0.6}_{-0.6}$	$3.5^{+0.6}_{-0.9}\times10^{56}$	990^{+320}_{-380}	$0.20^{+0.05}_{-0.07}$	340
GW170814	$30.7^{+5.7}_{-3.0}$	$25.3^{+2.9}_{-4.1}$	$24.2^{+1.4}_{-1.1}$	$0.07^{+0.12}_{-0.11}$	$53.4^{+3.2}_{-2.4}$	$0.72^{+0.07}_{-0.05}$	$2.7^{+0.4}_{-0.3}$	$3.7^{+0.4}_{-0.5}\times10^{56}$	580^{+160}_{-210}	$0.12^{+0.03}_{-0.04}$	87
GW170817	$1.46^{+0.12}_{-0.10}$	$1.27^{+0.09}_{-0.09}$	$1.186^{+0.001}_{-0.001}$	$0.00^{+0.02}_{-0.01}$	≤ 2.8	≤ 0.89	≥ 0.04	$\geq 0.1\times10^{56}$	40^{+10}_{-10}	$0.01^{+0.00}_{-0.00}$	16
GW170818	$35.5^{+7.5}_{-4.7}$	$26.8^{+4.3}_{-5.2}$	$26.7^{+2.1}_{-1.7}$	$-0.09^{+0.18}_{-0.21}$	$59.8^{+4.8}_{-3.8}$	$0.67^{+0.07}_{-0.08}$	$2.7^{+0.5}_{-0.5}$	$3.4^{+0.5}_{-0.7}\times10^{56}$	1020^{+430}_{-360}	$0.20^{+0.07}_{-0.07}$	39
GW170823	$39.6^{+10.0}_{-6.6}$	$29.4^{+6.3}_{-7.1}$	$29.3^{+4.2}_{-3.2}$	$0.08^{+0.20}_{-0.22}$	$65.6^{+9.4}_{-6.6}$	$0.71^{+0.08}_{-0.10}$	$3.3^{+0.9}_{-0.8}$	$3.6^{+0.6}_{-0.9}\times10^{56}$	1850^{+840}_{-840}	$0.34^{+0.13}_{-0.14}$	1651

- Most massive and distant source

Abbott et al, arXiv:1811.12907 (2018)

GWTC-1 results

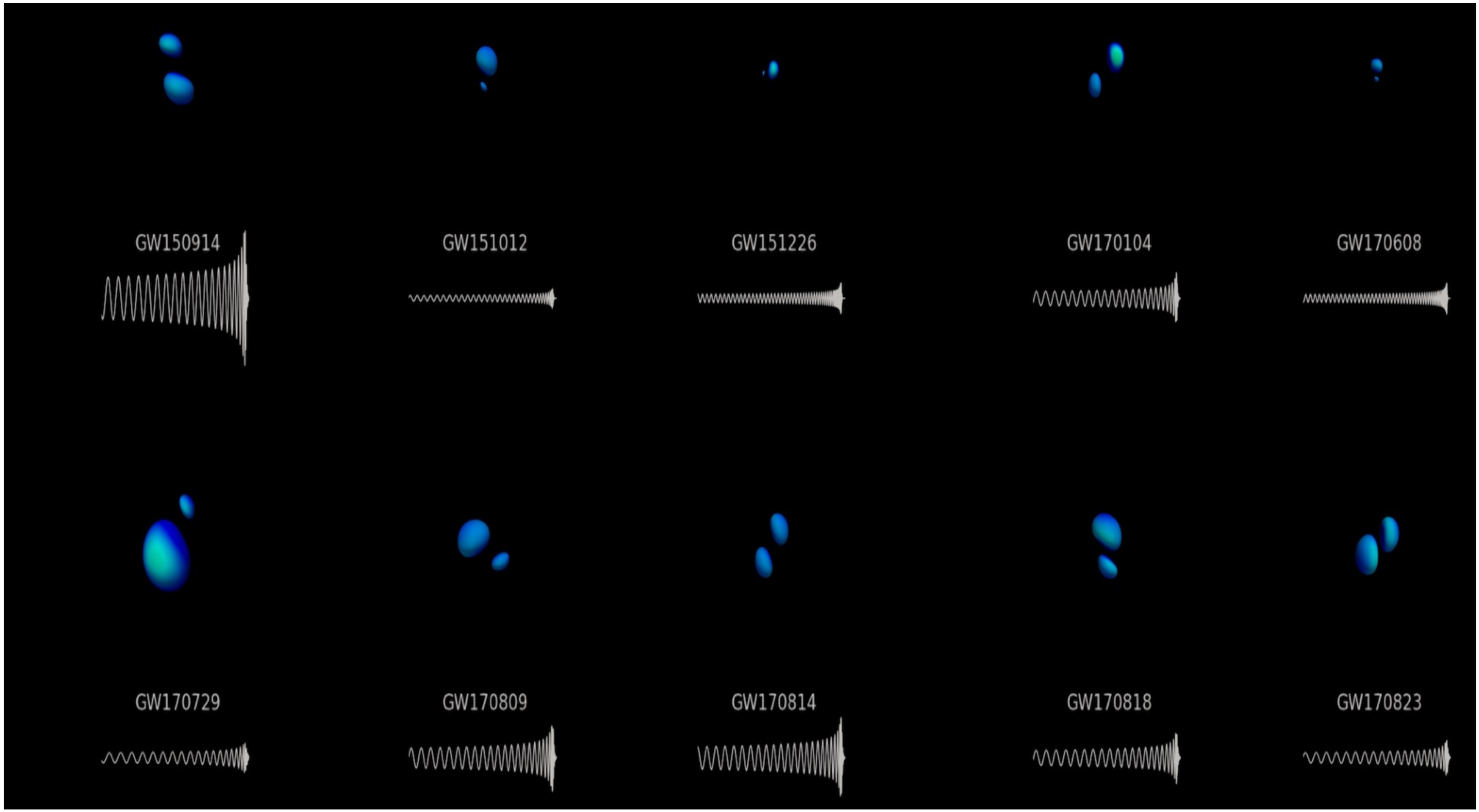

ligo.caltech.edu

BBH Masses

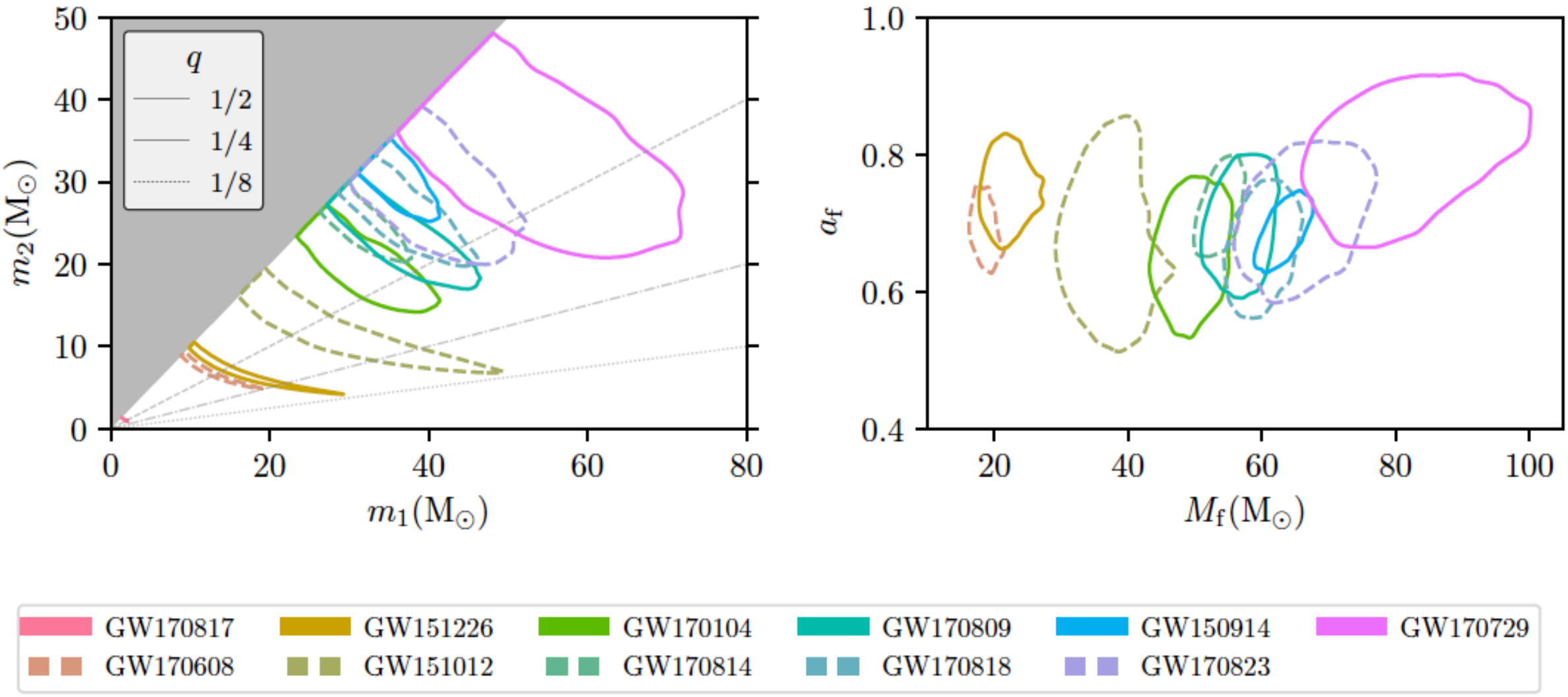

Abbott et al, arXiv:1811.12907 (2018)

BBH Distance

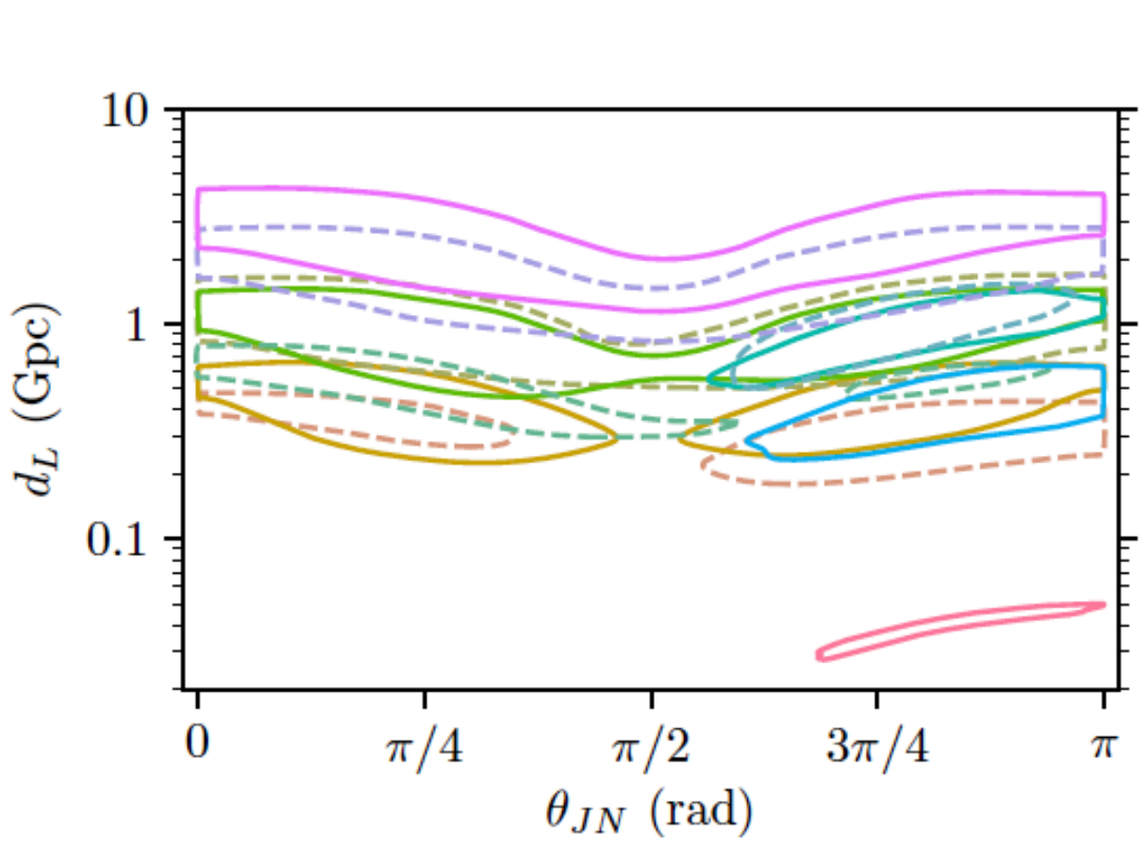

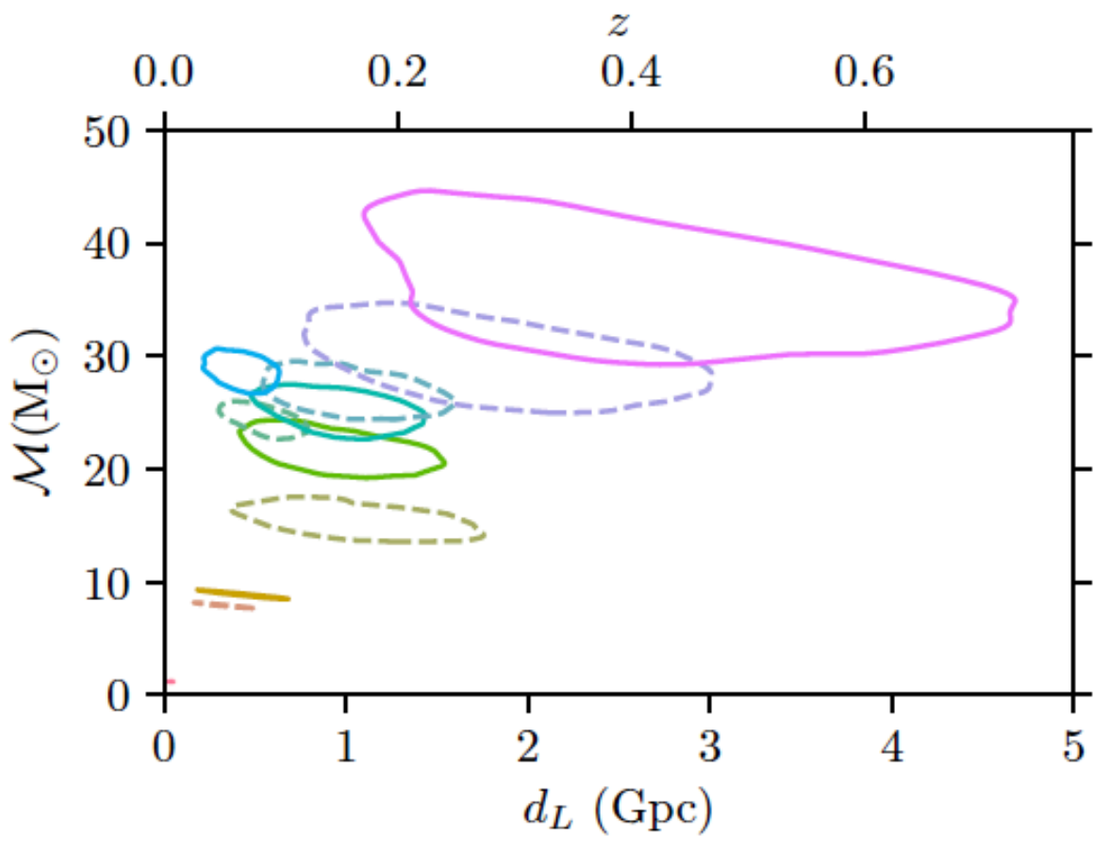

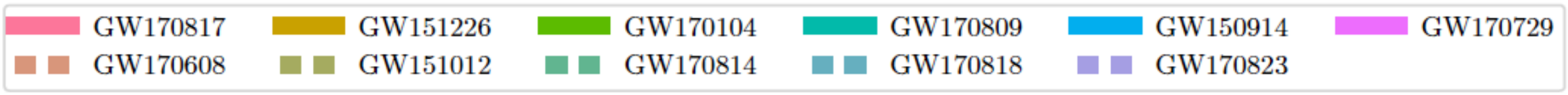

Abbott et al, arXiv:1811.12907 (2018)

BBH Spins

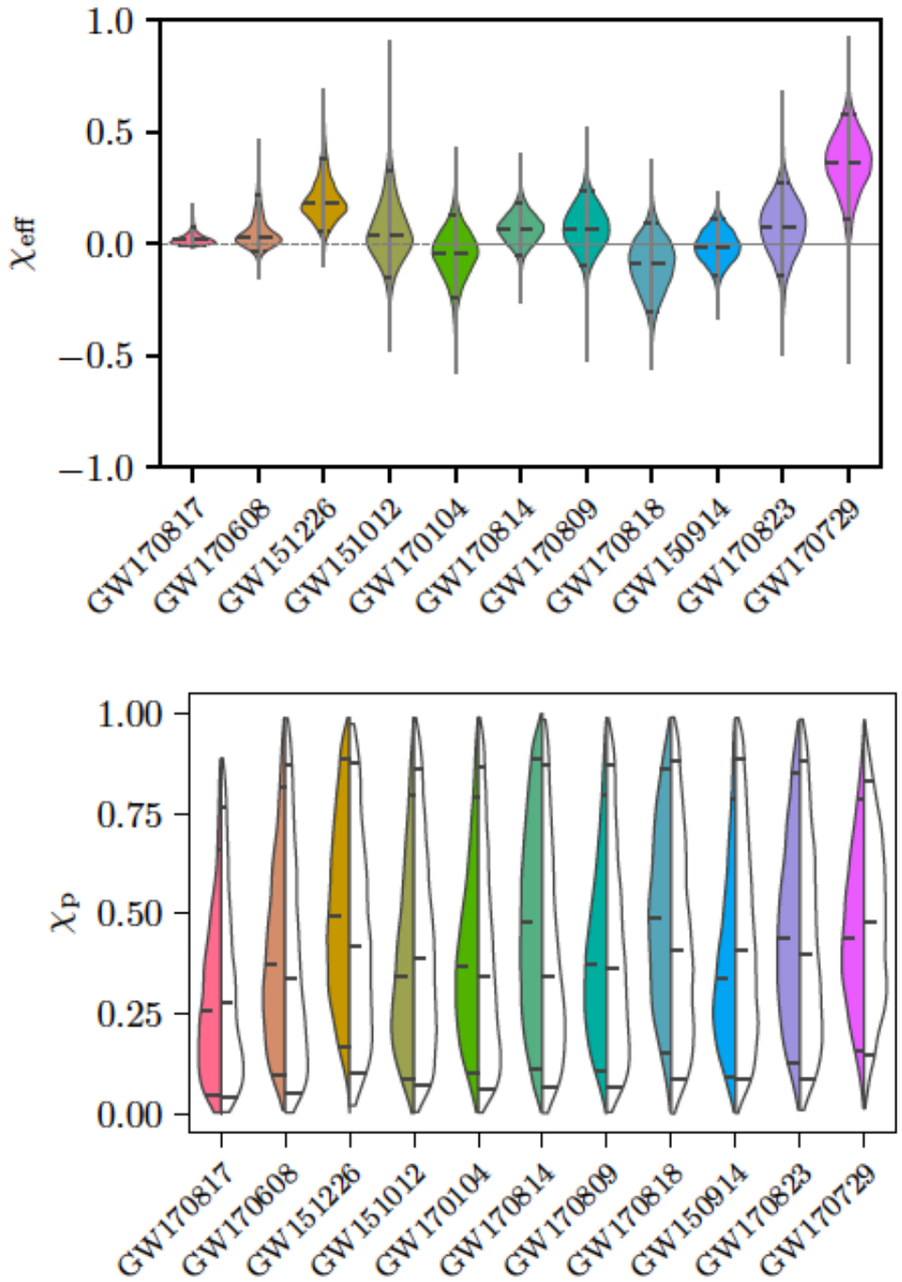

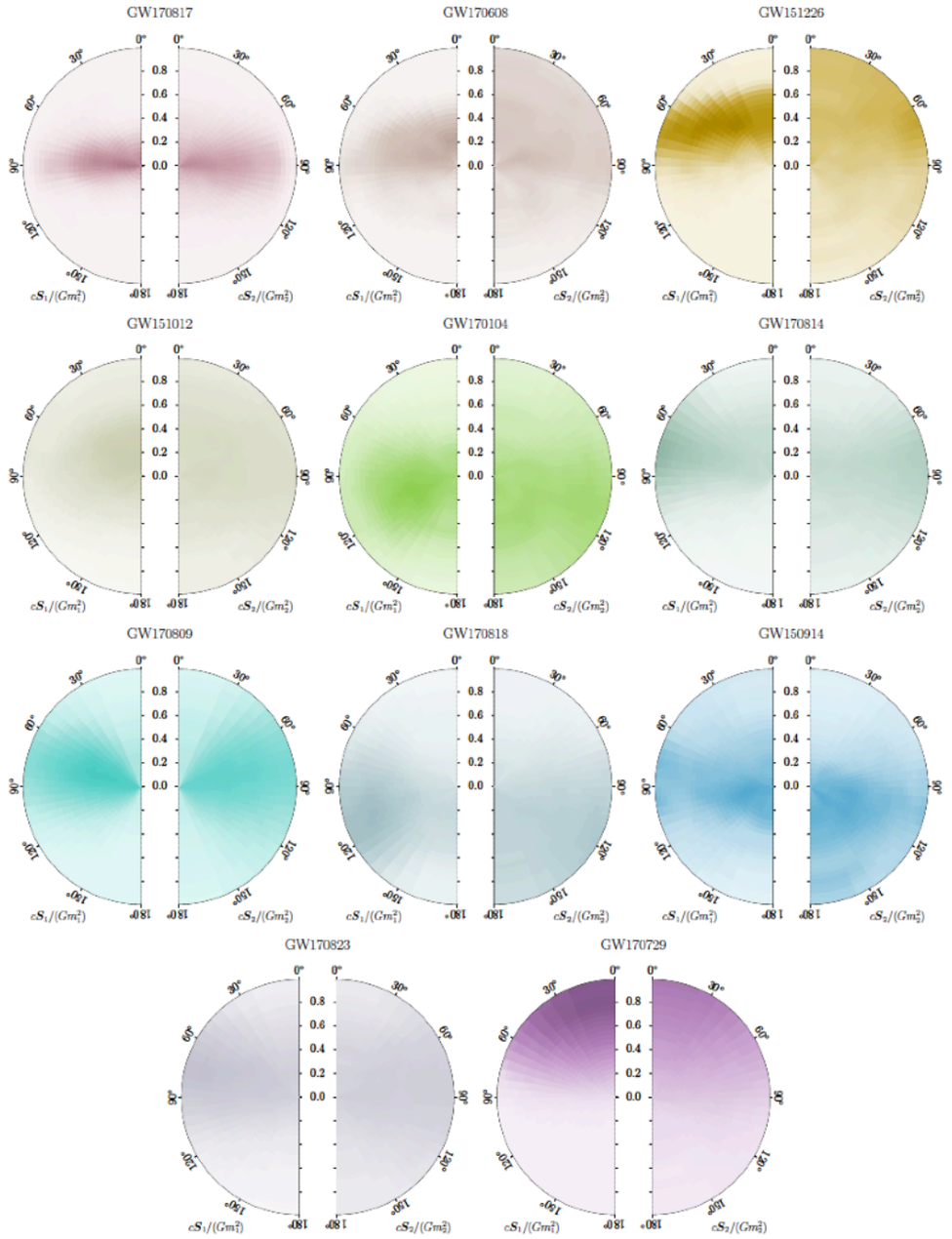

Abbott et al, arXiv:1811.12907 (2018)

GWTC-1 results

Event	$m_1/M_\odot$	$m_2/M_\odot$	$\mathcal{M}/M_\odot$	$\chi_{\rm eff}$	$M_{\rm f}/M_\odot$	$a_{\rm f}$	$E_{\rm rad}/(M_\odot c^2)$	$\ell_{\rm peak}/({\rm erg\,s^{-1}})$	$d_L/{\rm Mpc}$	z	$\Delta\Omega/{\rm deg}^2$
GW150914	$35.6^{+4.8}_{-3.0}$	$30.6^{+3.0}_{-4.4}$	$28.6^{+1.6}_{-1.5}$	$-0.01^{+0.12}_{-0.13}$	$63.1^{+3.3}_{-3.0}$	$0.69^{+0.05}_{-0.04}$	$3.1^{+0.4}_{-0.4}$	$3.6^{+0.4}_{-0.4}\times10^{56}$	430^{+150}_{-170}	$0.09^{+0.03}_{-0.03}$	180
GW151012	$23.3^{+14.0}_{-5.5}$	$13.6^{+4.1}_{-4.8}$	$15.2^{+2.0}_{-1.1}$	$0.04^{+0.28}_{-0.19}$	$35.7^{+9.9}_{-3.8}$	$0.67^{+0.13}_{-0.11}$	$1.5^{+0.5}_{-0.5}$	$3.2^{+0.8}_{-1.7}\times10^{56}$	1060^{+540}_{-480}	$0.21^{+0.09}_{-0.09}$	1555
GW151226	$13.7^{+8.8}_{-3.2}$	$7.7^{+2.2}_{-2.6}$	$8.9^{+0.3}_{-0.3}$	$0.18^{+0.20}_{-0.12}$	$20.5^{+6.4}_{-1.5}$	$0.74^{+0.07}_{-0.05}$	$1.0^{+0.1}_{-0.2}$	$3.4^{+0.7}_{-1.7}\times10^{56}$	440^{+180}_{-190}	$0.09^{+0.04}_{-0.04}$	1033
GW170104	$31.0^{+7.2}_{-5.6}$	$20.1^{+4.9}_{-4.5}$	$21.5^{+2.1}_{-1.7}$	$-0.04^{+0.17}_{-0.20}$	$49.1^{+5.2}_{-3.9}$	$0.66^{+0.08}_{-0.10}$	$2.2^{+0.5}_{-0.5}$	$3.3^{+0.6}_{-0.9}\times10^{56}$	960^{+430}_{-410}	$0.19^{+0.07}_{-0.08}$	924
GW170608	$10.9^{+5.3}_{-1.7}$	$7.6^{+1.3}_{-2.1}$	$7.9^{+0.2}_{-0.2}$	$0.03^{+0.19}_{-0.07}$	$17.8^{+3.2}_{-0.7}$	$0.69^{+0.04}_{-0.04}$	$0.9^{+0.05}_{-0.1}$	$3.5^{+0.4}_{-1.3}\times10^{56}$	320^{+120}_{-110}	$0.07^{+0.02}_{-0.02}$	396
GW170729	$50.6^{+16.6}_{-10.2}$	$34.3^{+9.1}_{-10.1}$	$35.7^{+6.5}_{-4.7}$	$0.36^{+0.21}_{-0.25}$	$80.3^{+14.6}_{-10.2}$	$0.81^{+0.07}_{-0.13}$	$4.8^{+1.7}_{-1.7}$	$4.2^{+0.9}_{-1.5}\times10^{56}$	2750^{+1350}_{-1320}	$0.48^{+0.19}_{-0.20}$	1033
GW170809	$35.2^{+8.3}_{-6.0}$	$23.8^{+5.2}_{-5.1}$	$25.0^{+2.1}_{-1.6}$	$0.07^{+0.16}_{-0.16}$	$56.4^{+5.2}_{-3.7}$	$0.70^{+0.08}_{-0.09}$	$2.7^{+0.6}_{-0.6}$	$3.5^{+0.6}_{-0.9}\times10^{56}$	990^{+320}_{-380}	$0.20^{+0.05}_{-0.07}$	340
GW170814	$30.7^{+5.7}_{-3.0}$	$25.3^{+2.9}_{-4.1}$	$24.2^{+1.4}_{-1.1}$	$0.07^{+0.12}_{-0.11}$	$53.4^{+3.2}_{-2.4}$	$0.72^{+0.07}_{-0.05}$	$2.7^{+0.4}_{-0.3}$	$3.7^{+0.4}_{-0.5}\times10^{56}$	580^{+160}_{-210}	$0.12^{+0.03}_{-0.04}$	87
GW170817	$1.46^{+0.12}_{-0.10}$	$1.27^{+0.09}_{-0.09}$	$1.186^{+0.001}_{-0.001}$	$0.00^{+0.02}_{-0.01}$	≤ 2.8	≤ 0.89	≥ 0.04	$\geq 0.1\times10^{56}$	40^{+10}_{-10}	$0.01^{+0.00}_{-0.00}$	16
GW170818	$35.5^{+7.5}_{-4.7}$	$26.8^{+4.3}_{-5.2}$	$26.7^{+2.1}_{-1.7}$	$-0.09^{+0.18}_{-0.21}$	$59.8^{+4.8}_{-3.8}$	$0.67^{+0.07}_{-0.08}$	$2.7^{+0.5}_{-0.5}$	$3.4^{+0.5}_{-0.7}\times10^{56}$	1020^{+430}_{-360}	$0.20^{+0.07}_{-0.07}$	39
GW170823	$39.6^{+10.0}_{-6.6}$	$29.4^{+6.3}_{-7.1}$	$29.3^{+4.2}_{-3.2}$	$0.08^{+0.20}_{-0.22}$	$65.6^{+9.4}_{-6.6}$	$0.71^{+0.08}_{-0.10}$	$3.3^{+0.9}_{-0.8}$	$3.6^{+0.6}_{-0.9}\times10^{56}$	1850^{+840}_{-840}	$0.34^{+0.13}_{-0.14}$	1651

- 1st ever BNS and best resolved event

Abbott et al, arXiv:1811.12907 (2018)

Common question....

- ...how do we know GW170817 was a BNS?

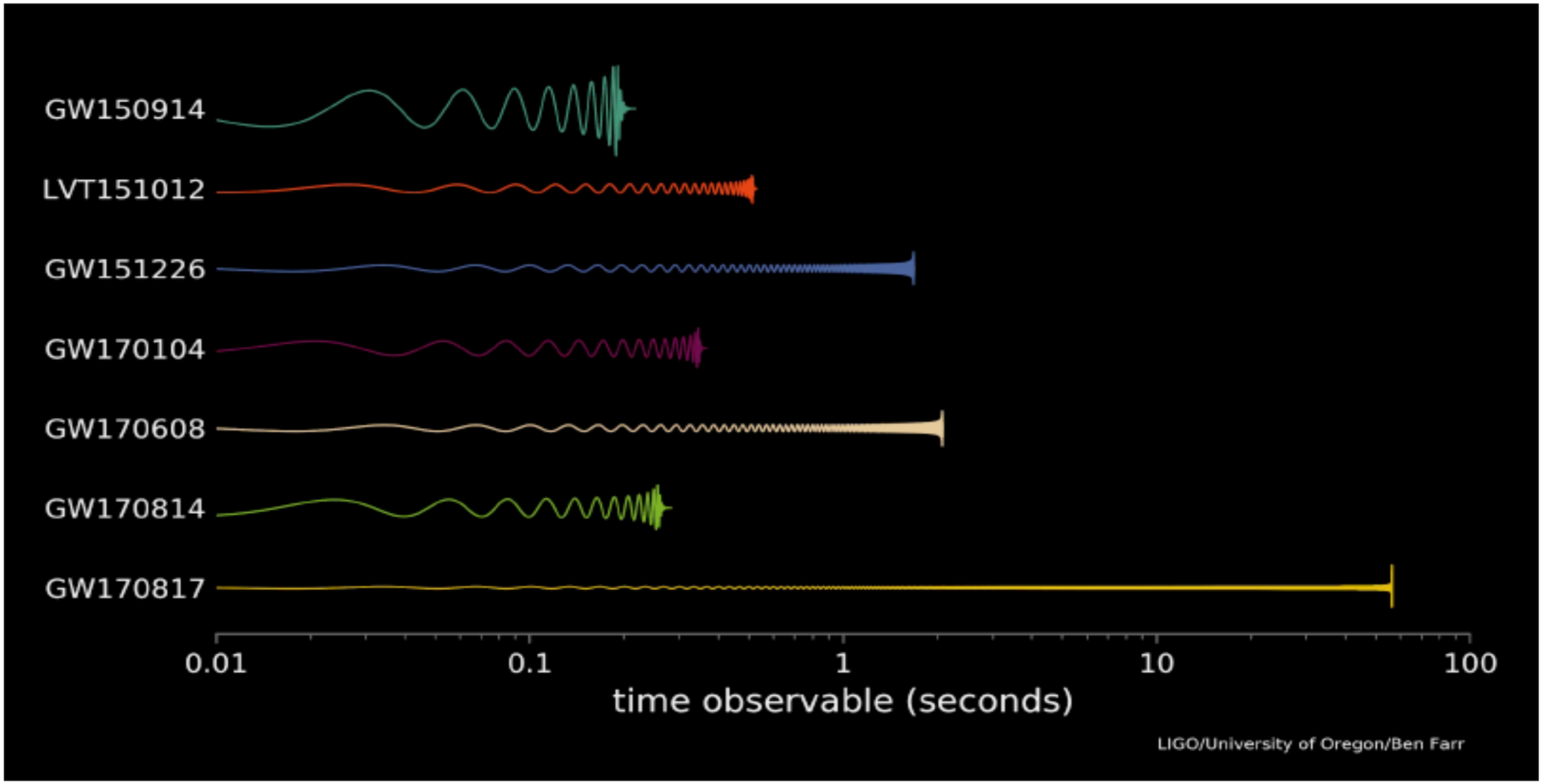

How well do we measure NS mass?

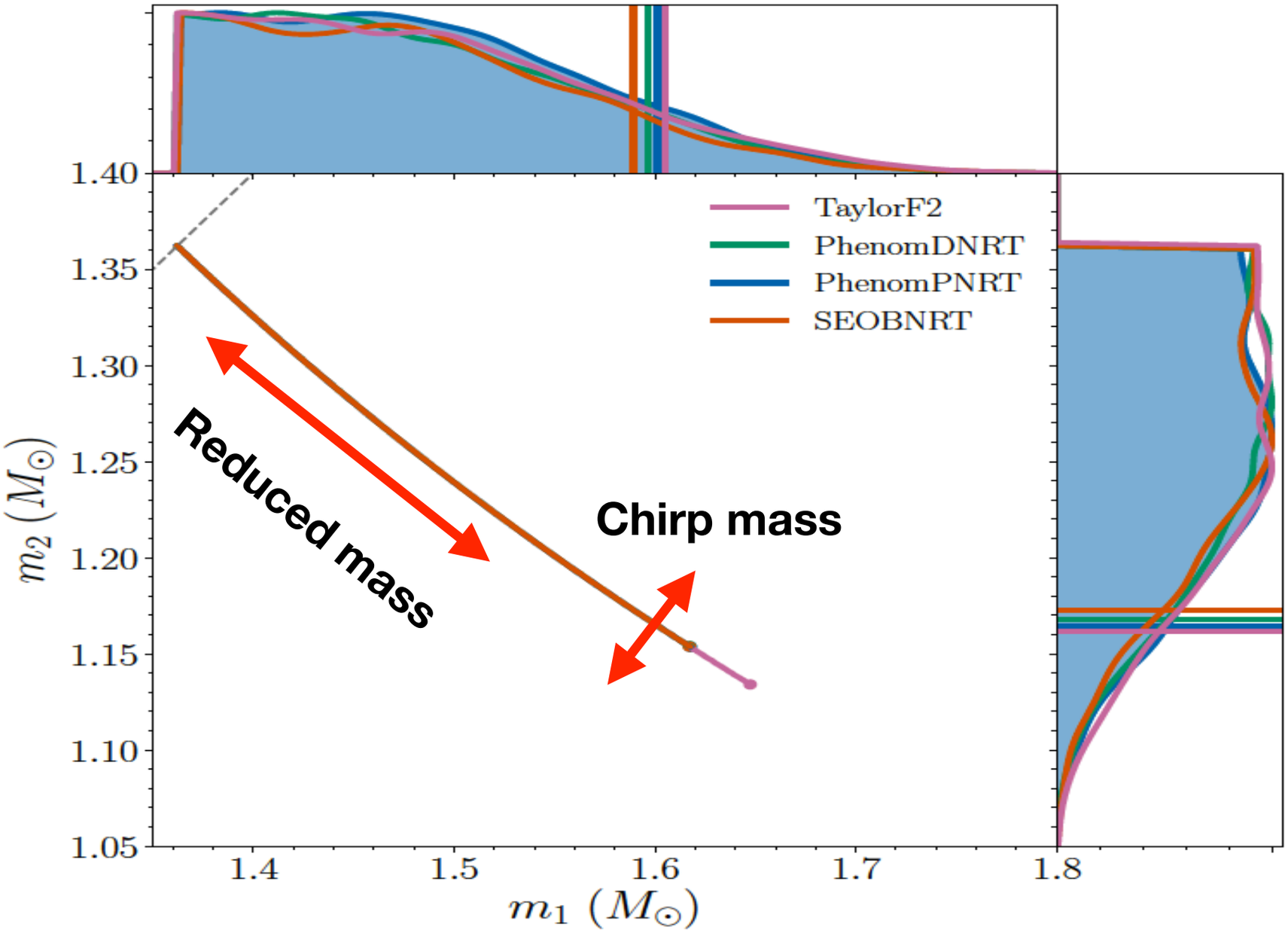

Abbott et al, arXiv:1805.11579 (2018)

How well do we measure NS mass?

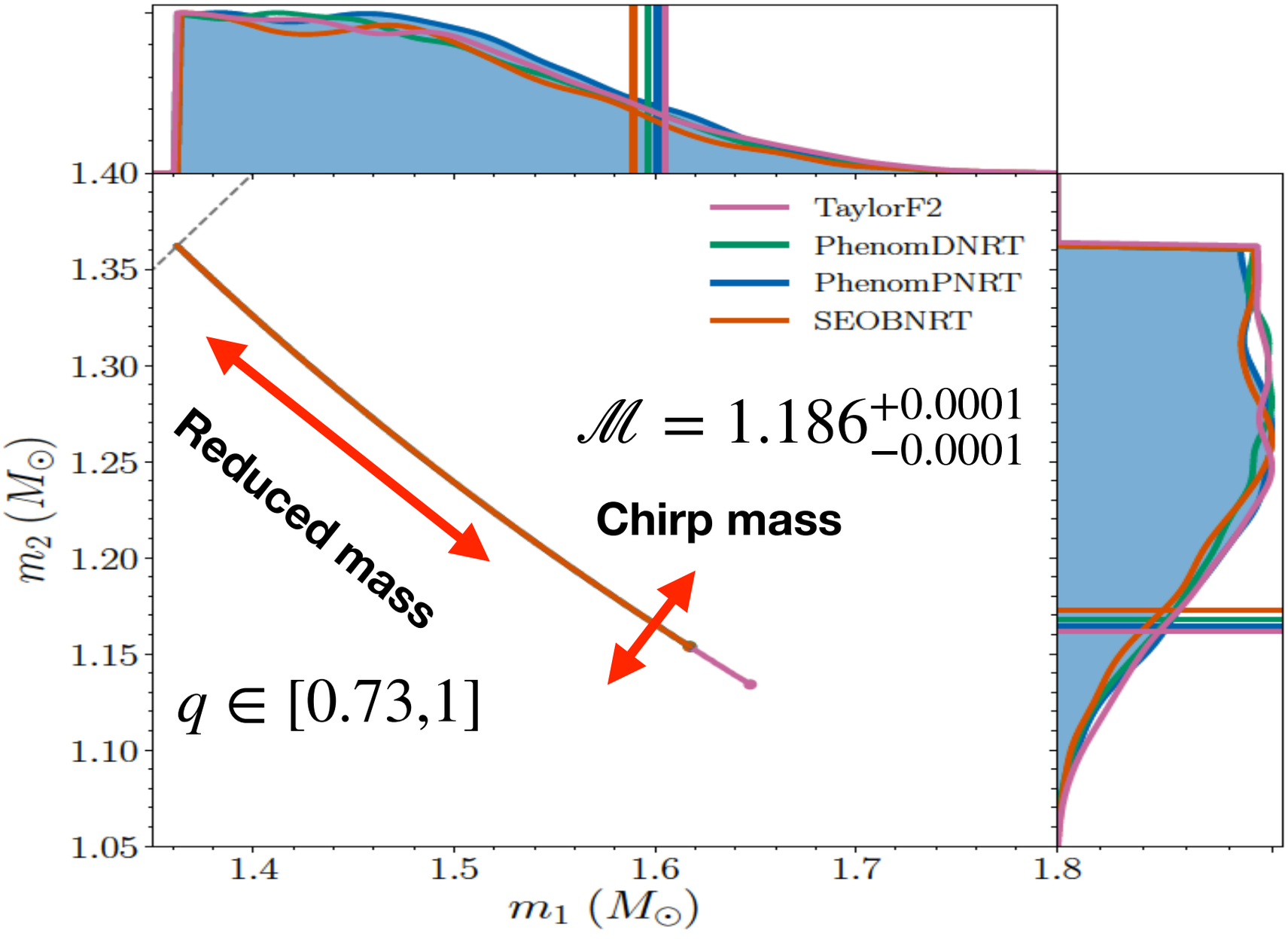

Abbott et al, arXiv:1805.11579 (2018)

GRB Association

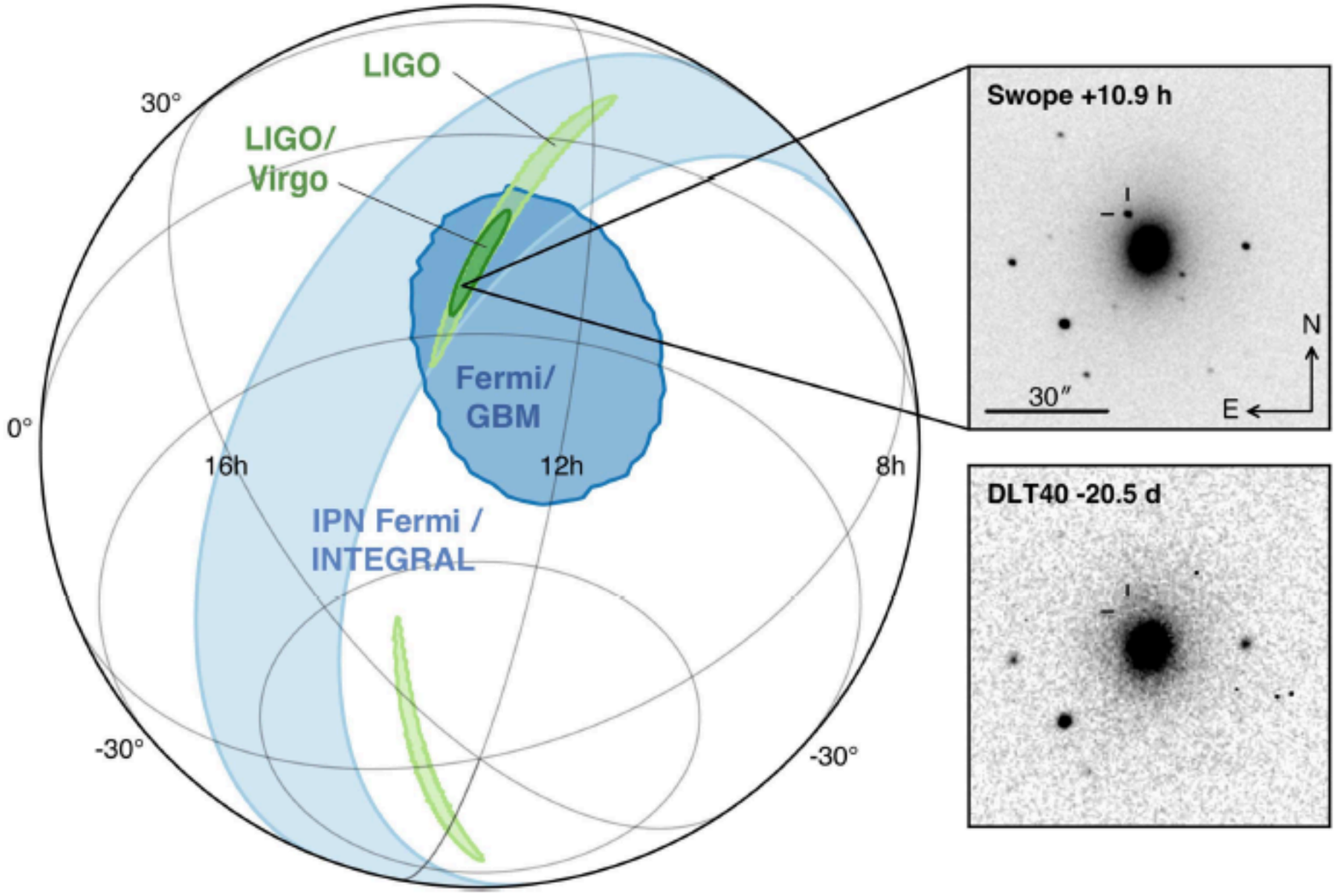

www.ligo.caltech.edu/images

EM Follow-up Timeline

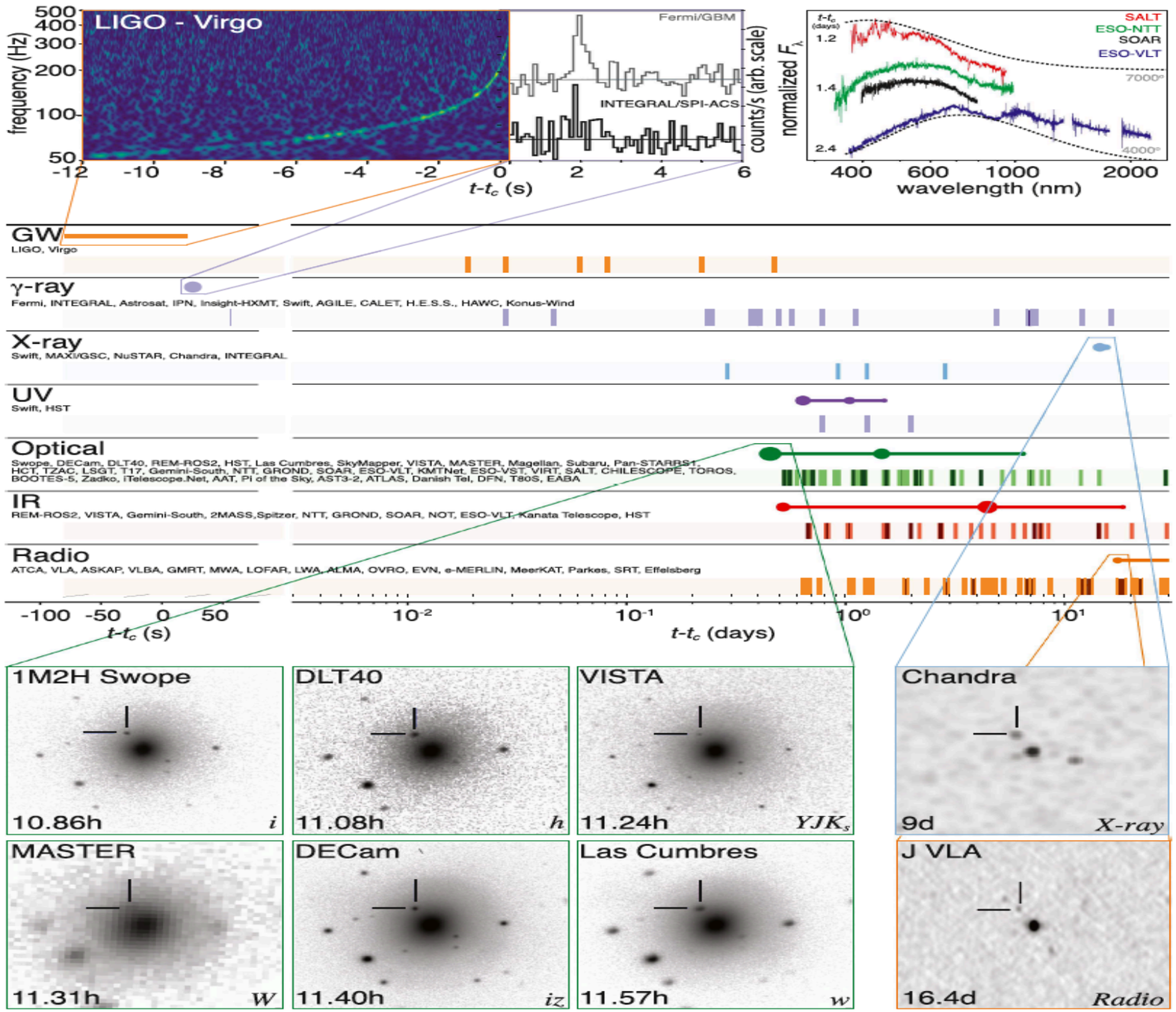

Abbott et al, ApJ Letters 848, L13 (2017)

01/02

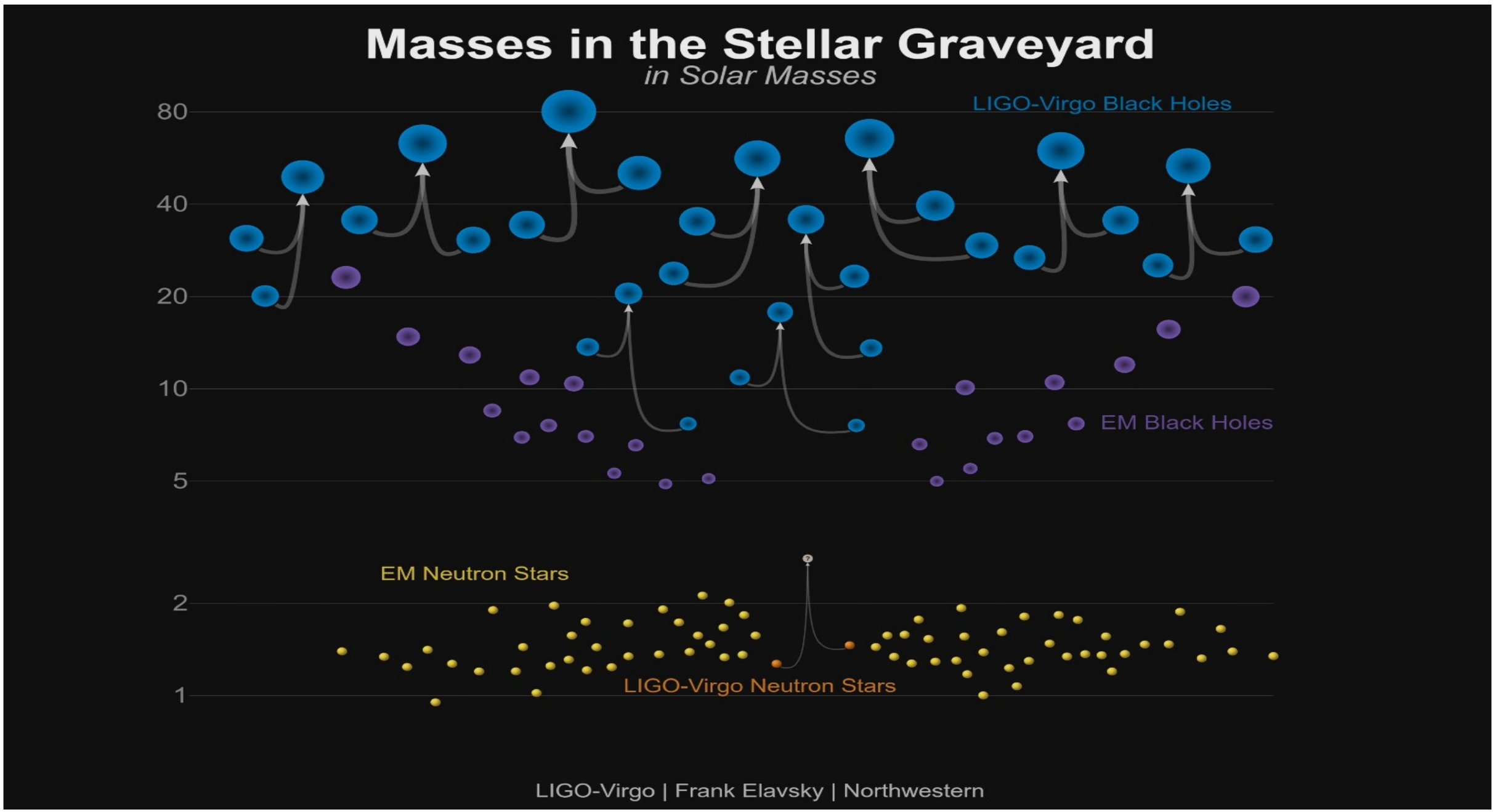

www.ligo.caltech.edu/images

O1/O2

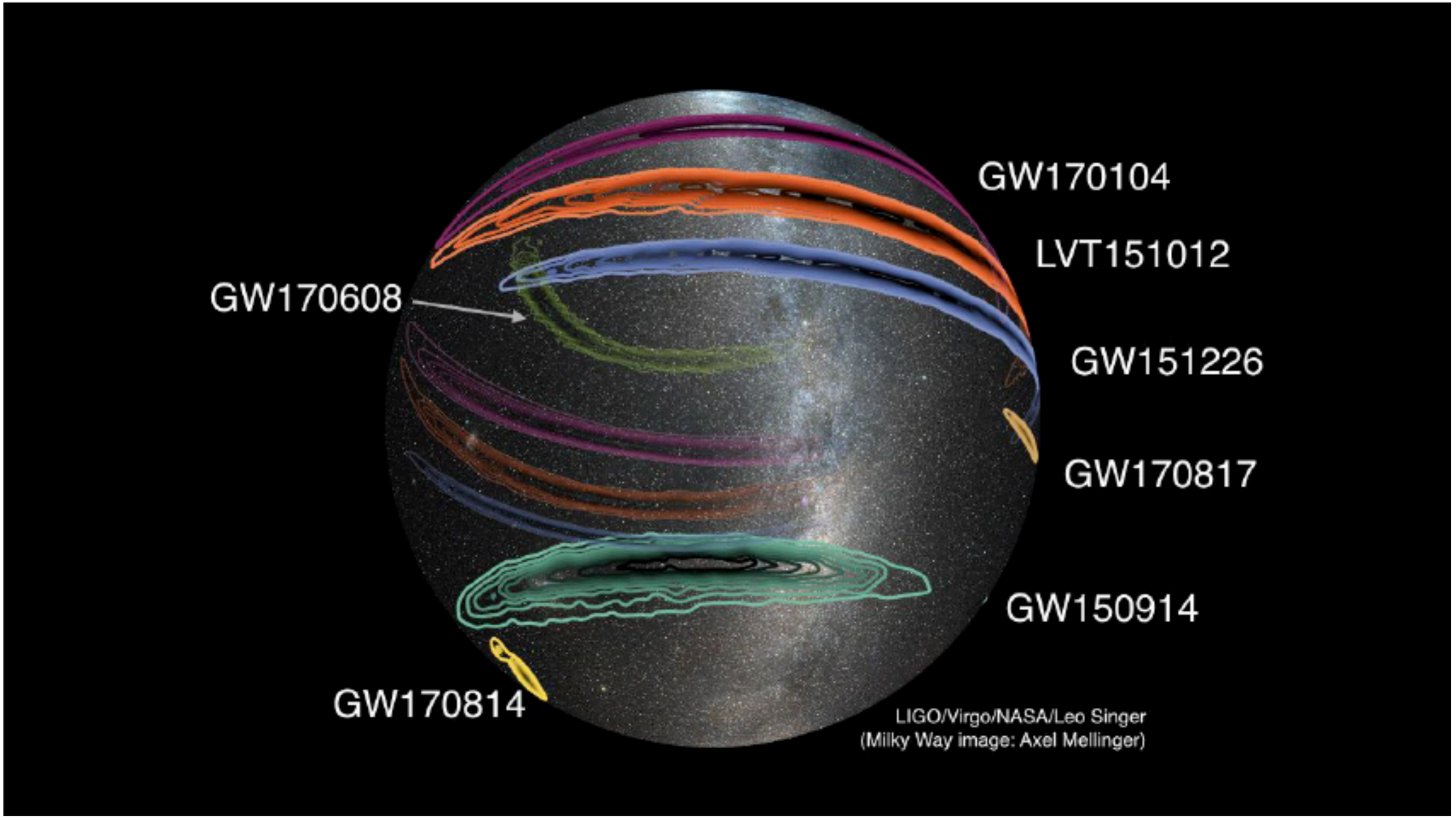
GW170104
LVT151012
GW170608
GW151226
GW170817
GW150914
GW170814
LIGO/Virgo/NASA/Leo Singer
(Milky Way image: Axel Mellinger)

So, what can we do?

- Fundamental physics
- Astrophysics
- Extreme MatterCosmology
- Cosmology

Fundamental Physics

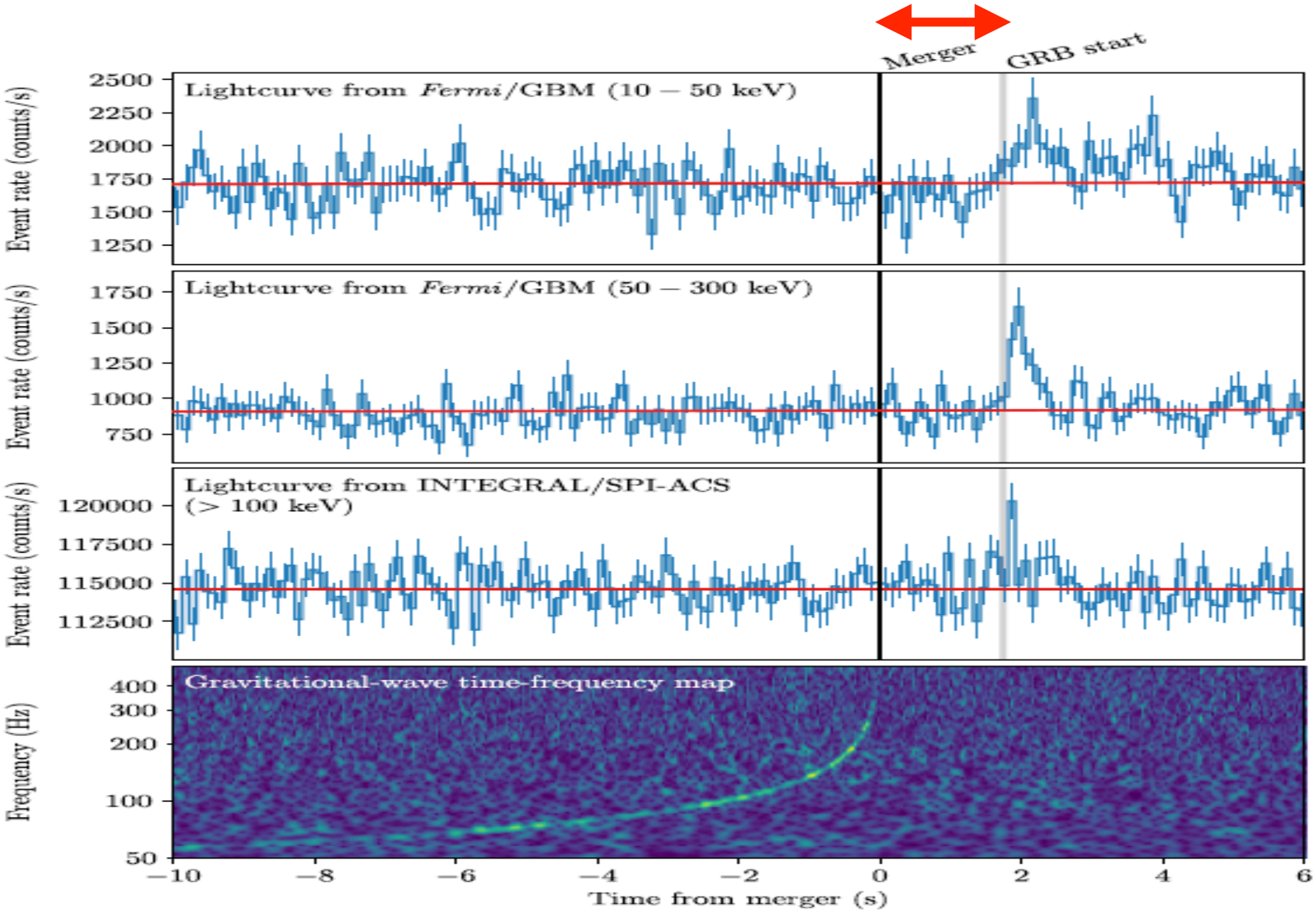

Abbott et al, ApJ Letters 848, L13 (2017)

Fundamental Physics

- The time delay between the GW and GRB detections over 1.3x10^8 Lyrs was (N.B. analysis allows for +/- 10 secs)

$$\Delta t = (1.74 \pm 0.05)\, s$$

- Defining the fractional difference between the speed of light and GWs as

$$\frac{c_g - c}{c} \approx c\frac{\Delta t}{D_L}$$

- We find the following constraint

$$-3 \times 10^{-15} \leq \frac{\Delta c}{c} \leq 7 \times 10^{-16}$$

- Large consequences for cosmological theories

Abbott et al, ApJ Letters 848, L13 (2017)

Fundamental Physics

	$c_g = c$	$c_g \neq c$
Horndeski	General Relativity quintessence/k-essence [42] Brans-Dicke/$f(R)$ [43, 44] Kinetic Gravity Braiding [46]	quartic/quintic Galileons [13, 14] Fab Four [15, 16] de Sitter Horndeski [45] $G_{\mu\nu}\phi^\mu\phi^\nu$ [47], Gauss-Bonnet
beyond H.	Derivative Conformal (20) [18] Disformal Tuning (22) DHOST with $A_1 = 0$	quartic/quintic GLPV [19] DHOST [20, 48] with $A_1 \neq 0$
	Viable after GW170817	Non-viable after GW170817

- with extension to: Einstein-Aether, Horava gravity, Generalised Proca, TeVeS, massive gravity, bigravity, multi-gravity, MOND-like theories

arXiv:1710.05901, 1710.06394, 1710.05893, 1710.05877….

Fundamental Physics

- Shapiro delay is defined as $\Delta t_s = -\frac{1+\gamma}{c}\int_{r_e}^{r_o} U(r(l))dl$
- γ is the PPN parameter parameterising a deviation from Einstein-Maxwell theory
- Conservative bound on $\Delta\gamma = |\gamma_{GW} - \gamma_{EM}| \leq 2\frac{\Delta t}{\Delta t_s}$
- is $-2.6 \times 10^{-7} \leq \Delta\gamma \leq 1.2 \times 10^{-6}$
- Newer result (S. Boran et al, 1710.06168) using more sophisticated dark matter halo model gives

$$\Delta\gamma \leq 3.9 \times 10^{-8}$$

- implying that MOND-like dark matter emulator theories are ruled out, as the GWs would have arrived 1000 days before the EM emission

Fundamental Physics

- Fourier domain waveform

$$\tilde{h}(f) = A(f)e^{i\Psi_{GR}(f)}$$

- GW inspiral phase to 3.5 PN order, i.e. ***(v/c)^7***

$$\Psi_{GR}(f) = 2\pi f t_c + \phi_c - \frac{\pi}{4} + \frac{3}{128}\Big[\psi_0(\pi M f)^{-5/3} + \psi_1(\pi M f)^{-4/3} + \psi_2(\pi M f)^{-1}$$
$$\psi_3(\pi M f)^{-2/3} + \psi_4(\pi M f)^{-1/3} + \psi_5 + \psi_6(\pi M f)^{1/3} + \psi_7(\pi M f)^{2/3} + \Big]$$

Fundamental Physics

- Fourier domain waveform

$$\tilde{h}(f) = A(f) e^{i\Psi_{GR}(f)}$$

- GW inspiral phase to 3.5 PN order, i.e. ***(v/c)^7***

Einstein-Aether
Khronometric

Massive Graviton

$$\Psi_{GR}(f) = 2\pi f t_c + \phi_c - \frac{\pi}{4} + \frac{3}{128}\Big[\psi_0(\pi M f)^{-5/3} + \psi_1(\pi M f)^{-4/3} + \psi_2(\pi M f)^{-1}$$
$$\psi_3(\pi M f)^{-2/3} + \psi_4(\pi M f)^{-1/3} + \psi_5 + \psi_6(\pi M f)^{1/3} + \psi_7(\pi M f)^{2/3} + \Big]$$

Dynamical Chern-Simons

+ scalar-tensor theory at the -1PN order, i.e. f$^{-7/3}$

Fundamental Physics

- Set $\psi_k \rightarrow \psi_k \left(1 + \delta\psi_k\right)$

- Phenomenological phase

$$\Psi(f) = \Psi_{GR}(f) + \Psi_{NGR}(f)$$

- Phenomenological waveform

$$\tilde{h}(f) = A(f) e^{i\Psi_{GR}(f)} e^{i\Psi_{NGR}(f)}$$

- Has been demonstrated that it is enough to search for the dominant effect

Fundamental Physics

- Test of the PN approximation during inspiral

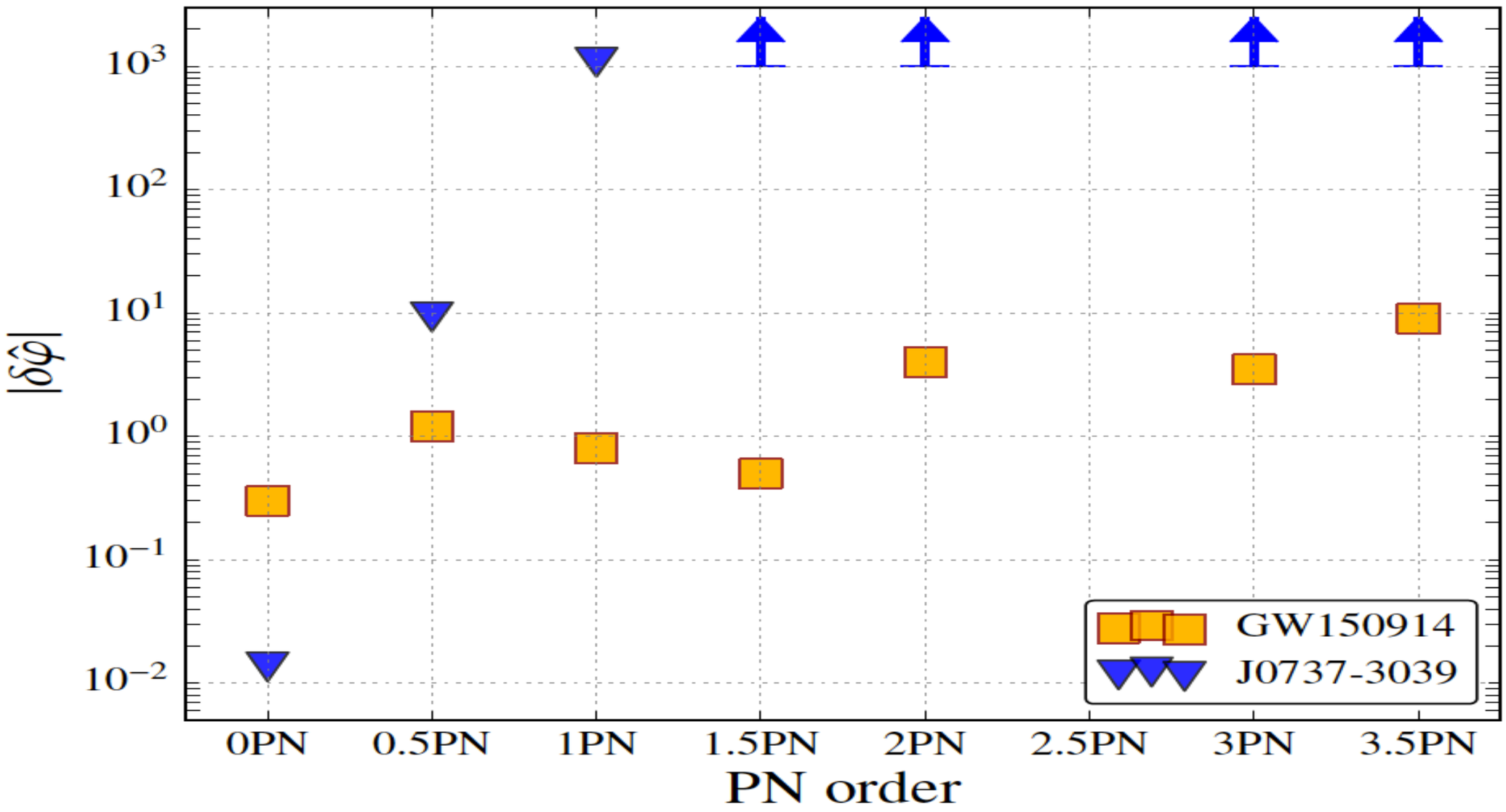

Abbott et al, arXiv:1903.04467

Fundamental Physics

- Test of the PN approximation during inspiral

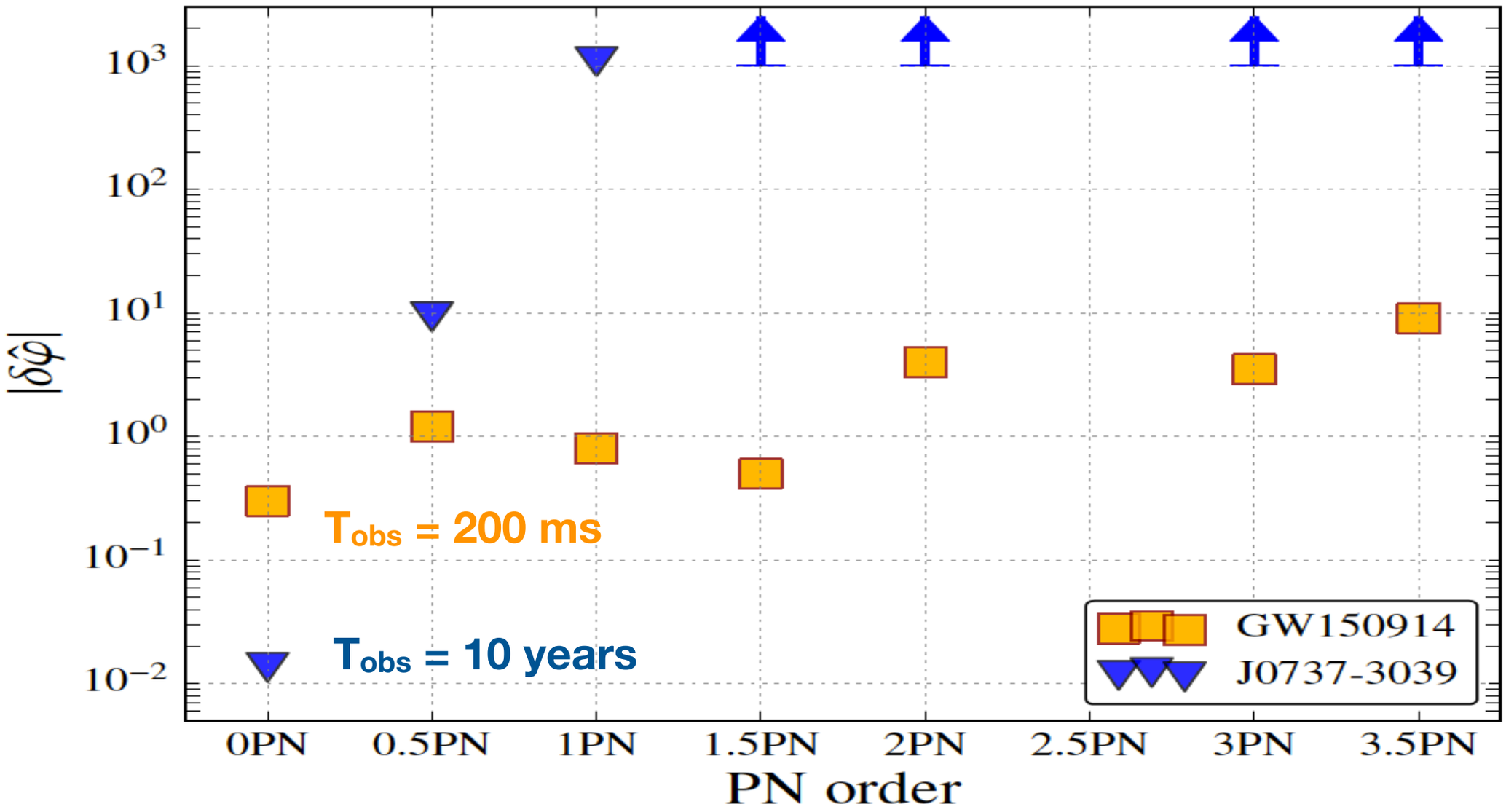

Abbott et al, arXiv:1903.04467

Fundamental Physics

- Test of the PN approximation during inspiral

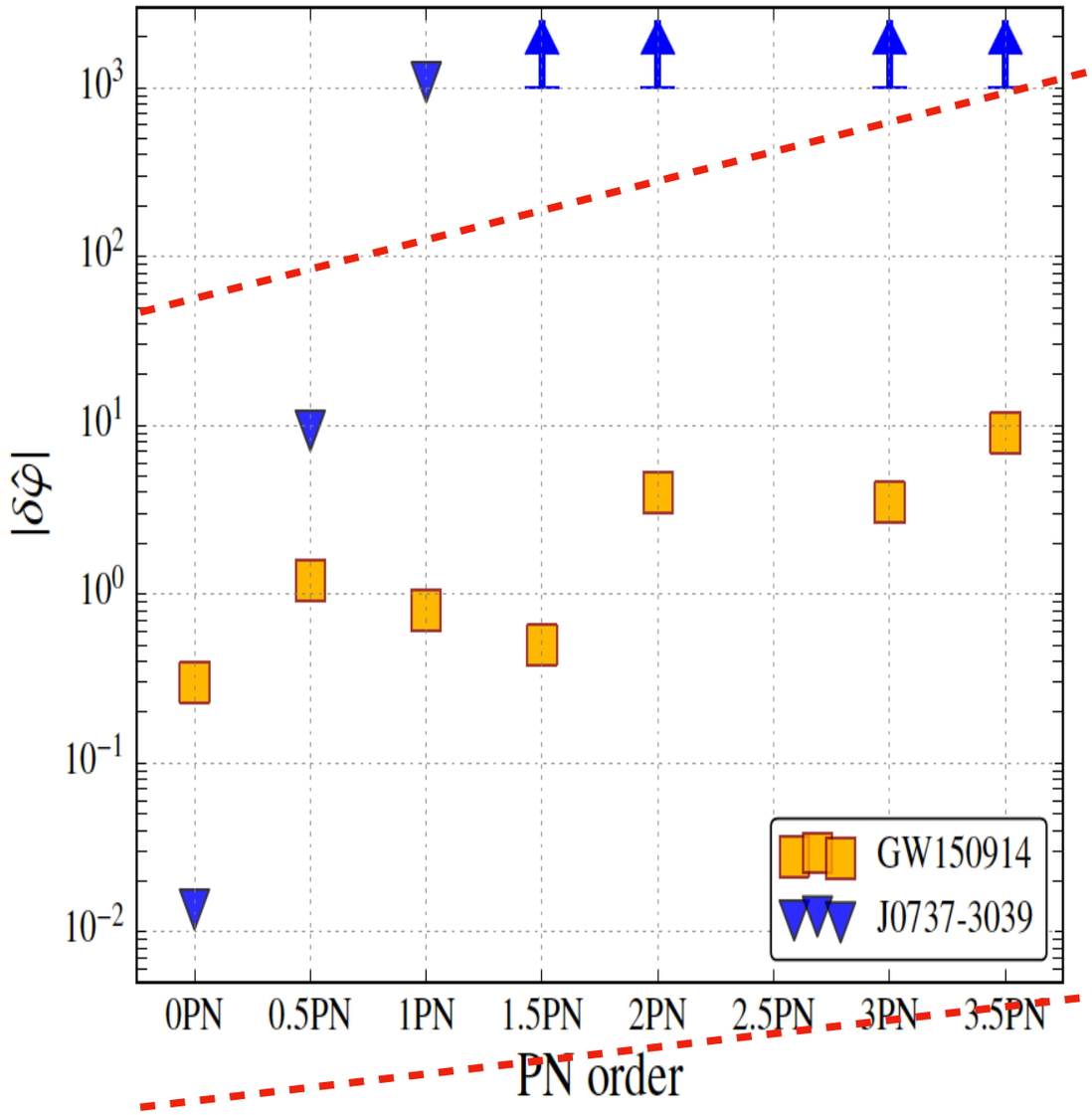

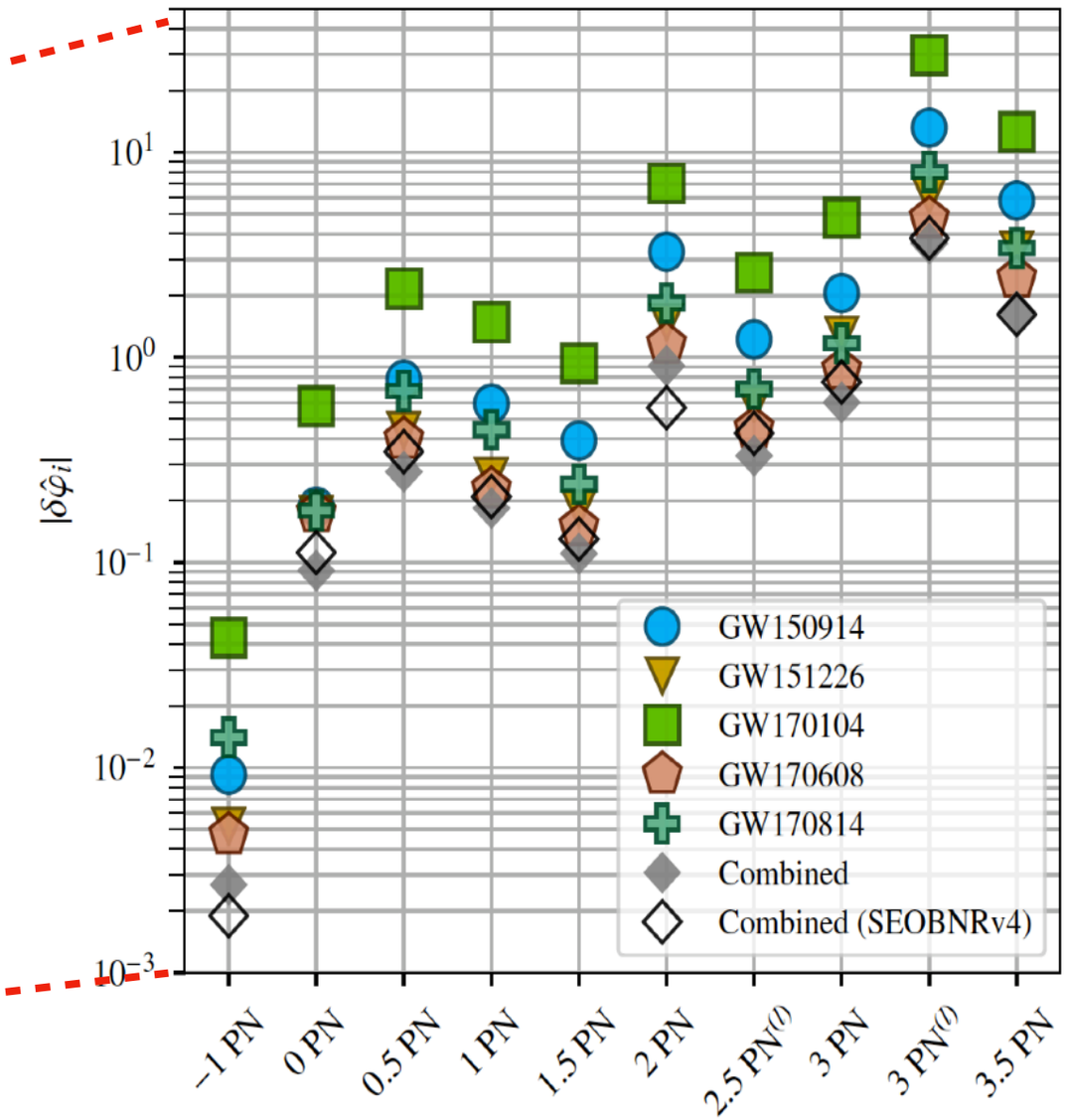

Abbott et al, arXiv:1903.04467

Fundamental Physics

- Test for dipole radiation

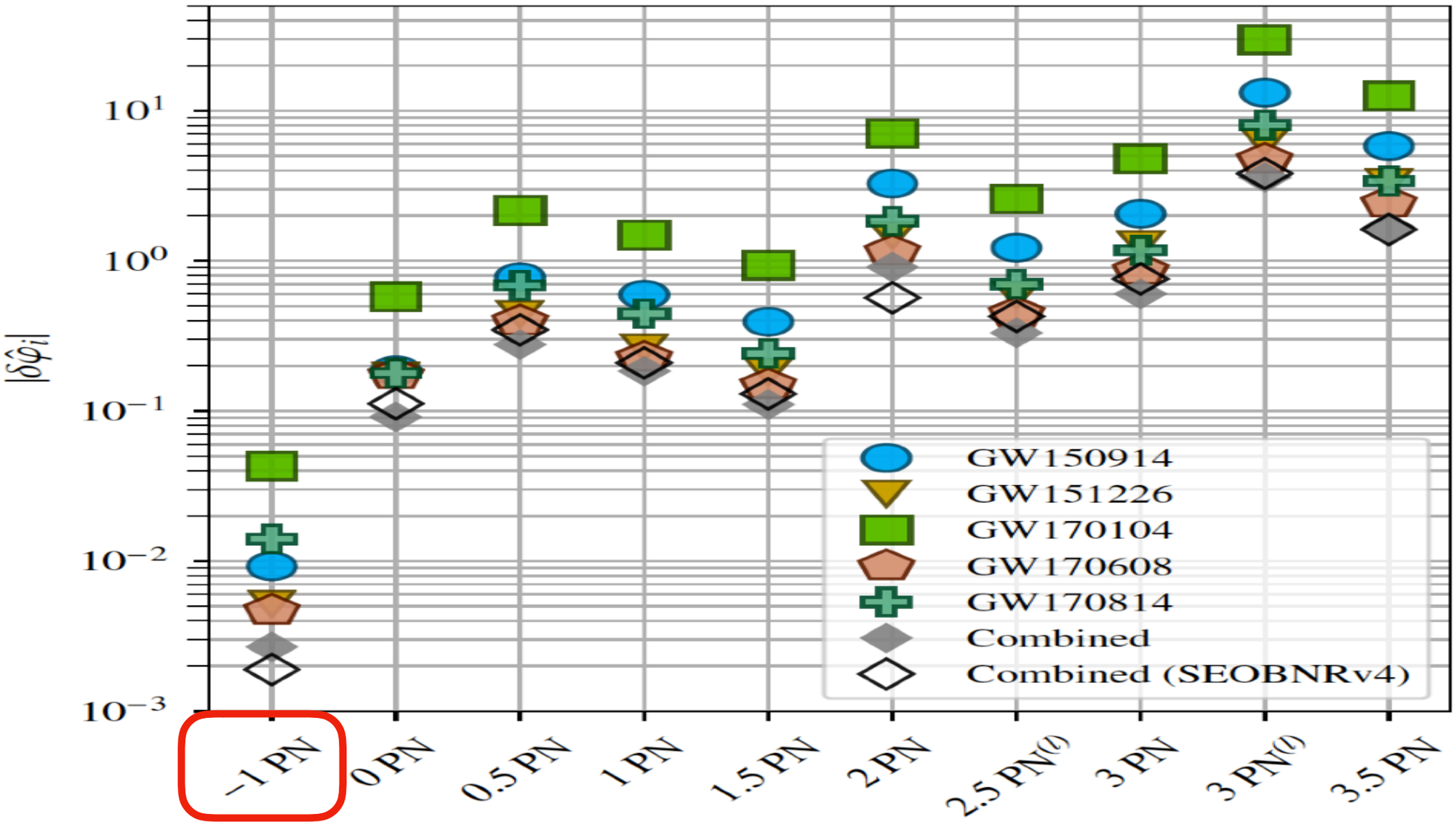

Abbott et al, arXiv:1903.04467

Fundamental Physics

If GR is correct, the deviation $\delta\hat{p}_i$ should be 0

GW150914

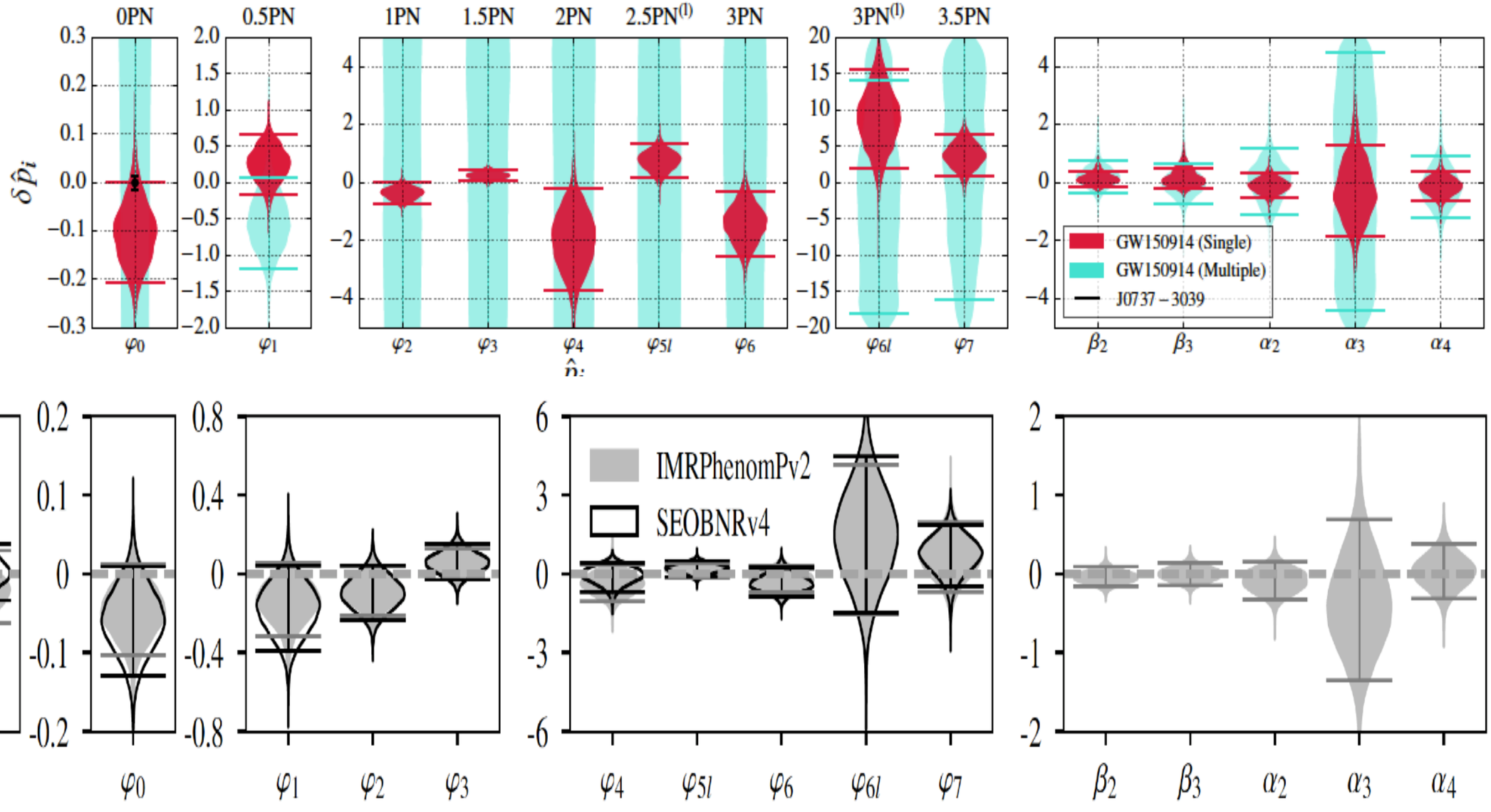

Abbott et al, arXiv:1903.04467

Fundamental Physics

- Assume a dispersion relationship of the form

$$E^2 = p^2c^2 + Ap^\alpha c^\alpha,\ \alpha \geq 0$$

- modifying the GW group velocity as

$$v_g/c = 1 + (\alpha - 1)AE^{\alpha-2}/2$$

- which changes the phase of the GW

$$\delta\Psi = \begin{cases} \dfrac{\pi}{\alpha - 1}\dfrac{AD_\alpha}{(hc)^{2-\alpha}}\left[\dfrac{(1+z)f}{c}\right]^{\alpha-1} & \alpha \neq 1 \\ \dfrac{\pi AD_\alpha}{hc}\ln\left(\dfrac{\pi G\mathcal{M}^{\rm det} f}{c^3}\right) & \alpha = 1 \end{cases}$$

Abbott et al, PRL 118, 221101 (2017)

Fundamental Physics

- Can probe the following theories:
  - Double special relativity $A = \eta_{dsrt}$, $\alpha = 3$
  - Extra-dimensional gravity $A = -\alpha_{edt}$, $\alpha = 4$
  - Horova-Lifshitz gravity $A = \kappa_{hl}^4 \mu_{hl}^2/16$, $\alpha = 4$
  - Massive gravity $A = (m_g c^2)^2$, $\alpha = 0$
  - Multifractional spacetime $A = (-3^{1-\alpha/2}) 2 E_*^{2-\alpha}/(3-\alpha)$, $\alpha = 2 - 3$

Fundamental Physics

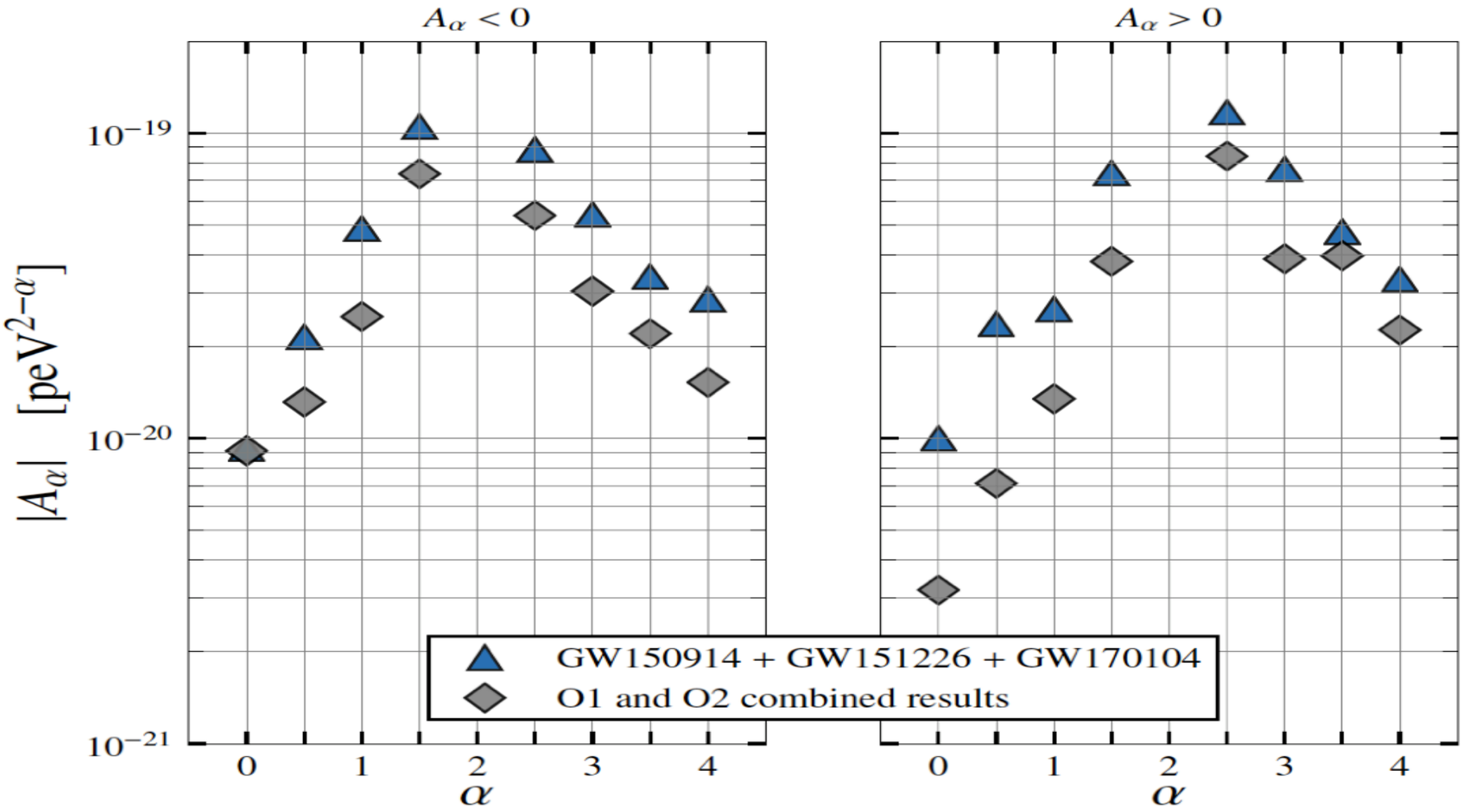

- A_0 corresponds to a massive graviton
- O1/O2 results give $m_g \leq 5 \times 10^{-23}\, eV/c^2$ or $\lambda_g > 2.4 \times 10^{13}\, km$

Abbott et al, arXiv:1903.04467

Fundamental Physics

- In generic metric theories, GWs can have up to 6 polarisations coming from the 6 independent components of the Riemann tensor.

- Test possible due to inclusion of Advanced Virgo

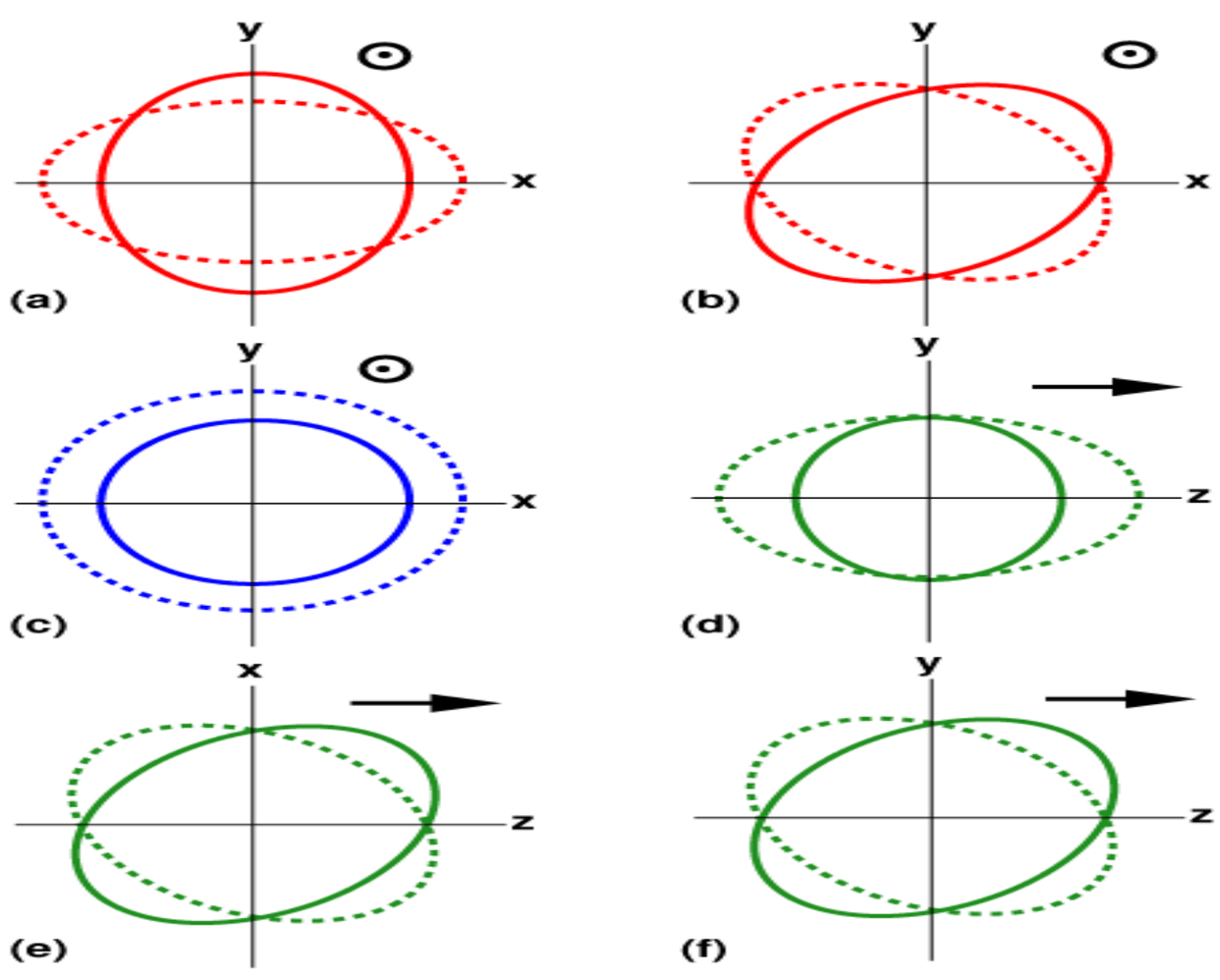

Fundamental Physics

Different polarisations produce a different response at the detector

Tensor

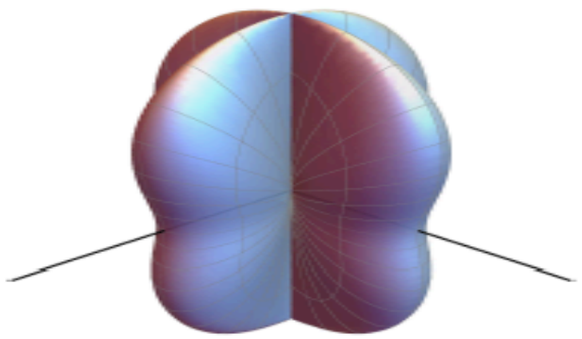

(a) Plus (+)

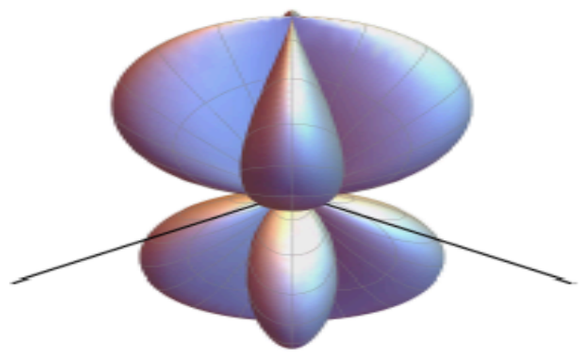

(b) Cross (×)

Vector

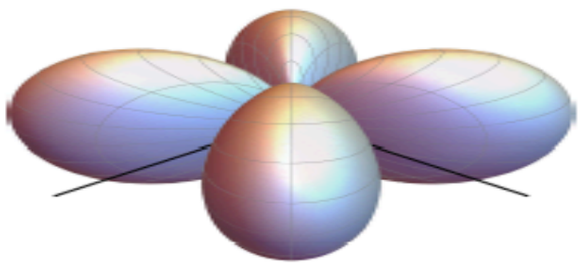

(c) Vector-x (x)

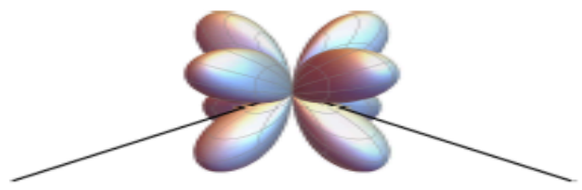

(d) Vector-y (y)

Scalar

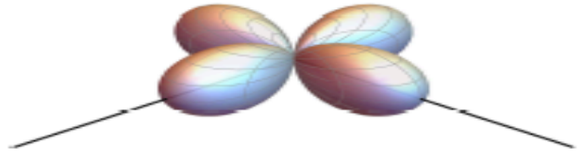

(e) Scalar (s)

T:V = 200:1

T:S = 1000:1

Credit: Max Isi

Fundamental Physics

Is this really surprising...?

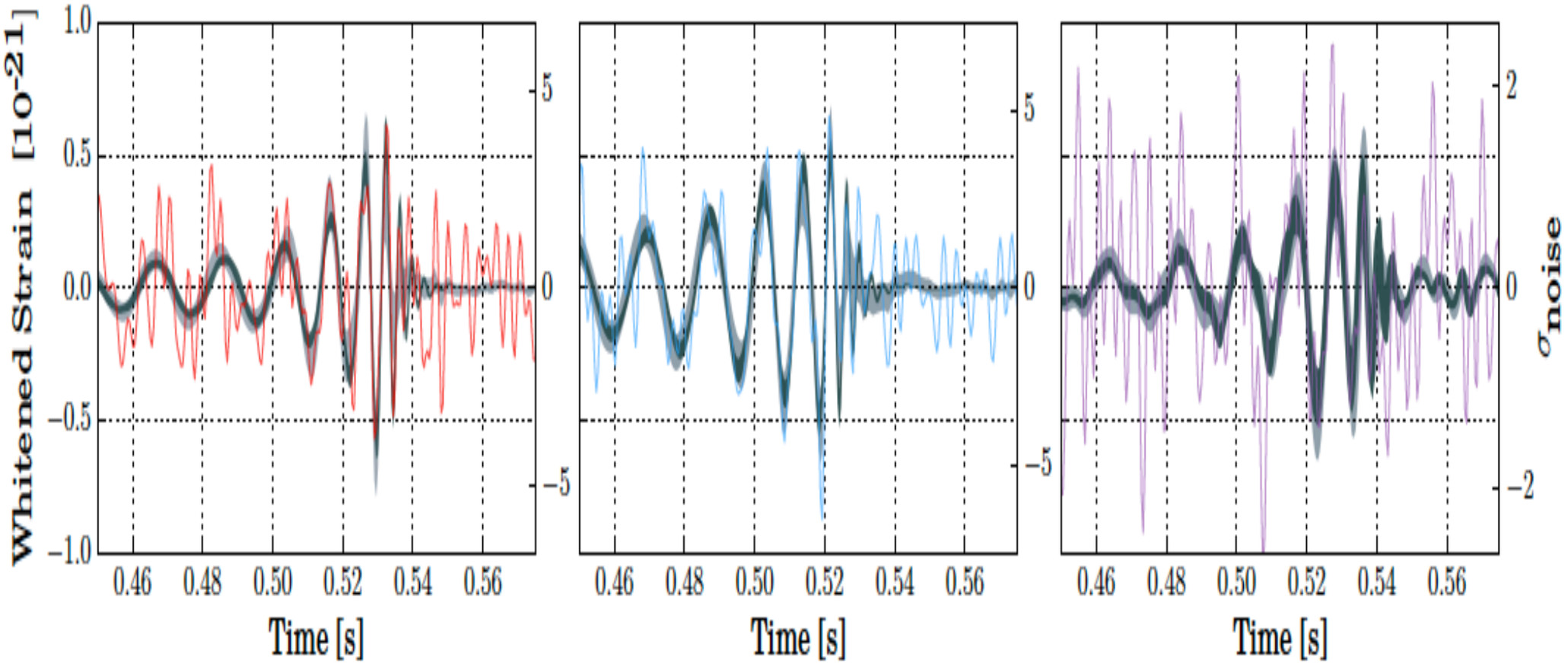

Abbott et al, PRL 119, 141101 (2017)

GR templates match the phase of the data extremely well!!

Already heavily constrains how much non-tensorial polarisation there can be, as well as the level of potential dipole radiation!

Astrophysics

- Uncertainty in formation channels
  - galactic field evolution
  - dynamical capture in globular clusters

- How does the common envelope phase actually work?
  - Role of metallicity?

- Do natal kicks in SN play a role?

- How does mass transfer efficiency affect binary evolution?

- What is the merger rate for binary systems?

Astrophysics

- Two possible mass gaps
  - >3 $M_\odot$: nuclear EOS
  - <5 $M_\odot$: binary evolution
  - > 50 $M_\odot$: PISN

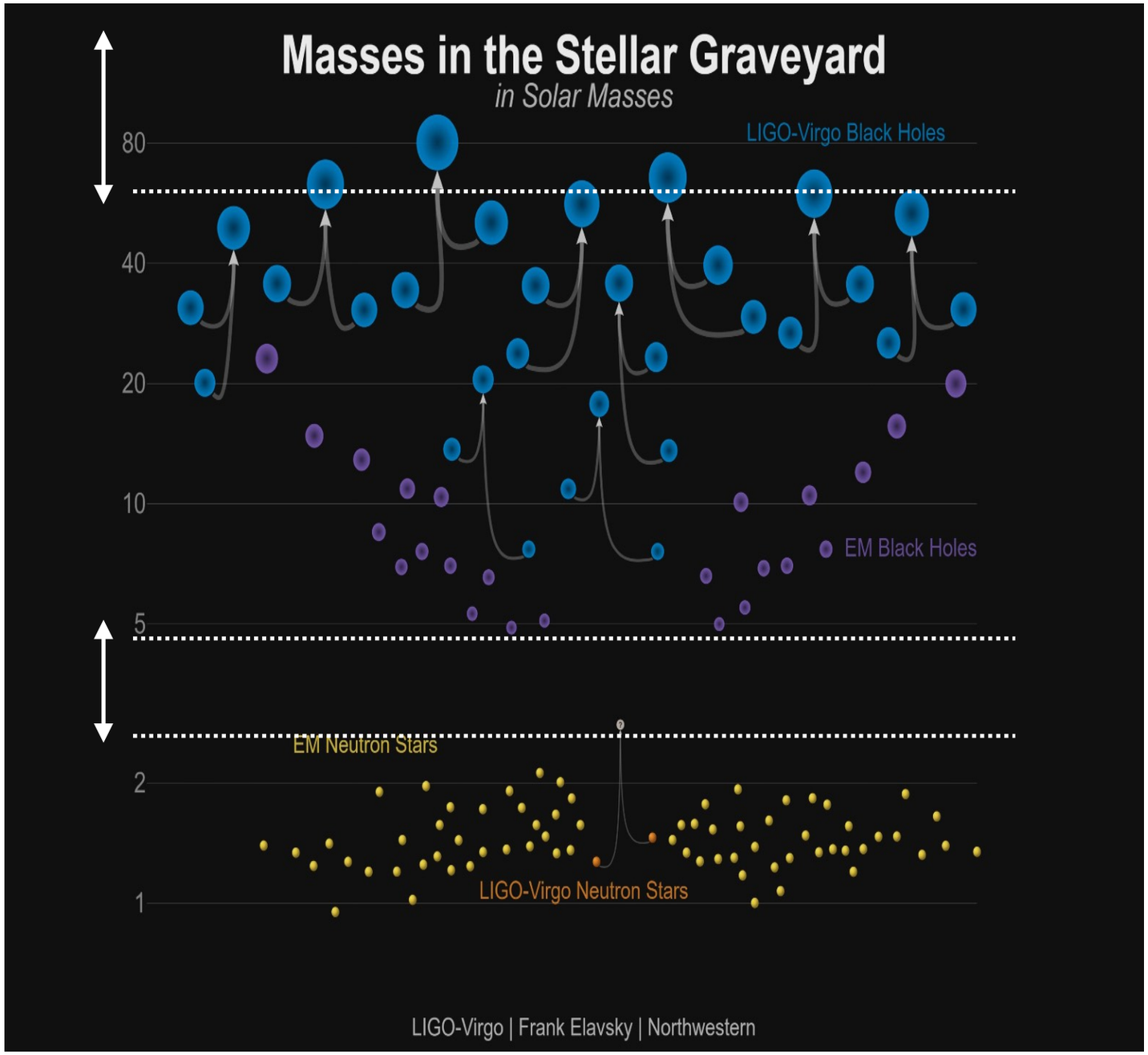

ligo.caltech.edu

BH FORMATION

e.g. GW150914

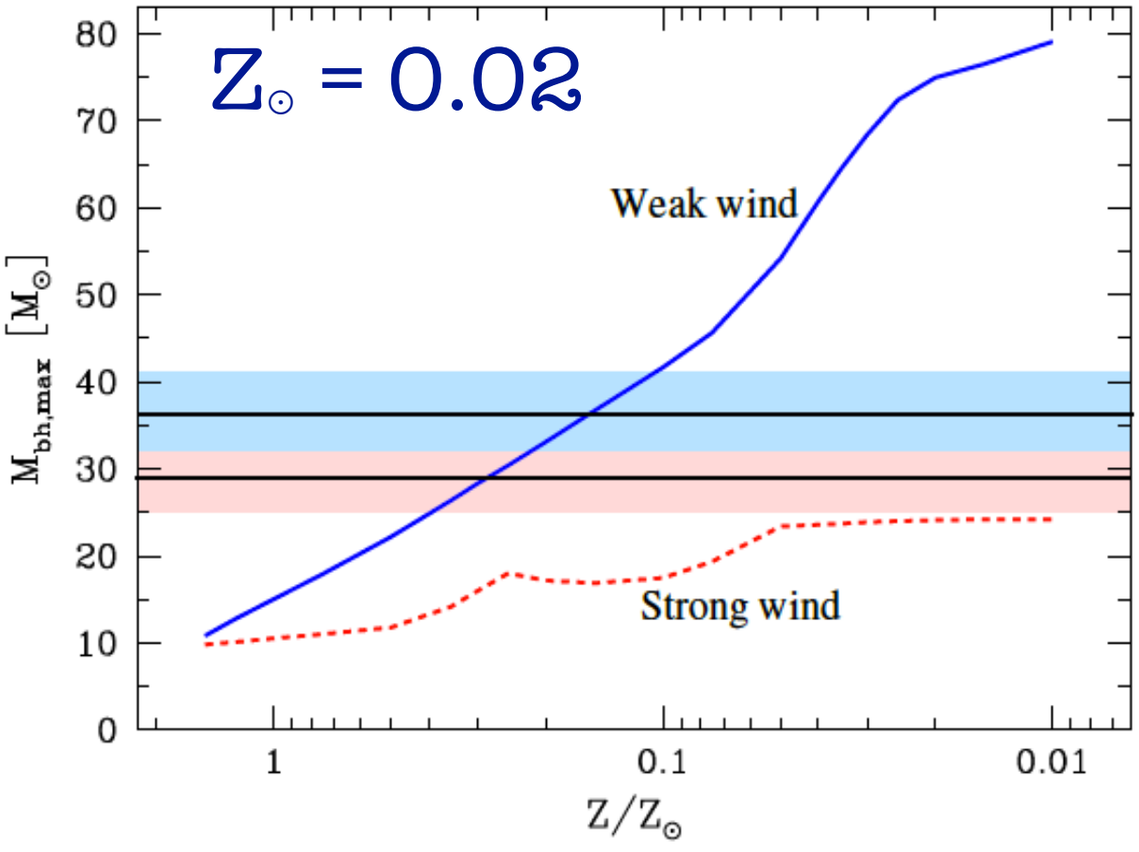

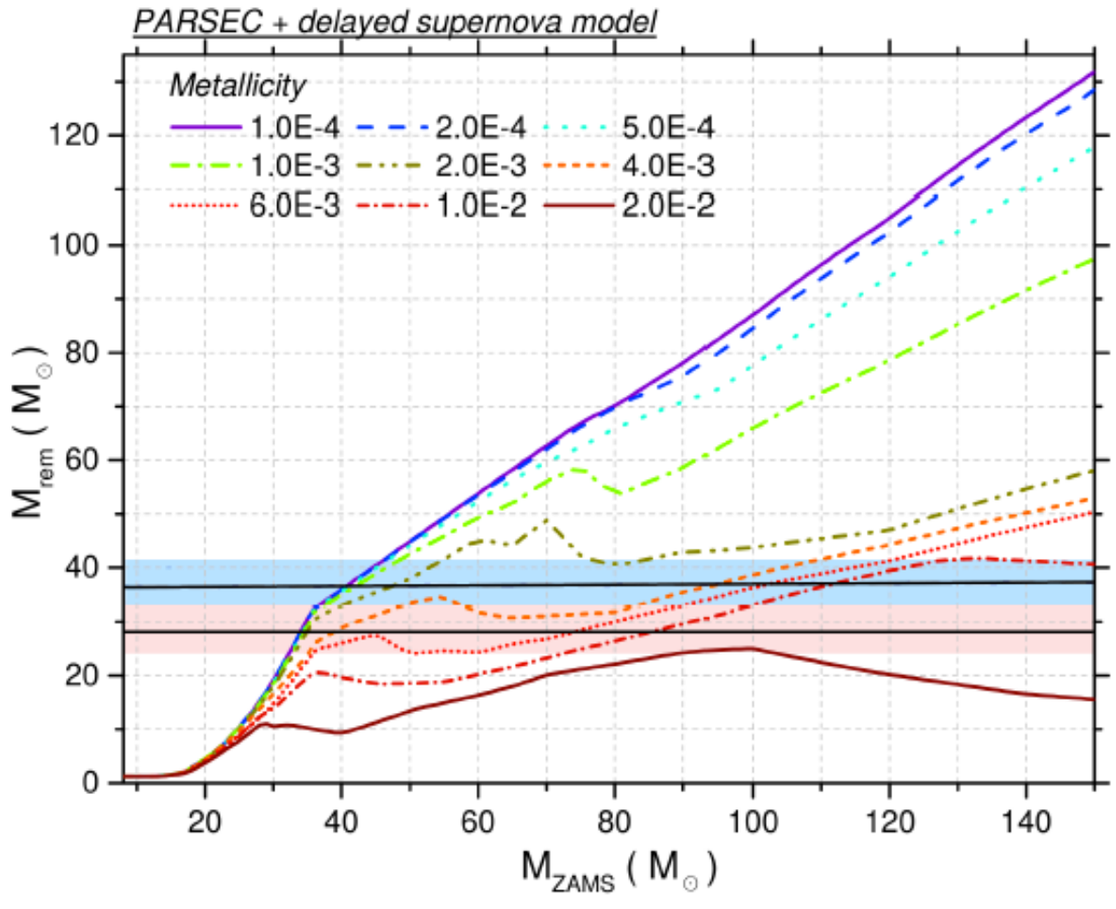

- Weak winds and low metallicity produce large BHs
- The lower the metallicity, the smaller the progenitor needed

Abbott et al, Astrophys.J. 818 (2016) L22

BBH mergers in the local Universe

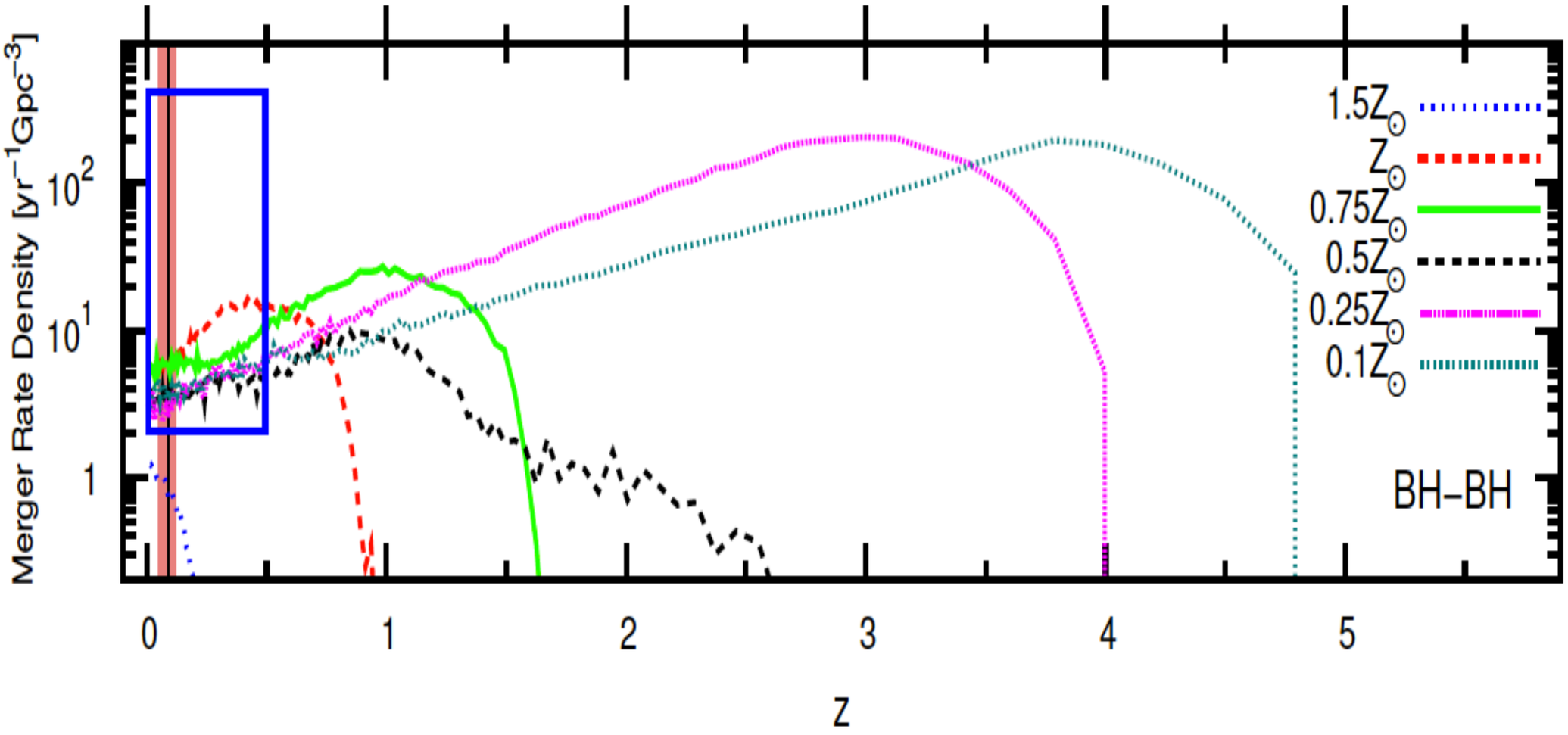

- Not yet possible to measure the BH mass function
- Our detections are consistent with
  - dynamical formation in GCs
  - isolated field binaries

Abbott et al, Astrophys.J. 818 (20 .3) 22

O1 BBH Rates

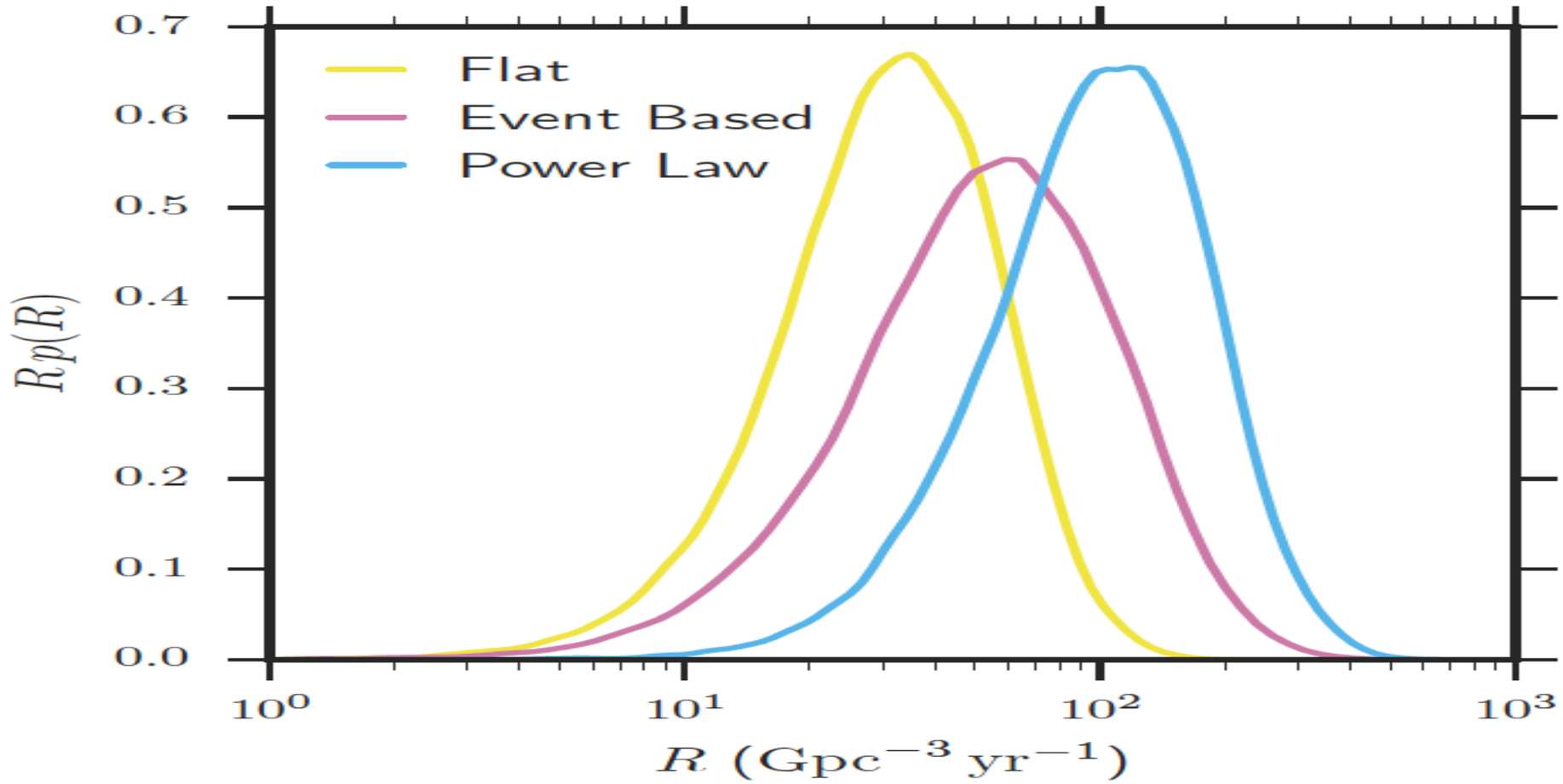

- Flat distribution in the log of the individual masses
- Power law distribution in the primary mass, uniform in the secondary
- Event based
- Combined O1 rate estimate : 9-240 Gpc^{-3} yr^{-1} (90% CI)

Abbott et al, Phys.Rev. X6 (2016) no.4, 041015

O1+O2 BBH Rates

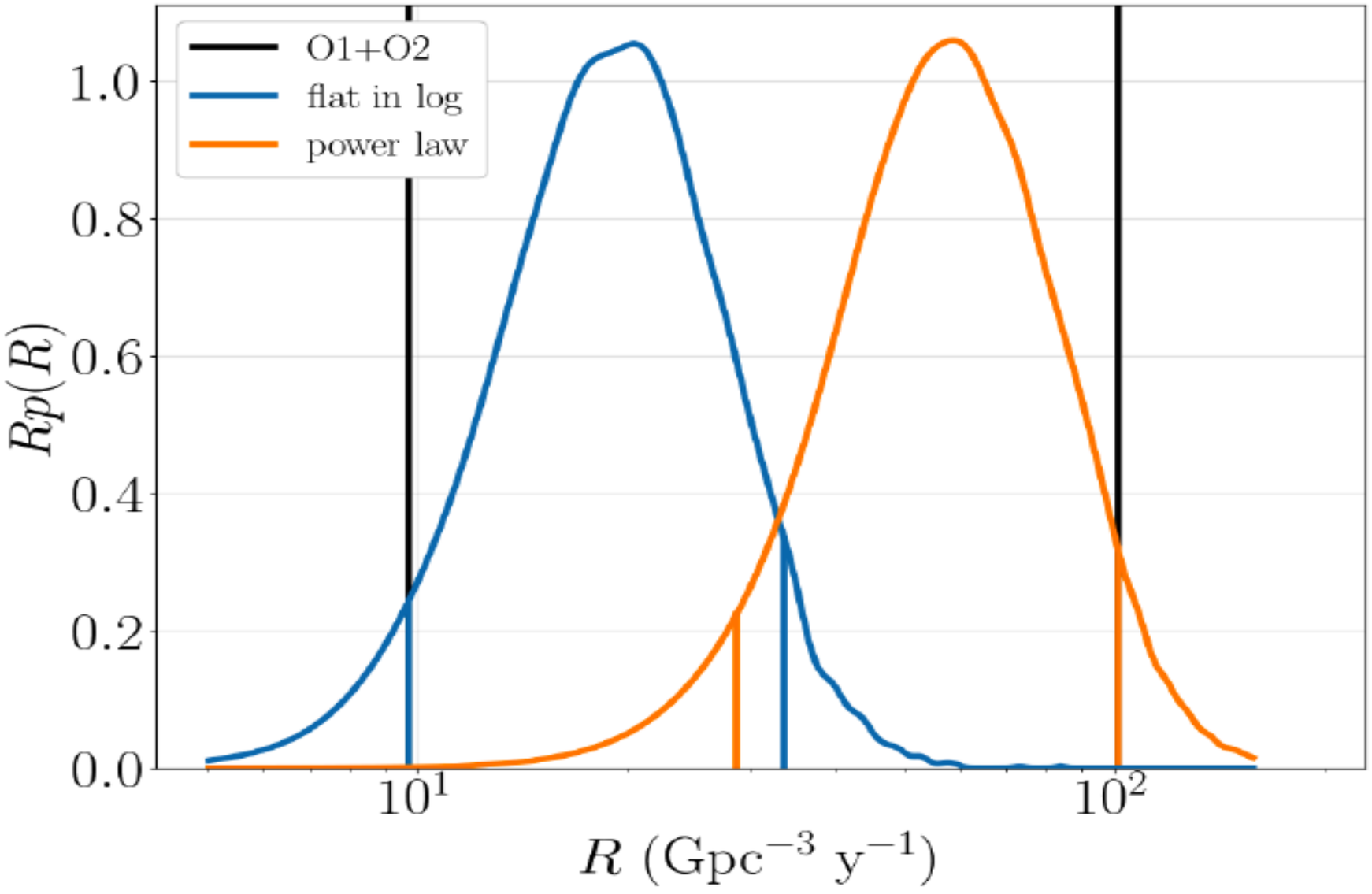

$$9.7 - 101\, Gpc^{-3} yr^{-1}$$

B. Abbott et al, arXiv:1811.12907

BBH Formation Channels

- If we assume a single formation channel, lower limit disfavours
  - dynamical formation in low-mass GCs
  - very high natal kicks in isolated binaries (> 100s km/s)
  - combination of very low CE binding energy with high efficiency ejection
- If we assume multiple simultaneous formation channels
  - nothing can be ruled out

BNS Event Rates

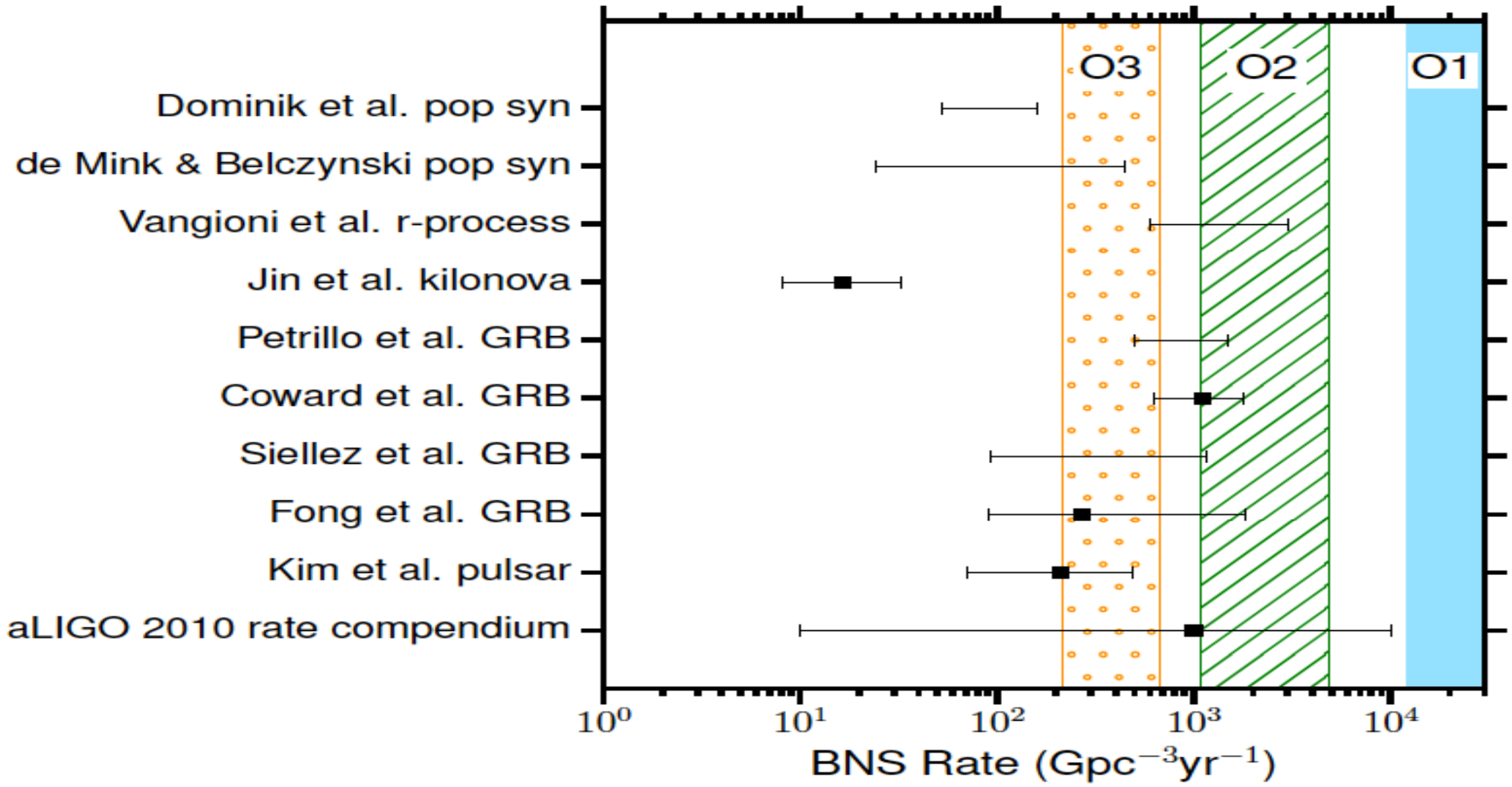

O1 : $\mathcal{R} < 12{,}600\ Gpc^{-3}\ yr^{-1}$

Abbott et al, ApJ 832, L21 (2016)

BNS Event Rates

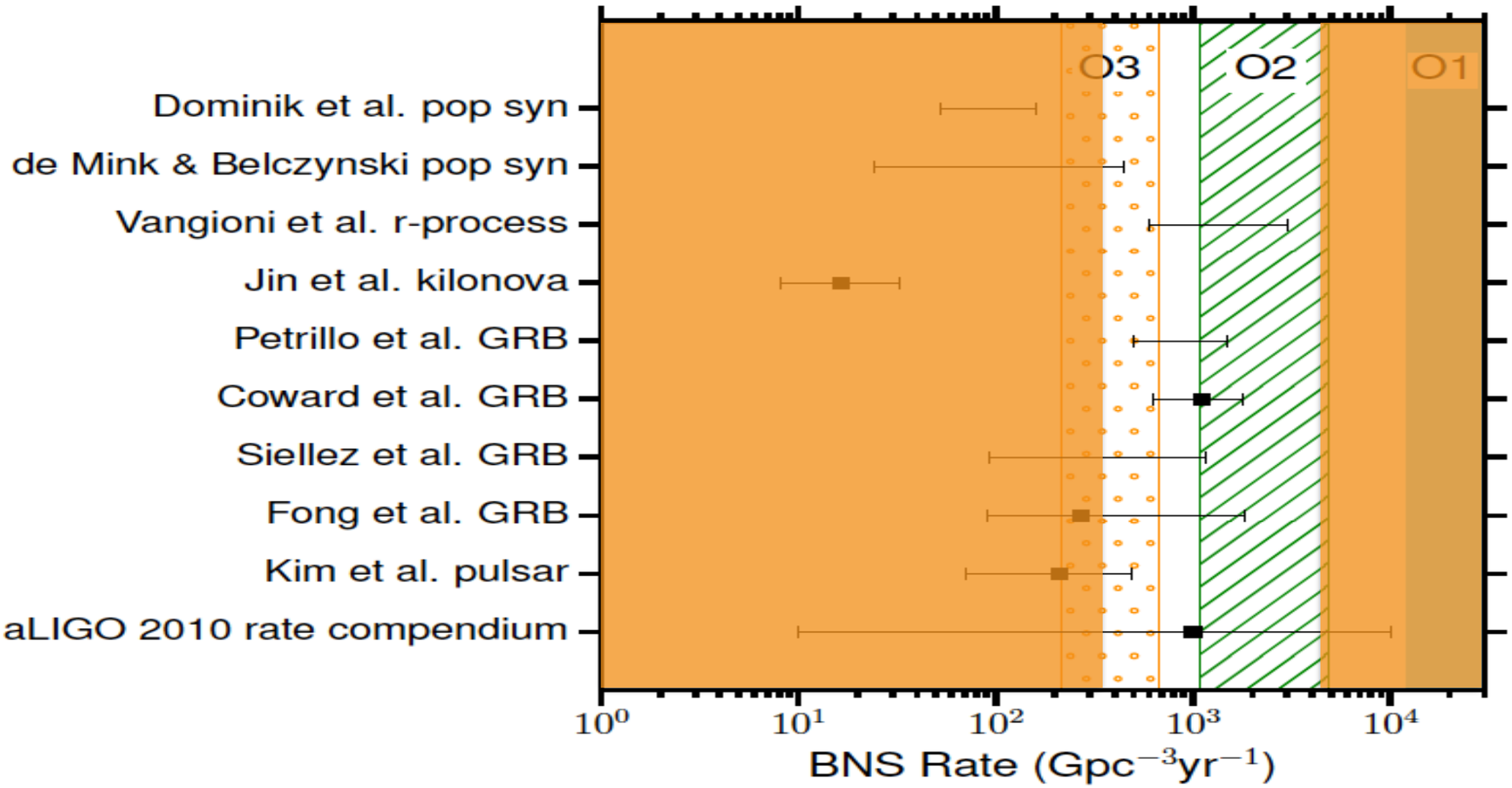

after GW170817, assuming a population uniform in with uniform component mass in the range [1,2] $M_\odot$: $\mathcal{R}$ = 320 - 4740 Gpc^{-3} yr^{-1}

Abbott et al, PRL 119, 161101 (2017)

BNS Event Rates

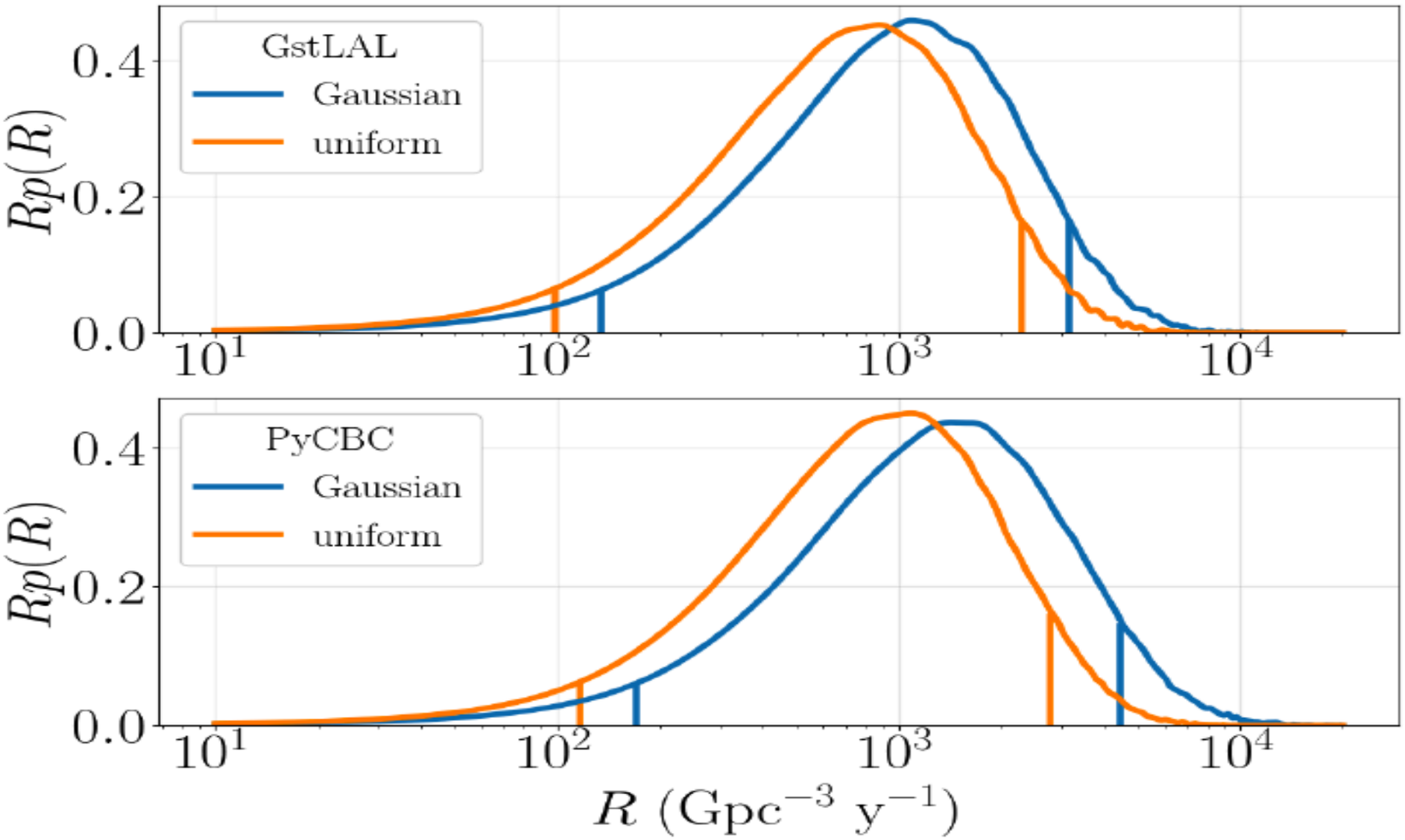

Combined O1+O2 result using new population models : $\mathcal{R}$ = 110 - 3840 Gpc^{-3} yr^{-1}

BHNS Rates

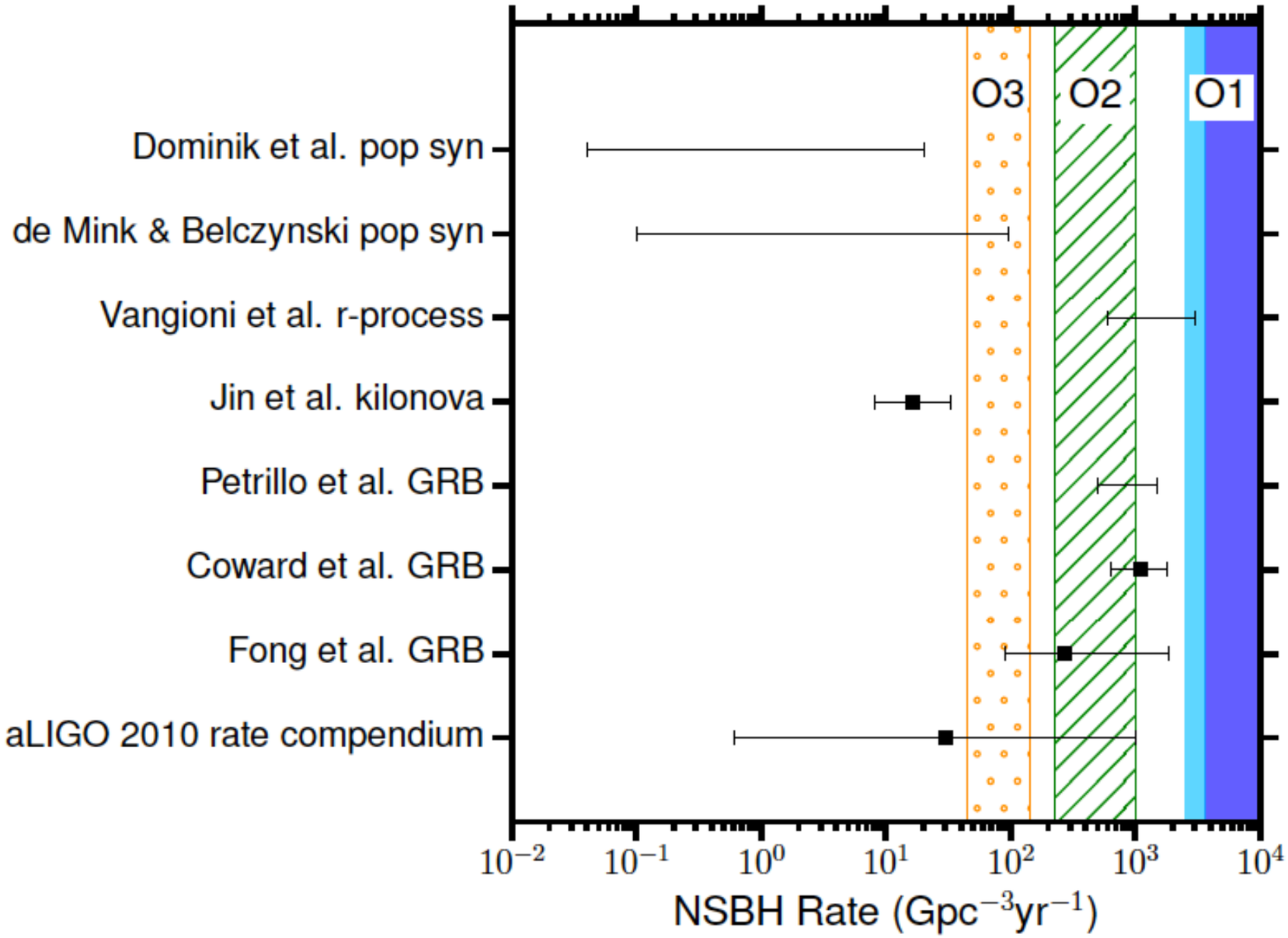

O1 : $\mathcal{R} < 3{,}600\ \mathrm{Gpc^{-3}\ yr^{-1}}$

BHNS Rates

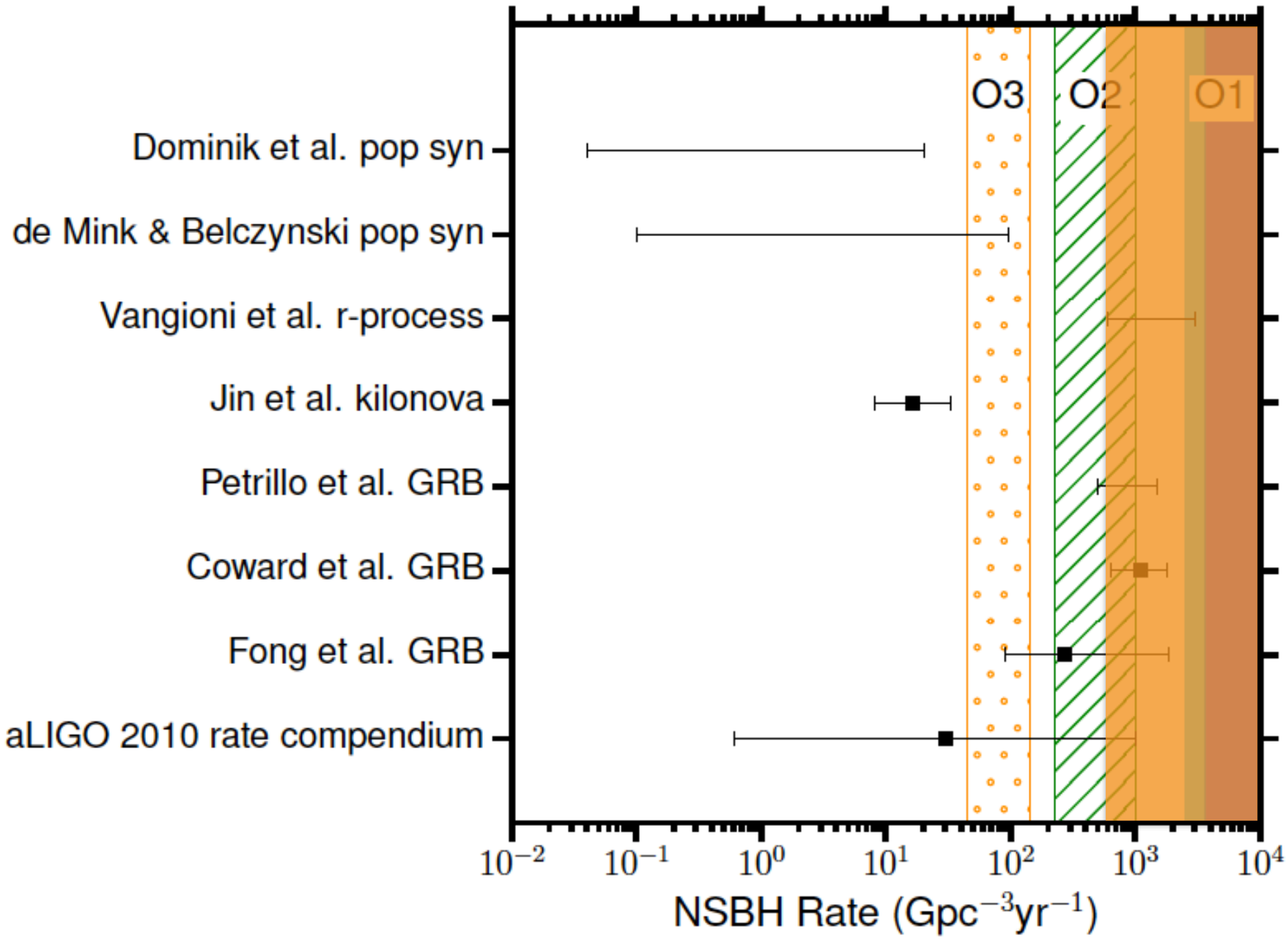

O2 : $\mathcal{R} < 610\ \mathrm{Gpc^{-3}\ yr^{-1}}$

NS Equation of State

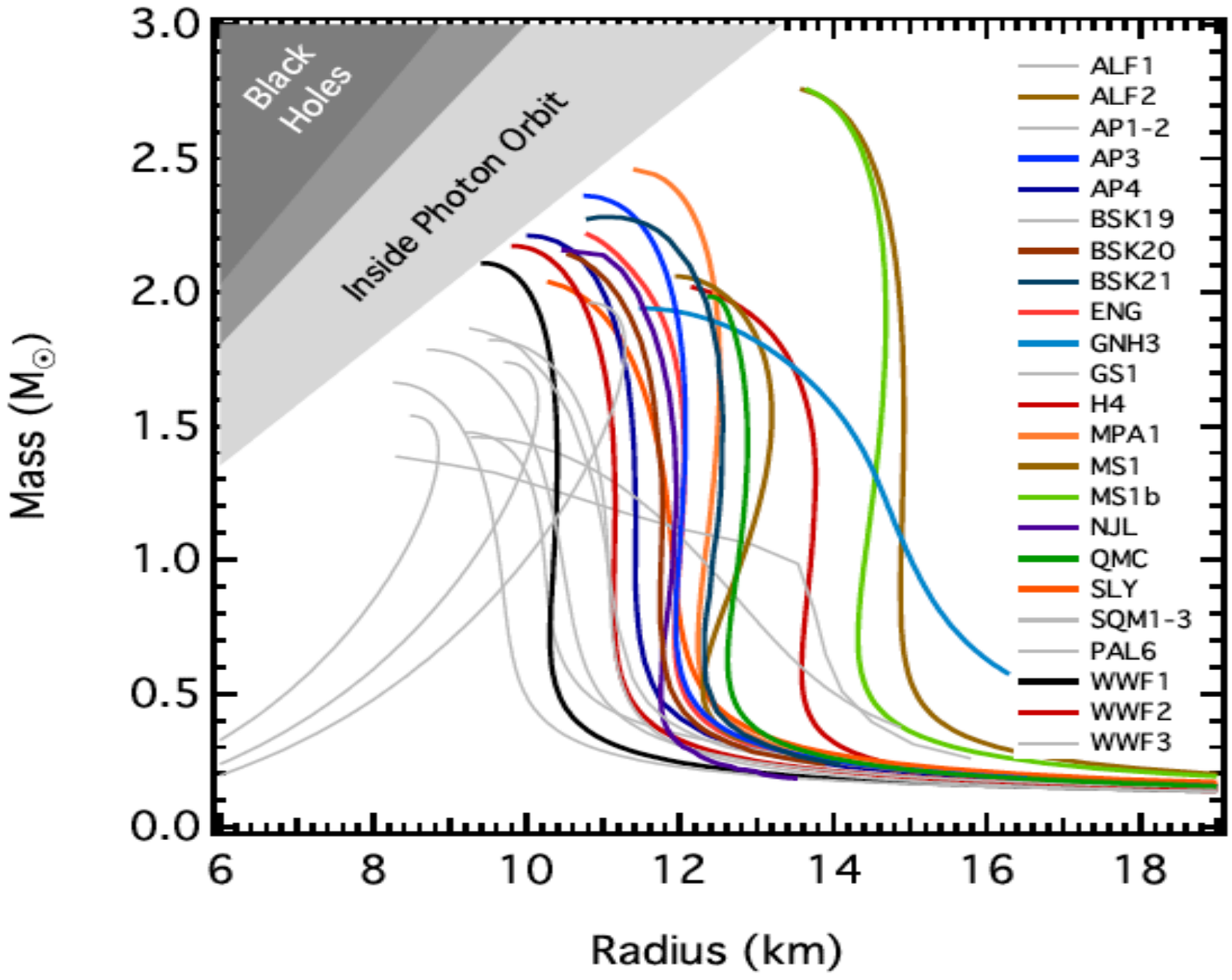

Özel & Freire, Ann.Rev.Astron.Astrophys 54, 401 (2017)

NS Equation of State

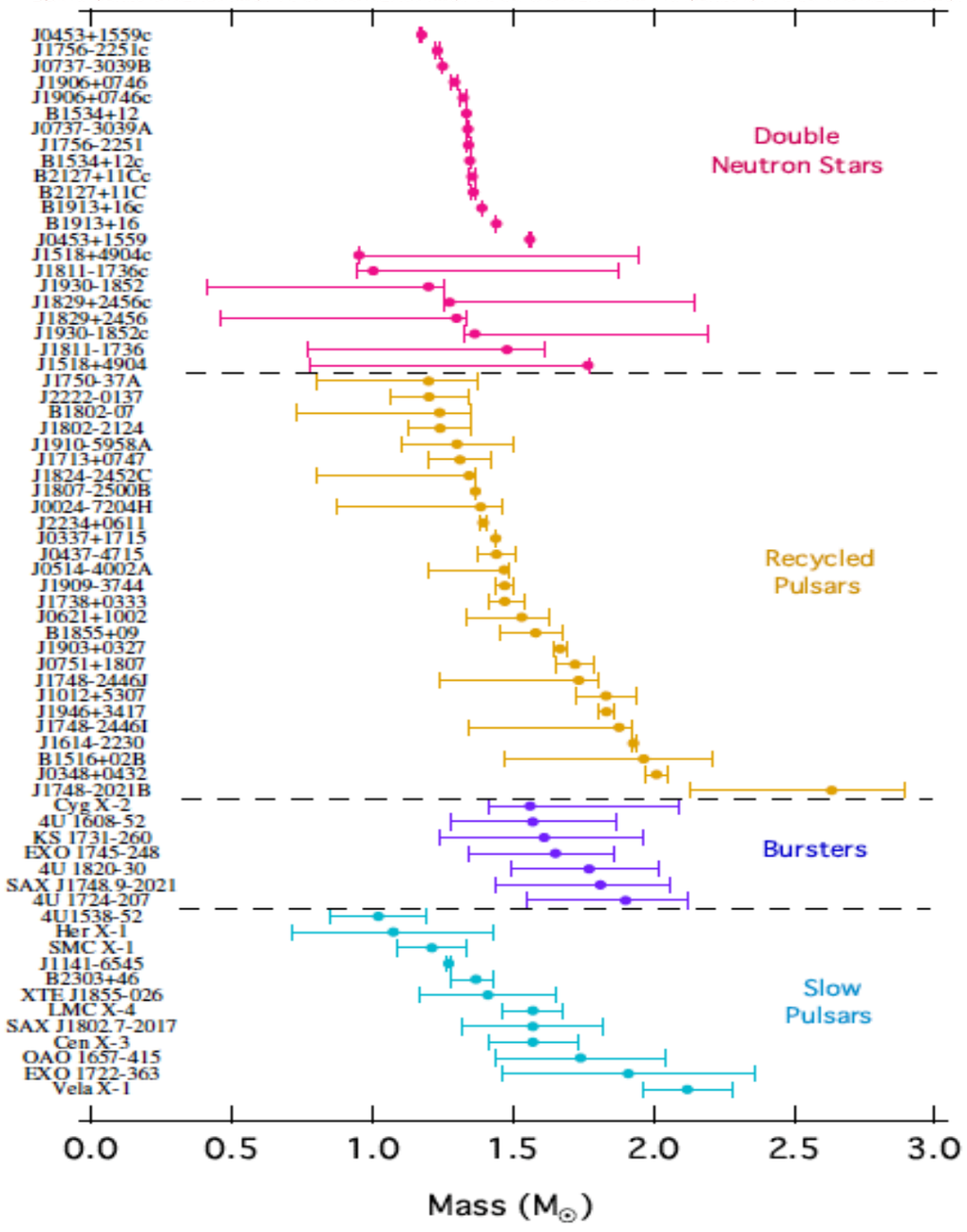

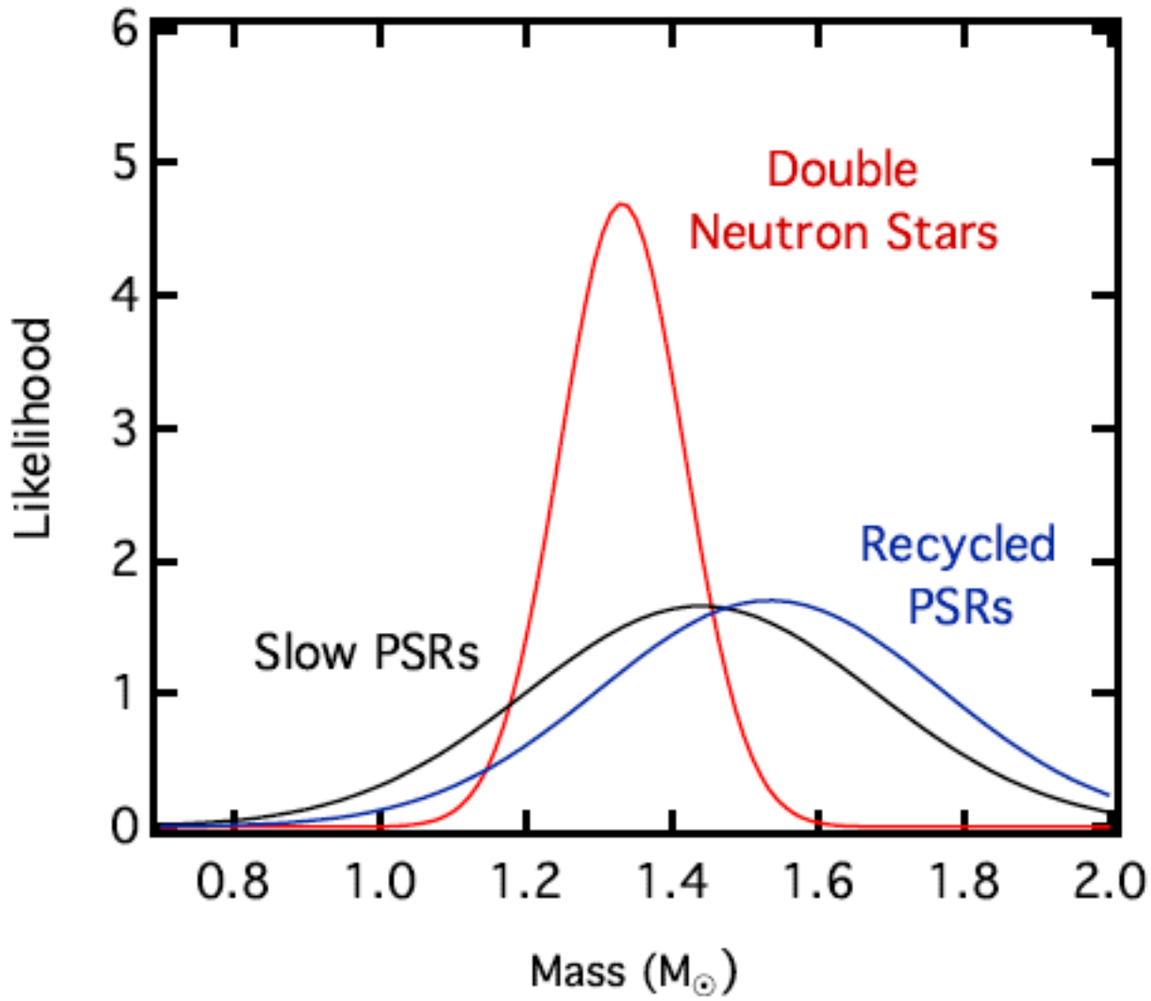

J0348+0432 : 2.01±0.04 M⊙

Özel & Freire, Ann.Rev.Astron.Astrophys 54, 401 (2017)

NS Equation of State

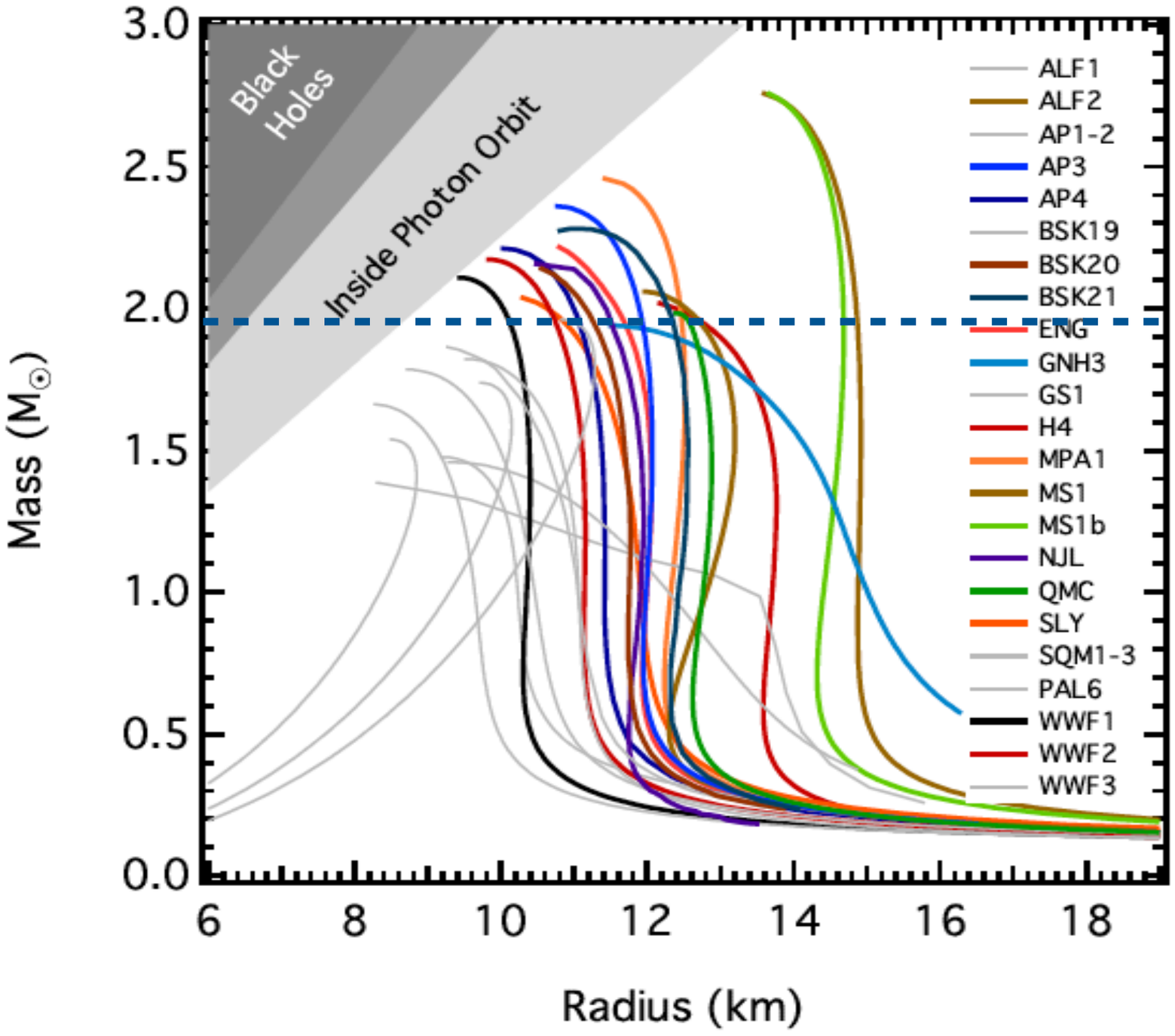

J0348+0432 (MSP-WD)

NS Equation of State

$$30 \leq f/Hz \leq 2048$$

$$m_1 \in (1.36, 1.6)\, M_\odot$$

$$m_2 \in (1.17, 1.36)\, M_\odot$$

$$\tilde{\Lambda}_{1.4} \leq 900$$

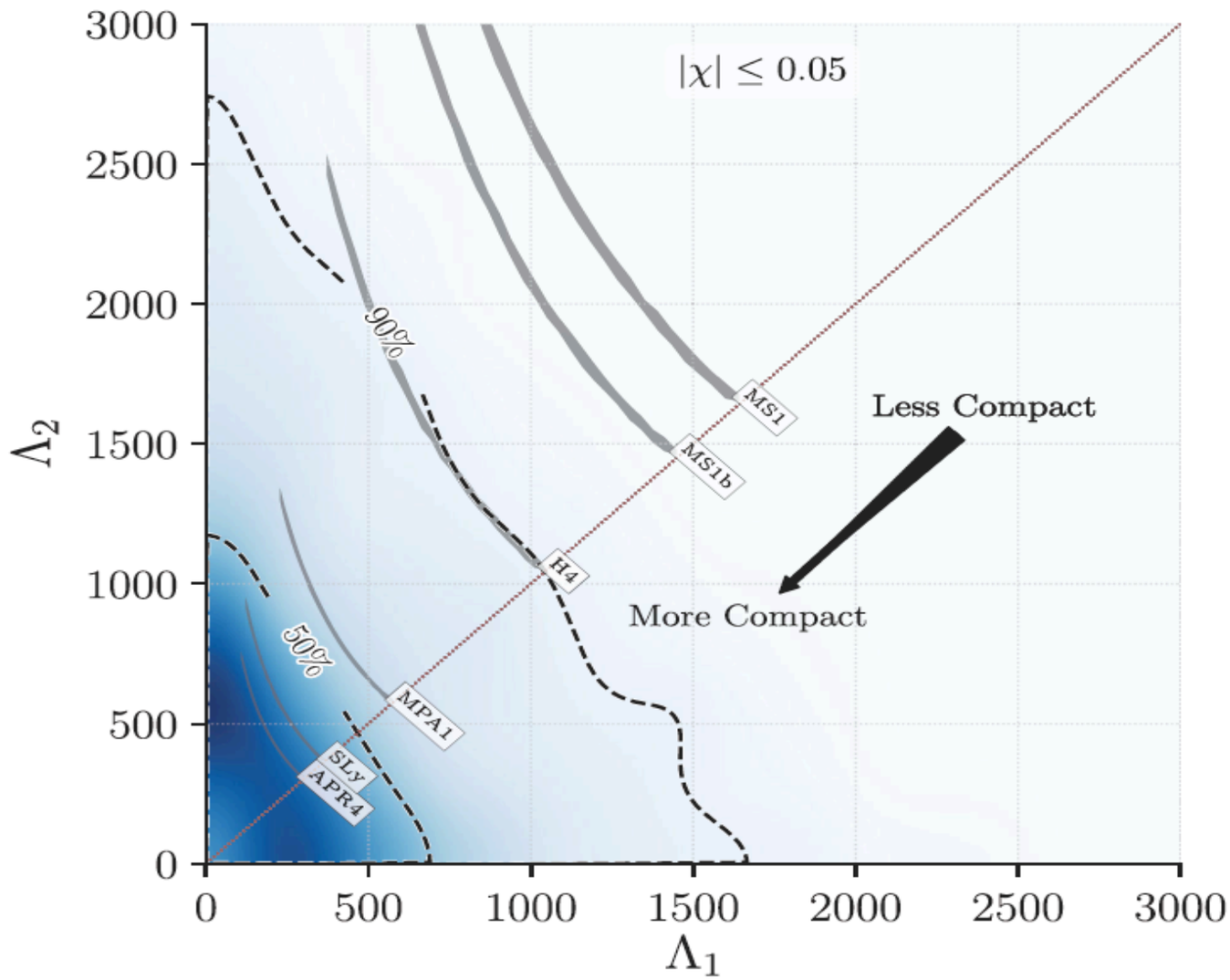

Assume low spins - consistent with NS observations

Abbott et al, PRL 119, 161101 (2017)

NS Equation of State

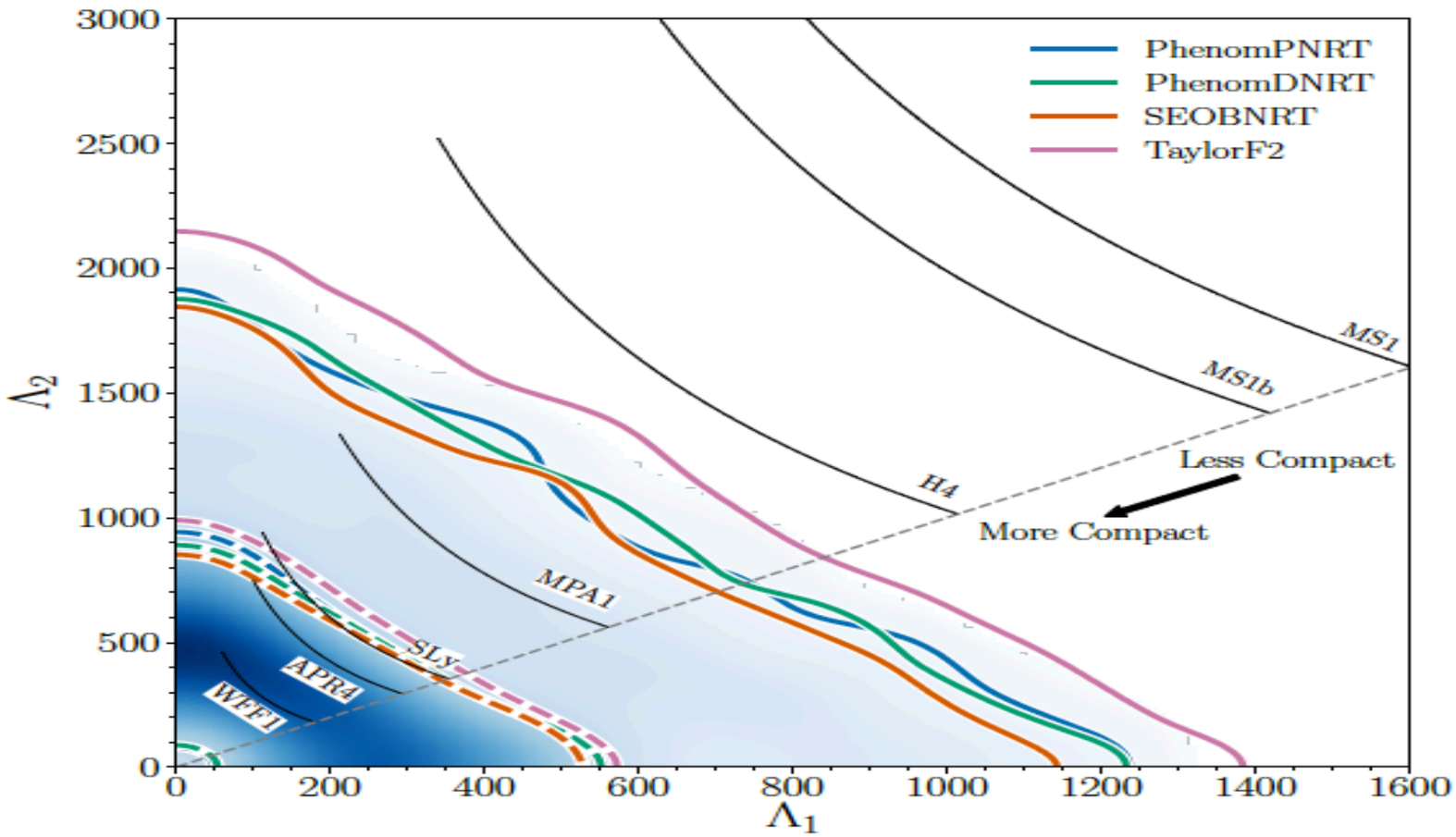

- New analysis beginning at 23 Hz (~1500 extra cycles) with better modelling
- No assumption on binary components
- No assumptions on EOS - independent variation
- sky error reduced to 16 deg^2 (using sky position given by SSS17A/AT 2017 gfo)
- Bound on Λ_1 - Λ_2 is 20% smaller

Abbott et al, arXiv:1805.11579 (2018)

NS Equation of State

- Assume 2 NSs with identical EOS
- 2 EOS methodologies
  - EOS-insensitive :
    - i. $\Lambda_a(\Lambda_s, q)$
    - ii. Λ - C
  - Parameterised EOS (no max mass)
    i. Spectral parameterisation
  - Original detection results
- 90% CI for Λ_1 - Λ_2 shrinks by ~3

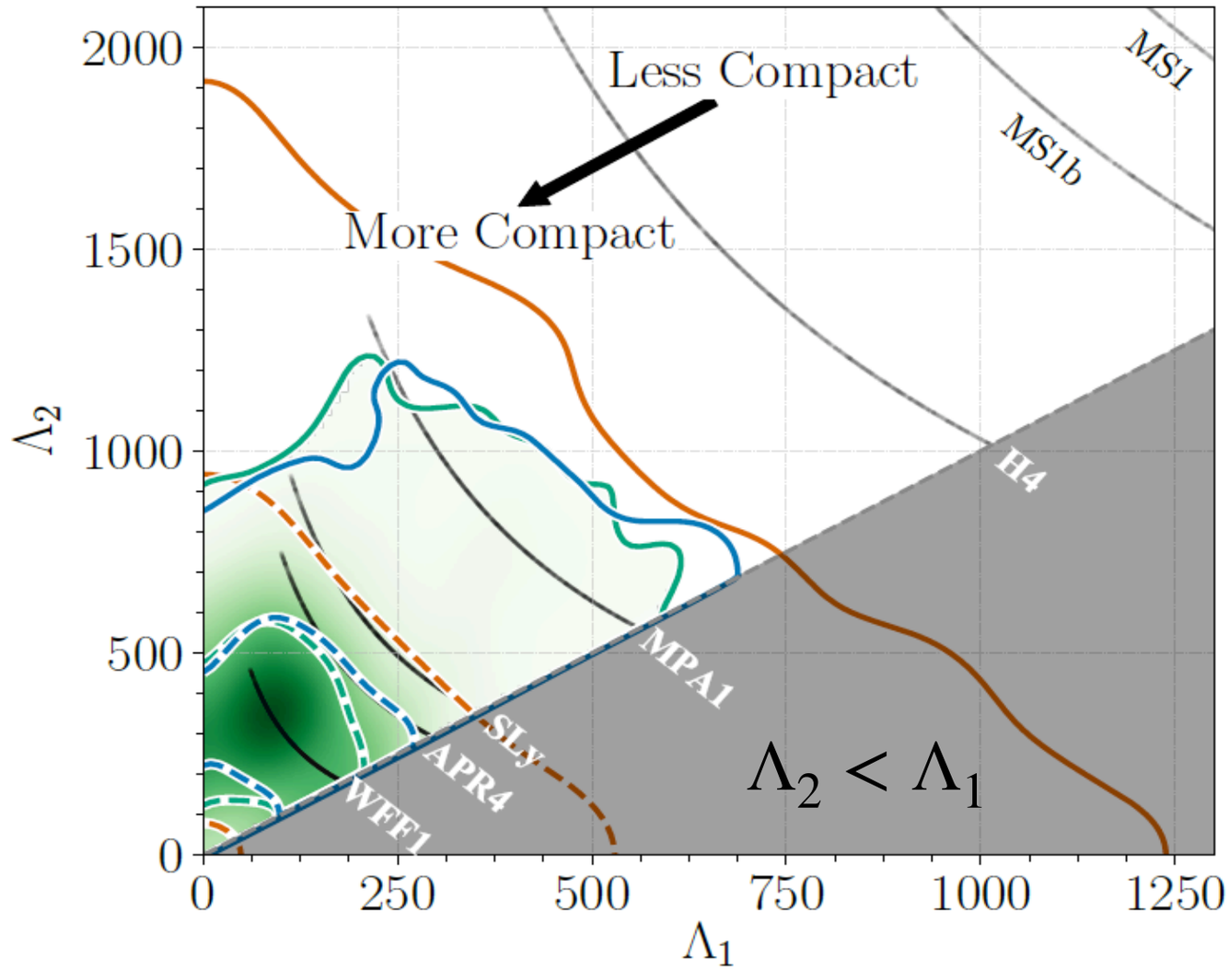

$$\Lambda_{1.4} = 190^{+390}_{-120}$$

Abbott et al, arXiv:1805.11581 (2018)

NS Equation of State

Now assume spectral parameterisation + maximum NS mass = 1.97 $M_\odot$

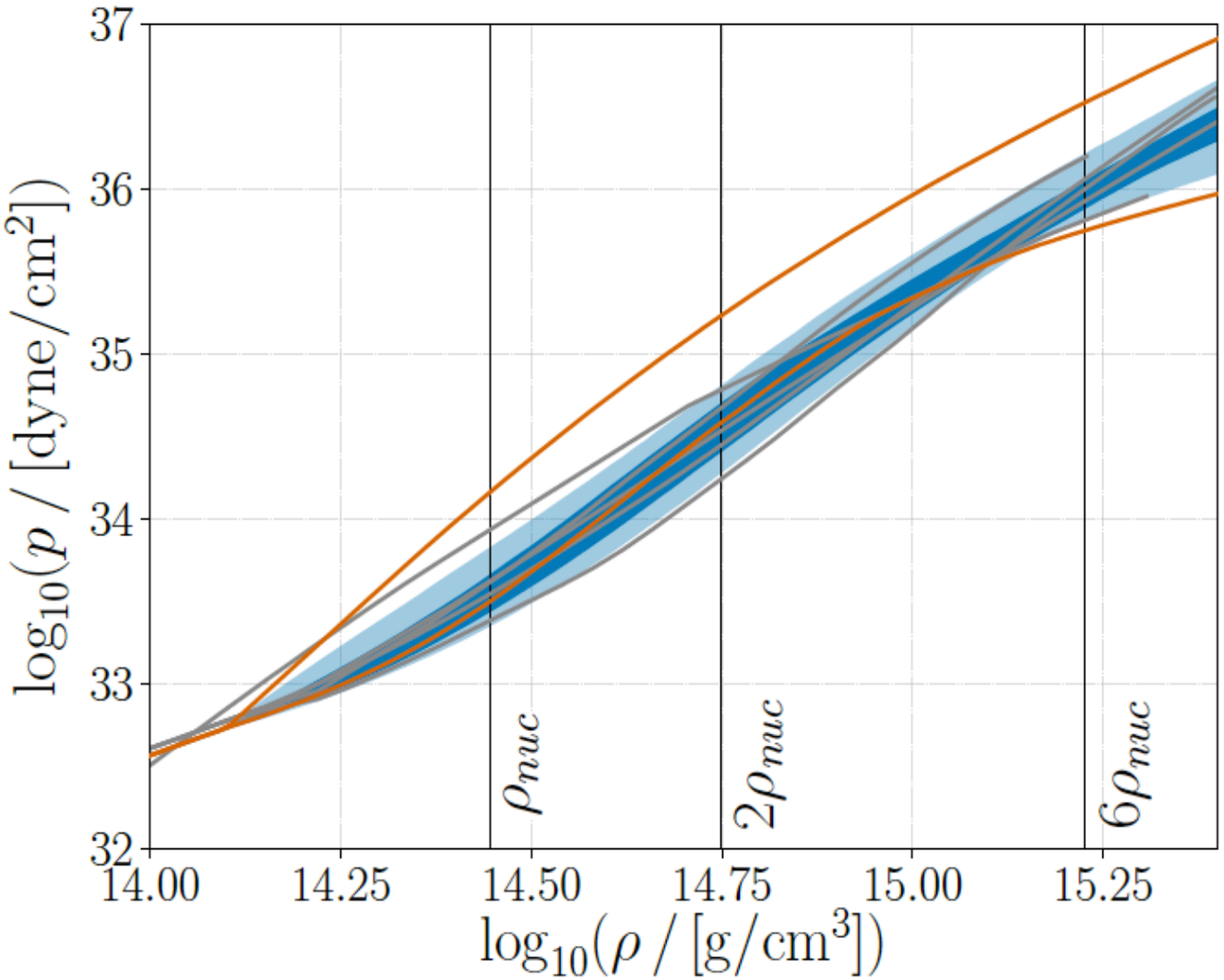

$$p(2\rho_{nuc}) = 3.5^{+2.5}_{-1.7} \times 10^{34}\, dyne\, cm^{-2}$$

Abbott et al, arXiv:1805.11581 (2018)

NS Equation of State

EOS-ins
(GW only)

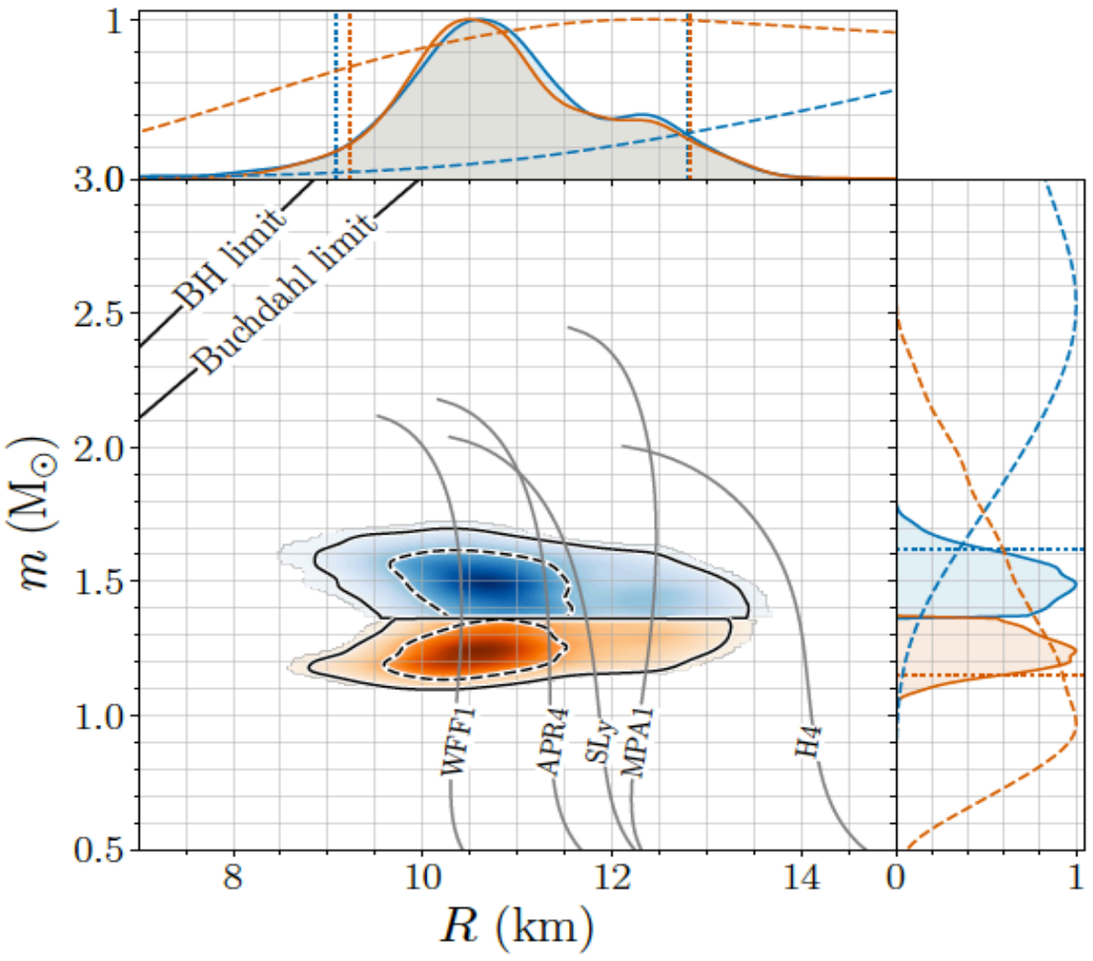

$$R_1 = 10.8^{+2.0}_{-1.7}\, km$$
$$R_2 = 10.7^{+2.1}_{-1.5}\, km$$

Spec.Param + max. NS mass
(GW + EM)

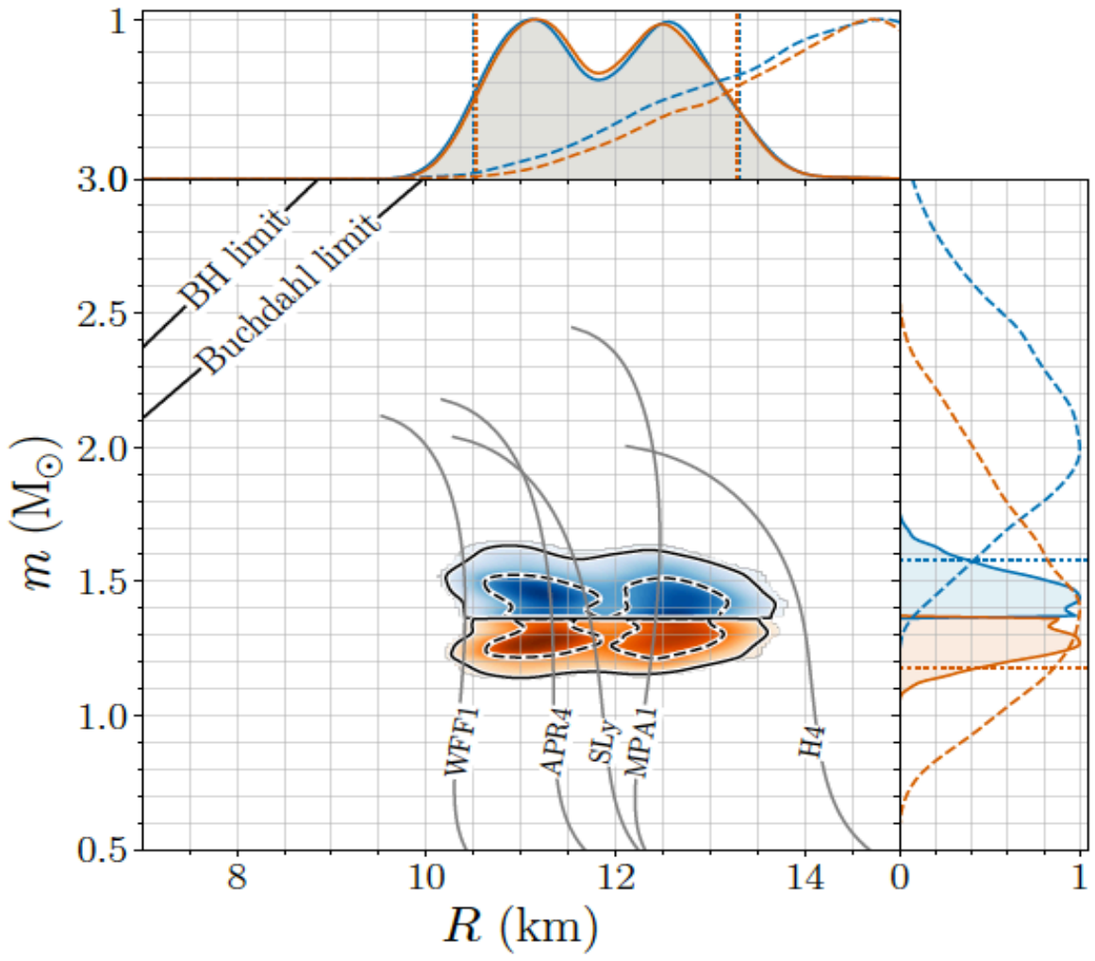

$$R_1 = 11.9^{+1.4}_{-1.4}\, km$$
$$R_2 = 11.9^{+1.4}_{-1.4}\, km$$

Abbott et al, arXiv:1805.11581 (2018)

NS Equation of State

EOS-ins

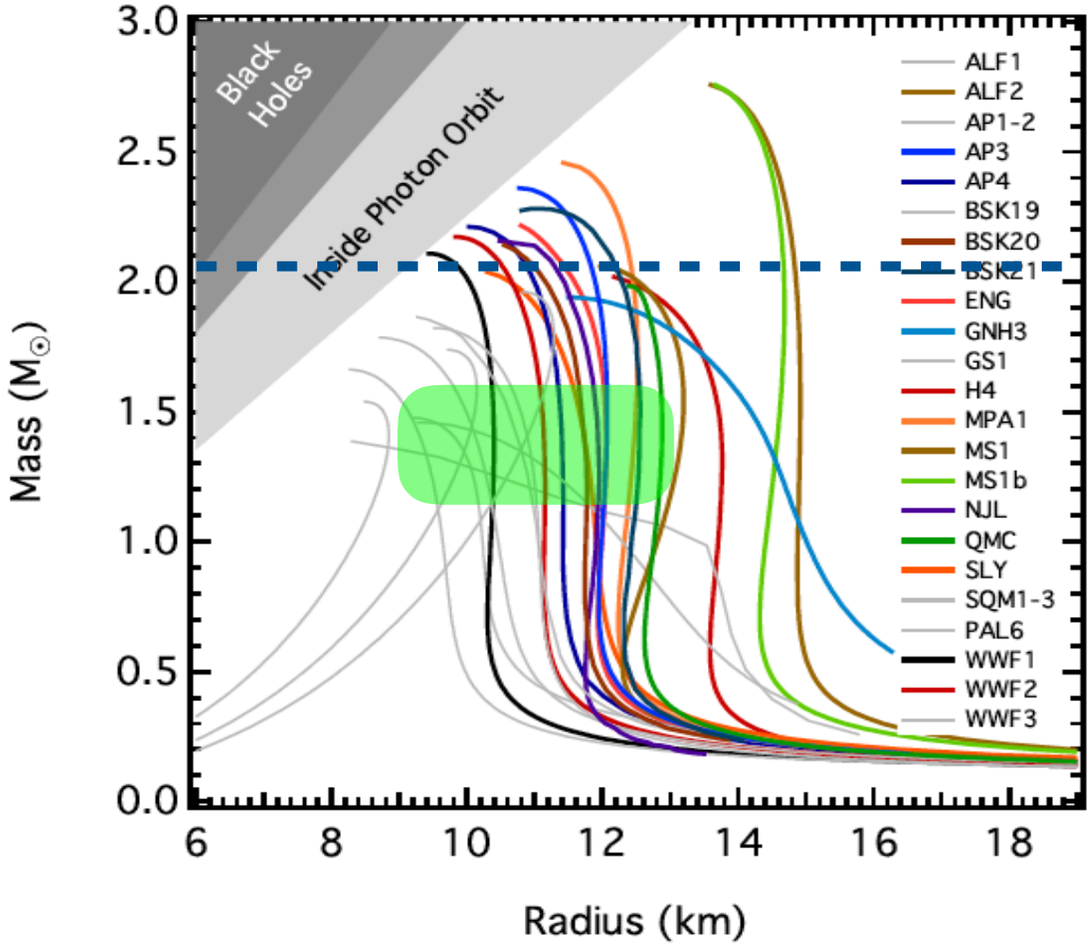

Spec.Param + min. NS mass

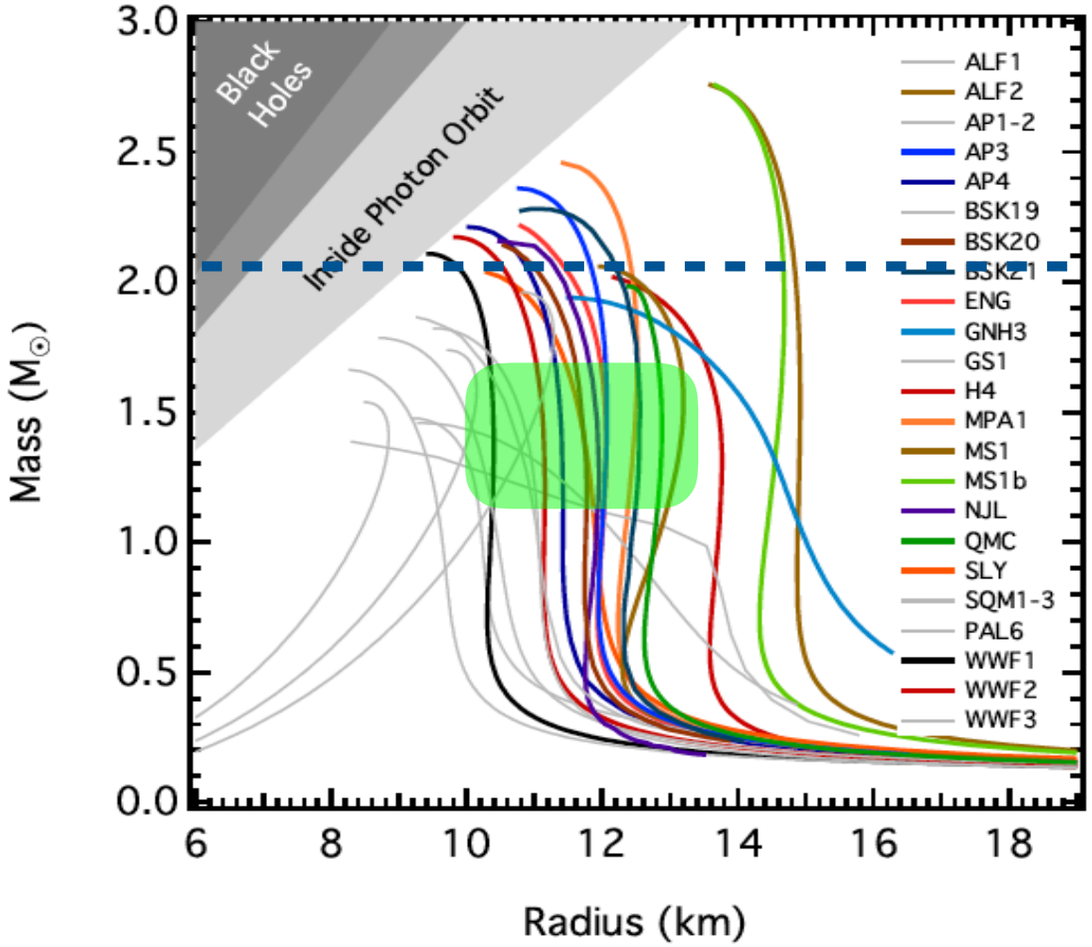

GW + EM gives much tighter constraint

Post-merger remnant

Q:So what is the remnant of the merger?

A:From GWs - we don't know. High frequency signal dominated by photon shot noise

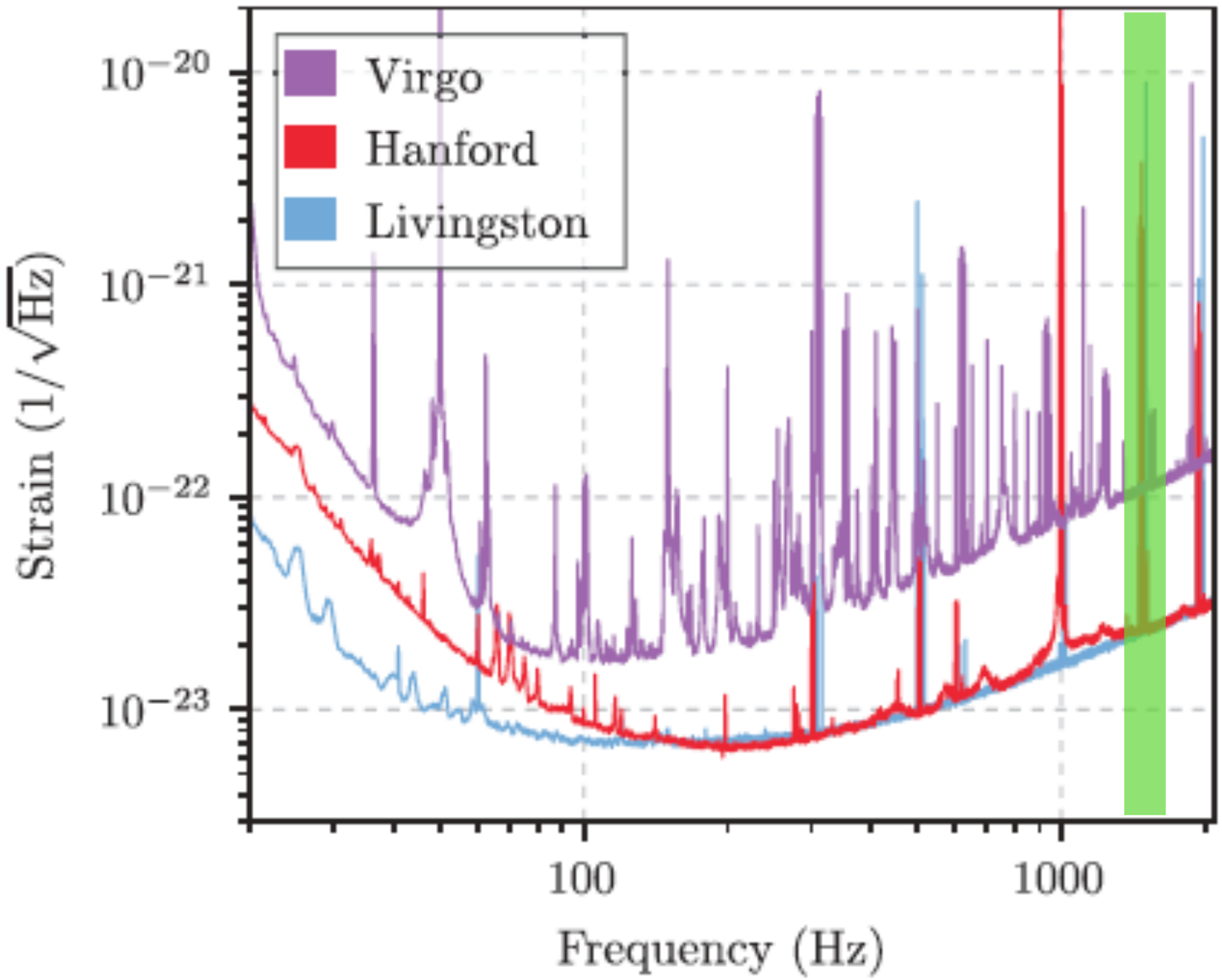

Post-merger remnant

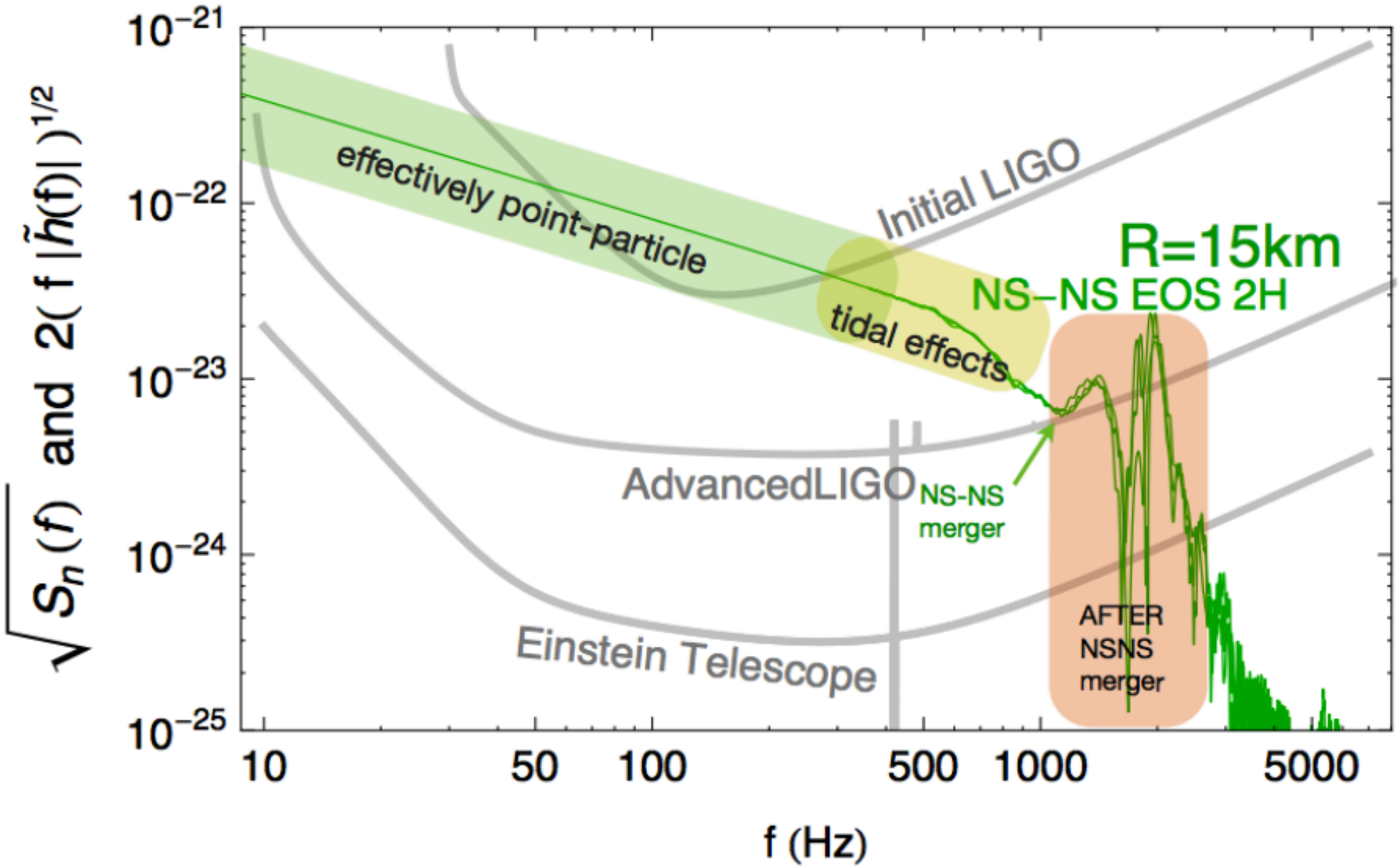

S. Usman et al (2018)

NS Equation of State

Q: So what is the remnant of the merger?

A: From EM - unclear! Some people believe prompt collapse to BH, others believe in the formation of a transient hypermassive NS

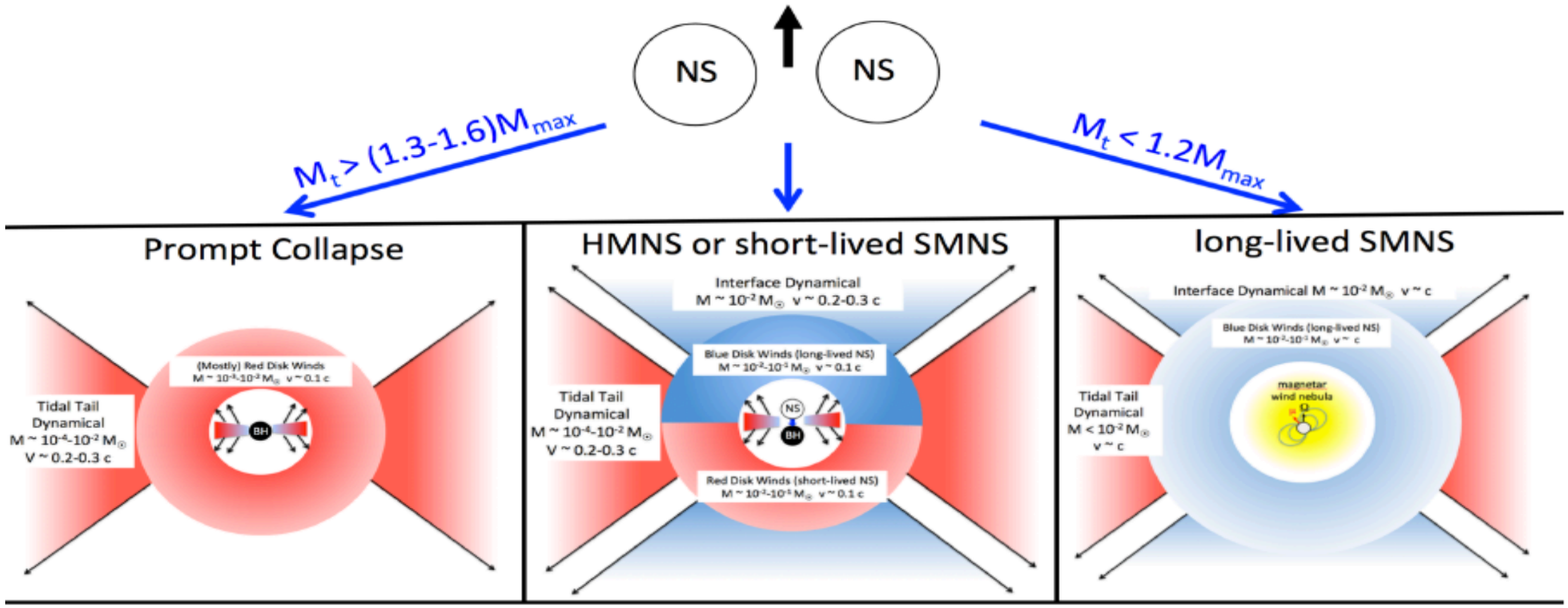

Margalit et al (2017)

Extreme Matter

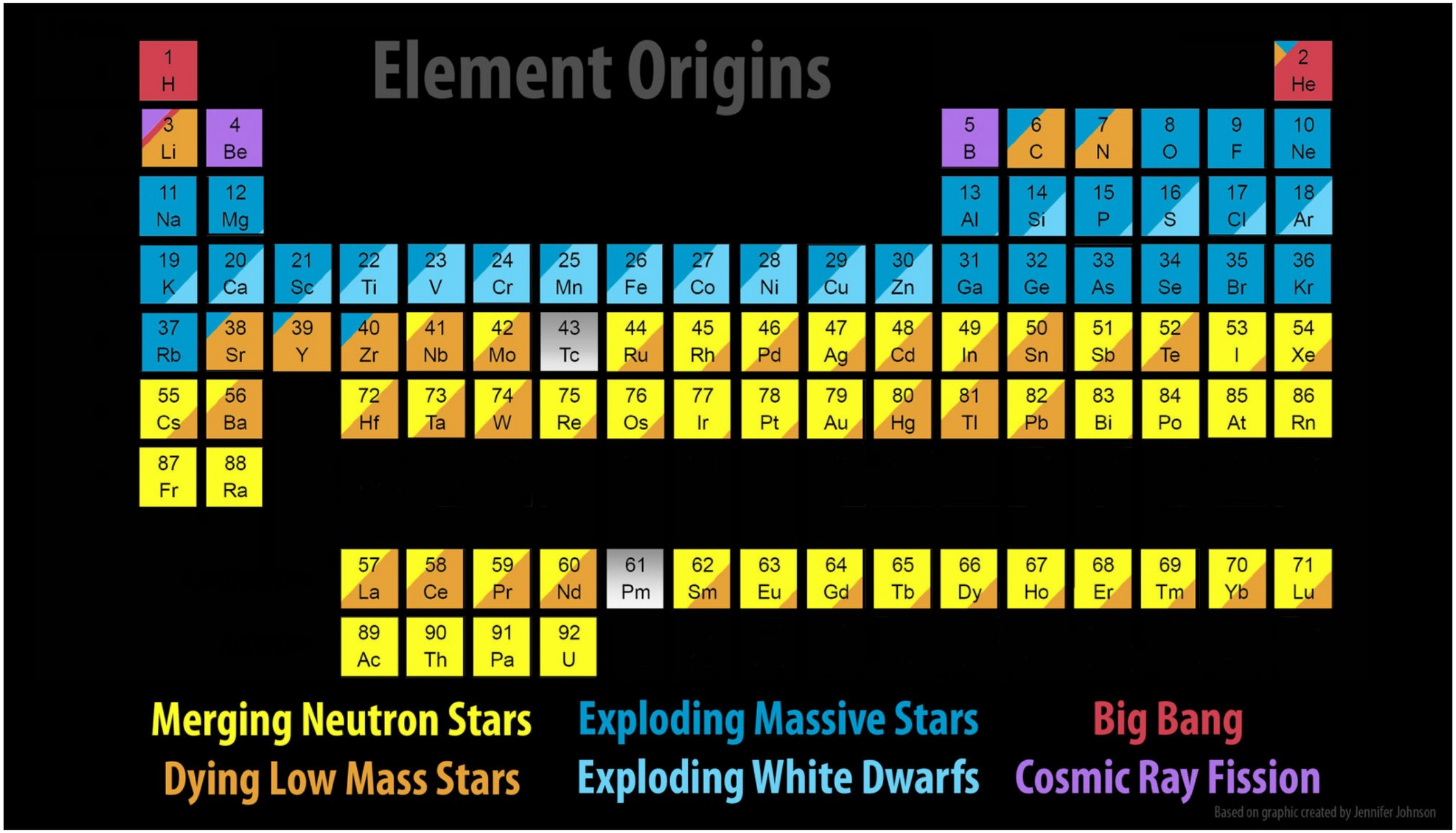

Credit: Jennifer Johnson/SDSS

Cosmology

Astrophysics

Cosmology

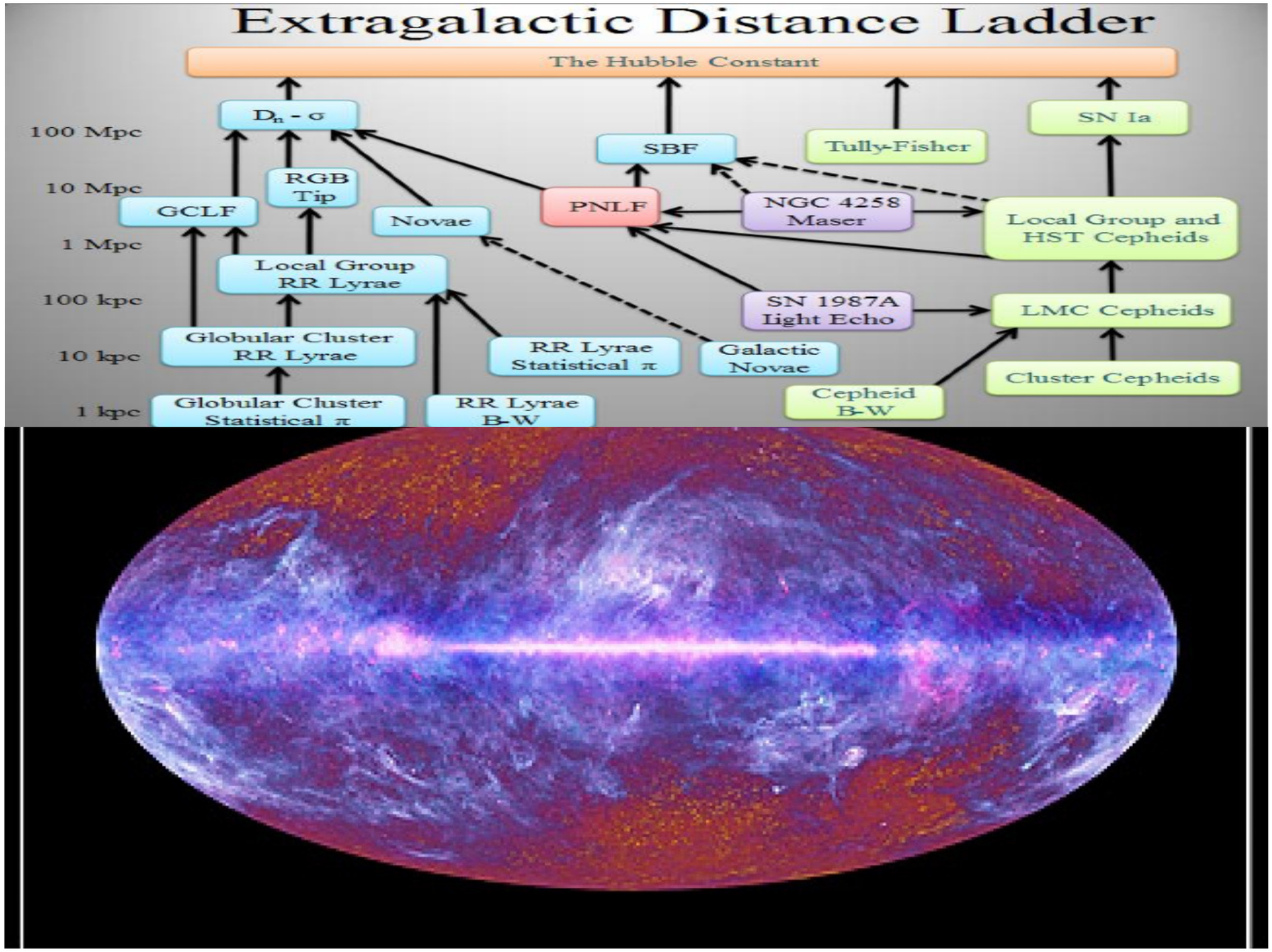

Cosmology

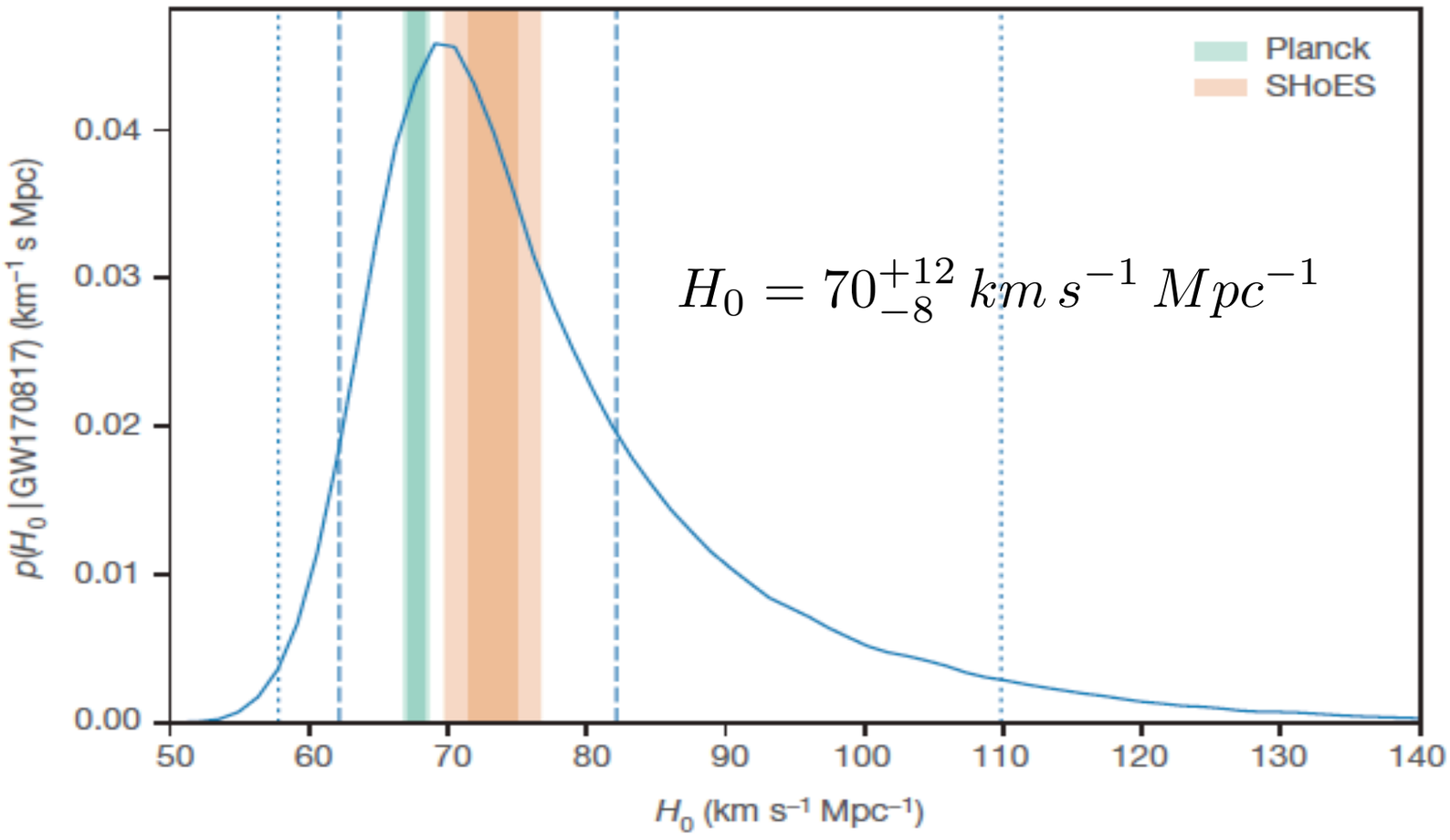

- **N.B. No cosmic distance ladder needed!!**
- **GW astronomy measures luminosity distance directly over cosmic scales**

Abbott et al, Nature (2017)

Conclusion

- Thank you for your attention